ENERGY TRANSFER IN MOLECULAR COLLISIONS

BY

EDUARDO F. VILALLONGA

A DISSERTATION PRESENTED TO THE GRADUATE COUNCIL
OF THE UNIVERSITY OF FLORIDA IN
PARTIAL FULFILLMENT OF THE REQUIREMENTS
FOR THE DEGREE OF DOCTOR OF PHILOSOPHY

UNIVERSITY OF FLORIDA

1981

AM39 81 2155

Bound by DOBBS BROS. LIBRARY BINDING CO., INC., St. Augustine, Florida

To my parents.

ACKNOWLEDGEMENTS

I wish to express my deepest appreciation and gratitude to my advisor, Professor David A. Micha, for his dedication, support and encouragement. I thank him for suggesting the study of the problems addressed in this dissertation, for many invaluable discussions, and for providing me many opportunities to broaden my experience as a scientist.

I am indebted to Professor Thomas L. Bailey for introducing me to the fascinating subject of atomic and molecular collisions. I wish to express to him my deepest appreciation and gratitude for his support during my first two graduate years and for his constant interest and encouragement.

I would like to thank all the faculty members of the Quantum Theory project and of the Department of Physics, all of whom have contributed to my development as a student and as a scientist. In particular, I thank Professors Per-Olov Löwdin and Charles F. Hooper, Jr., for providing me the opportunities to attend the International Summer School in Uppsala, Sweden, and the NATO Advanced Study Institute in Cortona, Italy, respectively.

I am deeply indebted to three very special persons, my parents and Kristin V. Bjorn. Much of the work presented here might not have been possible without their unwavering encouragement, patience and understanding.

TABLE OF CONTENTS

		Page
ACKNOWLEDGEMENTS.		iii
ABSTRACT.		vi
INTRODUCTION.		1
CHAPTER		
I	THE CORRELATION FUNCTION APPROACH	6
	1. The System Hamiltonian.	7
	2. The Differential Cross Section.	8
	3. Time-Evolution of the Correlation Function and Moments of the Energy Transfer.	12
	4. Cumulant and Moment Expansions.	15
	5. Short-Time Expansions	17
II	THE MANY-BODY CORRELATION FUNCTION APPROACH	20
	1. Outline of the Many-Body Approach	22
	2. Vibrational and Rotational Correlations . . .	26
	3. Cumulant Expansion of the Vibrational Correlation.	28
	4. Evaluation of the Displacement-Displacement Correlation Function.	34
	5. Effects of Molecular Anharmonicity in Hyperthermal Collisions.	42
	6. Short-Time Approximation to the Rotational Correlation	43
III	MULTICENTER POTENTIAL ENERGY SURFACES	48
	1. Single-Center vs. Multicenter Expansion . . .	48
	2. Atom-Pair Potentials for Ion/Linear Molecule Interactions.	52
	3. Multicenter Potential for the System Li^+/CO .	57
	4. Multicenter Potential for the System Li^+/CO_2.	73

TABLE OF CONTENTS (Continued)

		Page
IV	ROTATIONAL AND VIBRATIONAL ENERGY TRANSFER IN HYPERTHERMAL COLLISIONS OF Li^+ WITH N_2, CO AND CO_2	91
	1. The Atom-Pair Correlation Function of a Diatomic Molecule	91
	2. Rotational and Vibrational Energy Transfer in Hyperthermal Collisions of Li^+ with N_2 and CO	94
	3. Evaluation of the Atom-Pair Correlation Function of a Linear Triatomic Molecule	102
	4. Rotational and Vibrational Energy Transfer in Hyperthermal Collisions of Li^+ with CO_2	105
	5. Effects of Molecular Anharmonicity in N_2, CO and CO_2	113
V	A SEMICLASSICAL CORRELATION FUNCTION APPROACH TO MOLECULAR COLLISIONS	119
	1. The Semiclassical Approximation	121
	2. The Differential Probability of Energy Transfer	125
	3. Expansion of the Intermolecular Potential in Vibrational Displacements	130
	4. The Evolution Operator in the Interaction Representation	131
	5. Vibrational and Rotational Correlation	136
	6. The Vibrational Correlation	138
	7. The Rotational Correlation	140
	8. Discussion	145
BIBLIOGRAPHY		147
BIOGRAPHICAL SKETCH		152

Abstract of Dissertation Presented to the Graduate Council
of the University of Florida in Partial Fulfillment of the
Requirements for the Degree of Doctor of Philosophy

ENERGY TRANSFER IN MOLECULAR COLLISIONS

By

Eduardo F. Vilallonga

June, 1981

Chairman: David A. Micha
Major Department: Physics

Vibrational and rotational energy transfer in hyperthermal molecular collisions are investigated by means of time-correlation function methods. Within this approach, the collisional differential cross section is expressed as the Fourier transform of the time-correlation function of the transition operator, which evolves in time in accordance with the internal motions of the noninteracting molecules. The correlation function includes from the outset the experimental averages over initial distributions, so that only quantities directly related to experimental measurements need be calculated. The present approach allows the systematic introduction of approximations to the transition operator, which are based on models of the intermolecular forces and of the collision dynamics; the resulting correlation functions are readily evaluated for most polyatomics without need of internal-state or partial-wave expansions.

In particular, a many-body description of the dynamics, together with a multicenter representation of intermolecular forces, shows that, at hyperthermal energies, large-angle atom-polyatomic scattering is related to the correlation of the positions of pairs of atoms that constitute the target. The atom-pair correlation functions are evaluated by means of cumulant expansions and of Green-function techniques. The multicenter representation of the intermolecular potential is investigated, and multicenter surfaces are developed for the interaction of Li^+ with CO and with CO_2. Combining these developments, we calculate differential cross sections for the vibrational and rotational excitation of N_2, CO and CO_2 in collisions with hyperthermal Li^+ ions. Comparing these results with those obtained in experiments, we gain understanding of the features of the potential surface and of the dynamics that govern energy transfer processes.

We also develop a new semiclassical description of molecule-molecule collisions. Whenever the relative motion of the polyatomics may be described classically, we find that the differential probability of energy transfer is given by the Fourier transform of the time-correlation function of quantal transition amplitudes; the correlation function evolves in time in accordance with the Hamiltonians of the noninteracting polyatomics and describes the response of the molecules to the collision. The correlation function is evaluated for large

polyatomics by means of a procedure which includes the intermolecular potential to infinite order. We thus obtain simple analytical expressions for the differential probability of energy transfer in terms of action integrals; these integrals correspond to the actions that the intermolecular forces exert on the atoms of the polyatomics.

INTRODUCTION

During the past few years, there has been an explosive development of theoretical approaches to energy transfer processes in molecular collisions, generally in the thermal collision energy regime. These approaches range from fully quantal (Lester, 1976), in which the wave-function of the system is expanded in a more or less complete set of internal (vibrational and rotational) states of the colliding molecules, to completely classical (Porter and Raff, 1976), in which all the degrees of freedom of the system are described by Hamilton's equations of motion. Halfway between these two extremes lie the various semiclassical and time-dependent methods (McCann and Flannery, 1975, Miller, 1975, Child, 1976, Billing, 1978) that treat the relative motion of the collision partners classically while describing the internal motions by a wave-function expanded in internal states. Extensive reviews on these various approaches can be found in the book edited by Miller, 1976, in the monograph by Gianturco, 1979, and in the articles by Clark et al., 1977, by Dickinson, 1979 and by Micha, 1981a.

Concurrently with these theoretical developments, the progress of crossed molecular beams techniques (Toennies, 1976, Faubel and Toennies, 1977) has made available a wealth of new experimental information in atom-molecule collisions at hyperthermal energies (1 to 10 eV). The

systems which have been studied in detail include, among others, Li^+ ions in collision with N_2 and CO (Bottner et al., 1976, Eastes et al., 1979a), CO_2 and N_2O (Eastes et al., 1977), CH_4 (Eastes et al., 1979b) and SF_6 (Ellenbroek et al., 1979). Techniques based on time-of-flight or velocity analysis of the scattered ions have produced detailed velocity distributions of the products as functions of collision energy and scattering angle. These distributions show rich and varied structure due to the collisional excitation of the vibrational and rotational states of the target.

In spite of the recent theoretical advances outlined above, these new measurements present a challenge to theoretical interpretation. The fully classical approaches, which can give accurate values of average energy transfers, cannot describe the quantum-mechanical nature of the target, which is clearly shown by the experiments. Furthermore, for systems of more than about three or four atoms, several dynamical approximations must be introduced in order to decrease the number of Hamilton's equations which must be integrated numerically (Schatz, 1980). The quantal and semiclassical methods can, in principle, provide very detailed state-to-state transition probabilities. However, they become computationally impractical for energies above .1 eV because the number of internal states that are energetically accessible is unmanageably large. This necessitates the introduction of rather drastic computational approximations whose dynamical consequences are not yet fully understood. These approximations include the orbital-sudden or coupled states (McGuire and Kouri, 1974, Pack, 1974), the energy-sudden (Khare, 1977 and 1978), the infinite-order-sudden (Secrest, 1975, Goldflam et al., 1977) and the effective potential methods

(Rabitz, 1976). Furthermore, the ultimate test of accuracy of a theoretical model lies in a successful comparison with experimental results, which usually correspond to averages over initial distributions of internal states. The theoretician is forced to question the efficiency of state-expansion approaches when he is faced with the prospect of averaging over coarse experimental distributions the detailed results so laboriously obtained.

A complete description of molecular collision processes also requires knowledge of the potential energy surface of the colliding partners. Except for a limited number of small systems, accurate quantum-chemical calculations of potential energy surfaces are beyond the reach of present-day computational resources. This does not present a serious difficulty for the description of thermal collisions, because they are mediated mostly by the long and intermediate range forces. These forces can be accurately determined by combining the results of perturbation expansions (Hirschfelder et al., 1967, Chap. 13) with experimental measurements of the molecular properties (electrostatic multipole moments, polarizabilities, etc.) of the separate colliding partners. However, as the collision energy increases above a few tenths of an electron-volt, the projectiles probe the inner regions of the potential surface. At short distances, the usual perturbation expansions diverge, and accurate models for the forces have not yet been found.

We thus find that the description of hyperthermal collisions involving polyatomics presents a double challenge to the theoretician, due to the lack of knowledge of the intermolecular forces involved, and due to the inapplicability of the existent dynamical models. The

purpose of this dissertation is to develop and apply new theoretical approaches to the study of vibrational and rotational energy transfer in molecular collisions. We will consider in particular the range of collision energies above 1 eV but below the threshold for electronic excitation or dissociation of the colliding partners. In view of the previous discussion, these approaches must satisfy the following requirements:

1) The internal motions of the colliding molecules must be described quantum mechanically.

2) Expansions in internal states must be avoided; instead, we will focus our attention on the many-body nature of the system.

3) The new models should be interpretable in terms of molecular forces and dynamical processes so that we can gain understanding of the physical mechanisms involved.

4) The models should allow us to include averages over initial distributions of internal states without greatly increasing computational costs, in order to permit comparison with experimental measurements.

During the course of our investigations, we have found that the first two requirements lead us to express the collisional differential cross section in terms of the time-correlation function of the transition operator, as is shown in Chap. I; this function includes from the outset the averages over initial states, so that only quantities directly related to experimental measurements need be calculated. The present approach allows us to systematically introduce approximations to the transition operator, which are based on different models of the intermolecular forces and of the collision dynamics. In particular, a many

body description of the dynamics, together with a multicenter representation of the forces, shows that the large-angle scattering of hyperthermal projectiles is related to the correlation of the positions of pairs of atoms of the isolated target (Micha, 1979a). In Chap. II, we study these atom-pair correlation functions and extend them to include the effects of anharmonicity in the vibrational motion of the polyatomic. In Chap. III, we investigate the multicenter representation of intermolecular forces and develop multicenter potential surfaces for the systems Li^+/CO and Li^+/CO_2. Next, combining the developments of the previous two chapters, we calculate differential cross sections for the vibrational and rotational excitation of N_2, CO and CO_2 in collisions with hyperthermal Li^+ ions. By comparing these results with the experimental measurements (Bottner et al., 1976, Eastes et al., 1977), we gain understanding of the relative importance of the features of the potential surface and of the dynamics that govern energy transfer processes. Finally, in Chap. V, we develop a new semiclassical description of molecular collisions. Whenever the relative motion of the molecule may be described classically, we find that the differential cross section is related to the time-correlation of quantal transition amplitudes that evolve in accordance with the internal Hamiltonians of the isolated molecules. This correlation function completely describes the response of the molecules to the collision; furthermore, it is readily evaluated for a wide range of polyatomics, without need of internal-state expansions.

CHAPTER I
THE CORRELATION FUNCTION APPROACH

We consider collisions between two arbitrarily large molecules, A and B, each having closed electronic shells. In order to single out the mechanisms responsible for rotational and vibrational energy transfer, we consider the range of collision energies below the thresholds for electronic excitation and dissociation of the molecules. We are thus interested in process of the type

$$A(\alpha) + B(\beta) \overset{\varepsilon}{\rightarrow} A(\alpha') + B(\beta').$$

Initially A and B are in the internal states (rotational and/or vibrational) denoted by the sets of quantum numbers α and β, respectively. During the collision an amount of energy ε is transferred between them into internal motions, promoting A and B to their final internal states, which we indicate by α' and β'.

For the system Hamiltonian specified in Sec. 1, doubly-differential cross sections may be related to the time-correlation function of the collisional transition operator, as is shown in Sec. 2. In the following section, we examine the evolution of the correlation function and relate its time-derivatives at time equal zero to the moments of the energy transfer. In Sec. 4, we introduce the method of cumulant expansions which provides a powerful tool for evaluating the correlation functions. Finally, in Sec. 5, we show that internal motions that are

slower than relative ones lead to a Gaussian distribution of energy transfer.

Although we focus our attention on molecular scattering, we should emphasize that the analysis presented in this chapter applies, quite generally, to collisions between any two many-body systems whose interactions can be described by a single potential energy surface. These include, for example, scattering of molecules from surfaces of solids.

1. The System Hamiltonian

In the coordinate system fixed to the center of mass of the pair (A,B), indicating operators with carats, the Hamiltonian of the collision is

$$\hat{H} = \hat{K} + \hat{H}_M + \hat{V}. \tag{1.1.1}$$

Here, $\hat{K}$ is the operator for the kinetic energy of relative motion given by

$$\hat{K} = \frac{-\hbar^2}{2M} \frac{\partial^2}{\partial \vec{R}^2} \tag{1.1.2}$$

where $\vec{R}$ is the position of the center of mass of the projectile A with respect to that of target B, $M = M_A M_B/(M_A + M_B)$ is the reduced mass of the system with M_A and M_B the masses of the respective molecules. The Hamiltonian that describes the internal motions of the separated molecules, $\hat{H}_M$, is the sum of the internal Hamiltonians of each isolated molecule ($\hat{H}_A$ and $\hat{H}_B$, respectively). The operator $\hat{V}$ represents the intermolecular potential which generally depends on $\vec{R}$ and on $\vec{r}^M = \{\vec{r}^A, \vec{r}^B\}$, where $\vec{r}^X$ denotes the positions of the atoms of molecule X = A or B with respect to the center of mass of X.

The motion of the noninteracting molecules is described by

$$(\hat{K} + \hat{H}_M)|\vec{k}\nu\rangle = [\hbar^2 k^2/(2M) + E_\nu]|\vec{k}\nu\rangle, \tag{1.1.3a}$$

$$\langle \vec{R}\vec{r}^M|\vec{k}\nu\rangle = (2\pi)^{-3/2} \, e^{i\vec{k}\cdot\vec{R}} \, \langle \vec{r}^M|\nu\rangle, \tag{1.1.3b}$$

$$\langle \vec{r}^M|\nu\rangle = \langle \vec{r}^A|\alpha\rangle\langle \vec{r}^B|\beta\rangle, \tag{1.1.3c}$$

in which $\hbar\vec{k}$ is the relative momentum, ν represents the collection of vibrational and rotational quantum numbers of both molecules, $E_\nu = E_\alpha + E_\beta$, E_α and E_β are the energies of the internal states $|\alpha\rangle$ and $|\beta\rangle$ of A and B, respectively.

2. The Differential Cross Section

The scattering rate or transition probability per unit time between the free states defined in eqs. (1.1.3) is given by (Newton, 1966, chap. 8)

$$R(\vec{k}'\nu' \leftarrow \vec{k}\nu) = (2\pi/\hbar)|\langle \vec{k}'\nu'|\hat{T}^{(+)}(E)|\vec{k}\nu\rangle|^2, \tag{1.2.1}$$

where final and initial quantities are indicated by primed and unprimed symbols, respectively, and $E = \hbar^2 k^2/(2M) + E_\nu$ is the total energy of the system. The transition operator for the collision, $\hat{T}^{(+)}$, satisfies the Lippman-Schwinger equation for outgoing-wave boundary conditions

$$\hat{T}^{(+)}(E) = \hat{V} + \hat{V}\hat{G}_o^{(+)}(E)\hat{T}^{(+)}(E), \tag{1.2.2}$$

where $\hat{G}_o^{(+)}$ is the propagator for the free motion given by

$$\hat{G}_o^{(+)}(E) = (E + i\eta - \hat{K} - \hat{H}_M)^{-1}. \tag{1.2.3}$$

Experimental measurements usually correspond to thermal averages over initial distributions of internal states with $w_\alpha^{(X)}(T_X)$ with

temperature T_X for each collision partner X = A or B. Furthermore, experiments usually do not select the final internal states of the molecules. In these cases, we must consider the total rate for scattering between initial and final momenta,

$$R_{tot}(\vec{k}', \vec{k}) = (2\pi/\hbar) \sum_{v,v'} w_v(T_A, T_B) |\langle \vec{k}'v' | \hat{T}^{(+)}(E) | \vec{k}v \rangle|^2 \, \delta(E - E'), \quad (1.2.4)$$

where the delta function insures conservation of the total energy of the system.

Typical rotational excitation energies of most molecules (except those that contain several hydrogen atoms) are of the order of a few thousands of an electron volt. At hyperthermal collision energies, the sum over final states in eq. (1.2.4) contains a very large number of terms, even for small values of energy transfers. This also occurs in atom surface-scattering due to the low values of phonon excitation energies. However, the sum over final states may be formally eliminated by the following procedure (Micha, 1981a).

Introducing the integral representation of the delta function,

$$\delta(E - E') = \int_{-\infty}^{\infty} \frac{dt}{2\pi\hbar} \exp[-i(E - E')t/\hbar], \quad (1.2.5)$$

into the matrix elements of the transition operator of eq. (1.2.4) and using eq. (1.1.3a) yields

$$\langle \vec{k}'v' | \hat{T}^{(+)}(E) | \vec{k}v \rangle = \int_{-\infty}^{\infty} \frac{dt}{2\pi\hbar} \exp(-i\varepsilon t/\hbar) \langle \vec{k}'v' | \exp(i\hat{H}_M t/\hbar) \hat{T}^{(+)}(E) \times \exp(-i\hat{H}_M t/\hbar) | \vec{k}v \rangle, \quad (1.2.6)$$

where the energy transfer is given by $\varepsilon = \hbar^2[k^2 - (k')^2]/(2M)$. The matrix element of eq. (1.2.6) implies an integration over the relative coordinate $\vec{R}$ and over the internal coordinates $\vec{r}^M$. Before proceeding further it will prove convenient to explicitly factor these two integrations by defining the operator

$$\hat{T}_{\vec{k}',\vec{k}} = \langle \vec{k}' | \hat{T}^{(+)}(E) | \vec{k} \rangle, \tag{1.2.7}$$

which acts only on the internal coordinates of the molecules. Substituting eq. (1.2.7) into eq. (1.2.6) and the latter into eq. (1.2.4), the sum over final states may be eliminated by means of the completeness relation of the internal states $|\nu'\rangle$. One thus arrives at the following expression for the total scattering rate,

$$R_{tot}(\vec{k}',\vec{k}) = (2\pi/\hbar)^4 \int_{-\infty}^{\infty} \frac{dt}{2\pi\hbar} \exp(-i\varepsilon t/\hbar) \langle\langle \hat{T}^{\dagger}_{\vec{k}',\vec{k}}(0) \hat{T}_{\vec{k}',\vec{k}}(t)_M \rangle\rangle, \tag{1.2.8}$$

where the double brackets indicate the quantum mechanical and thermal averages over initial states,

$$\langle\langle \cdots \rangle\rangle = \sum_{\alpha,\beta} w_\alpha^{(A)}(T_A) w_\beta^{(B)}(T_B) \langle \alpha\beta | \cdots | \alpha\beta \rangle. \tag{1.2.9}$$

The time dependence of the transition operator is given by the Hamiltonian of the noninteracting molecules (indicated explicitly by the subscript M), as shown below

$$\hat{T}_{\vec{k}',\vec{k}}(t)_M = \exp(i\hat{H}_M t/\hbar)\, \hat{T}_{\vec{k}',\vec{k}}\, \exp(-i\hat{H}_M t/\hbar). \tag{1.2.10}$$

The doubly differential (energy-angle) cross section for scattering into a unit solid-angle Ω accompanied by a transfer of energy ε may be calculated from the ratio of the transition rate to the incident flux (Micha, 1979a), to give

$$\frac{d^2\sigma}{d\Omega d\varepsilon} = (2\pi/\hbar)^4 M^2(k'/k) \int_{-\infty}^{\infty} \frac{dt}{2\pi\hbar} \exp(-i\varepsilon t/\hbar) \langle\langle \hat{T}^{+}_{\vec{k}',\vec{k}}(0) \hat{T}_{\vec{k}',\vec{k}}(t)_M \rangle\rangle, \tag{1.2.11}$$

where the final momentum is related to the energy transfer by $k'=(k^2-2M\varepsilon/\hbar^2)^{\frac{1}{2}}$. The cross section is thus expressed as the Fourier transform of the time-correlation function of the transition operator, with the time dependence determined by the internal motions of the isolated molecules. Approximations to the cross section in terms of correlation functions have been previously used to describe scattering of cold neutrons from solids (Marshall and Lovesey, 1971) and from liquids (March and Tosi, 1976), and atoms from polyatomics (Micha, 1979a and 1981a) and from solid surfaces (Micha, 1981b,c). The present expression is more general than these models and is therefore applicable to a much wider range of many-body systems.

The direct evaluation of the time-correlation function of eq. (1.2.11) is as difficult as finding the solution to the many-body problem which is implicitly contained in the transition operators. At first sight, it seems that the sums over final states have been removed at the expense of introducing an added time dependence (due to the complicated internal molecular motions) into the already intricate transition operators. However, the correlation function approach allows the development of dynamical approximations to the

transition operator in a systematic way, as is shown in the following chapters. These approximations, based on the relevant features of the intermolecular potential surface and on the different types of molecular motions, will allow us to understand the physical mechanisms that govern energy transfer processes. The correlation function approach has the additional advantage of describing the collision in terms of time dependent Heisenberg operators which may be easily interpreted in terms of the classical dynamical variables of the colliding molecules.

3. Time-Evolution of the Correlation Function and Moments of the Energy Transfer

Other quantities usually measured by experiments are the moments of the energy transfer. These measurements are related to quantities that can be calculated theoretically, in the following way. For given values of the initial and final momenta, the nth order moment-average of the energy transfer with respect to the cross section is defined by

$$<\varepsilon^n>=[\int_{-\infty}^{\infty} d\varepsilon d^2\sigma/(d\Omega d\varepsilon)]^{-1} \int_{-\infty}^{\infty} d\varepsilon\ \varepsilon^n\ d^2\sigma/(d\Omega d\varepsilon) \qquad (1.3.1)$$

For the sake of brevity, we introduce the following notation for the correlation function,

$$C_{\vec{k}'\vec{k}}(t) = <<\hat{T}^{+}_{\vec{k}'\vec{k}}(0)\hat{T}_{\vec{k}'\vec{k}}(t)_M>>, \qquad (1.3.2)$$

and for its Fourier transform,

$$\tilde{C}_{\vec{k}'\vec{k}}(\varepsilon)=\int_{-\infty}^{\infty}\frac{dt}{2\pi\hbar}\exp(-i\varepsilon t/\hbar)\ C_{\vec{k}'\vec{k}}(t), \qquad (1.3.3a)$$

$$C_{\vec{k}'\vec{k}}(t) = \int_{-\infty}^{\infty} d\varepsilon\ \exp(i\varepsilon t/\hbar)\ \tilde{C}_{\vec{k}'\vec{k}}(\varepsilon), \qquad (1.3.3b)$$

and we drop the subscripts $\vec{k}$ and $\vec{k}'$ while keeping in mind that the following derivations correspond to fixed values of the initial and final momenta. Differentiating eq. (1.3.3b) with respect to time shows that the moments of the energy transfer are related to the time derivatives of the correlation function by

$$<\varepsilon^n>= \frac{(-i\hbar)^n}{C(0)} \frac{\partial^n}{\partial t^n} C(t)\Big|_{t=0} \tag{1.3.4}$$

and to the transition operator by

$$<\varepsilon^n>= <<\hat{T}^\dagger(0)([\hat{H}_M,)^n \hat{T}(0)]>><<\hat{T}^\dagger(0)\hat{T}(0)>>^{-1}, \tag{1.3.5}$$

through differentiation of eq. (1.2.10). This last equation provides the bridge between calculated values and experimental measurements.

However, the moments of the energy transfer, by themselves, do not provide information about the cross section in the most practical way. This can be seen by expanding the correlation function in a Taylor series in time, about t=0, and equating the time-derivatives to the moments of the energy transfer by eq. (1.3.4). One thus obtains an expansion for the cross section in moments of the energy transfer, but each term of this series diverges because it contains the Fourier transform of t^n. The origin of this divergence is further clarified by expressing the time dependence of the correlation function, as follows (1).

Differentiating eq. (1.2.10) with respect to time, yields Heisenberg's equation of motion for the transition operator,

$$\frac{\partial \hat{T}}{\partial t}(t)_M = \frac{i}{\hbar}[\hat{H}_M, \hat{T}(t)_M]. \tag{1.3.6}$$

---

1) The following derivation is based on class notes of Prof. D. A. Micha.

We now define the Liouville superoperator for the internal motions, L_M, by its action on any arbitrary operator $\hat{A}$ which acts on the internal coordinates of the molecules; this is given by

$$L_M \hat{A} = [\hat{H}_M, \hat{A}], \tag{1.3.7a}$$

and, more generally,

$$L_M^n \hat{A} = ([\hat{H}_M,)^n \hat{A}]. \tag{1.3.7b}$$

The time evolution of the transition operator may now be rewritten as

$$\frac{\partial \hat{T}}{\partial t}(t)_M = \frac{i}{\hbar} L_M \hat{T}(t)_M, \tag{1.3.8}$$

which has the formal solution

$$\hat{T}(t)_M = \exp(iL_M t/\hbar)\ \hat{T}\ (0). \tag{1.3.9}$$

Replacing eq. (1.3.9) into eq . (1.3.2) yields the following expression for the correlation function,

$$C(t) = C(0)\langle\langle \hat{T}^\dagger(0) \exp(iL_M t/\hbar)\ \hat{T}\ (0)\rangle\rangle \langle\langle \hat{T}^\dagger(0)\hat{T}(0)\rangle\rangle^{-1}. \tag{1.3.10}$$

The last two factors in the above equation are formally equivalent to the average of the operator $\exp(iL_M t/\hbar)$ over the "scattering" states defined by $|\nu\rangle_S = \hat{T}(0)|\nu\rangle$. Denoting this average by the subscript S, we write

$$C(t) = C(0)\langle\langle \exp(iL_M t/\hbar)\rangle\rangle_S. \tag{1.3.11}$$

A comparison of eqs. (1.3.4) and (1.3.8) shows that

$$\langle \varepsilon^n \rangle = \langle\langle L_M^n \rangle\rangle_S; \tag{1.3.12}$$

therefore, expanding the cross section in moments of the energy transfer is equivalent to an expansion of the exponential $\exp(iL_M t/\hbar)$ in powers of the exponent. We are not surprised that this expansion diverges when it is applied for all values of time.

In order to take full advantage of the theoretical and experimental information provided by the moments of the energy transfer, we must introduce the cumulant expansion methods which have been widely used in statistical mechanics (Kubo, 1962, Munster, 1969). These techniques will also provide us with powerful tools for evaluating the correlation functions that we will encounter in the following chapters.

4. Cumulant and Moment Expansions

For any operator $\hat{A}$ and complex number x, the average of $\exp(x\hat{A})$ is defined in terms of the moment averages of $\hat{A}$, $\langle\langle\hat{A}^n\rangle\rangle$, by

$$\langle\langle\exp(x\hat{A})\rangle\rangle = \sum_{n=0}^{\infty} x^n\langle\langle\hat{A}^n\rangle\rangle/n!. \qquad (1.4.1)$$

Truncating the above series to a finite number of terms might give a very poor (even divergent) approximation to $\langle\langle\exp(x\hat{A})\rangle\rangle$ for some values of x. We look for an alternate expansion which will hopefully give a better approximation when truncated. In particular, we write

$$\langle\langle\exp(x\hat{A})\rangle\rangle = \exp\sum_{n=1}^{\infty} x^n\langle\langle\hat{A}^n\rangle\rangle_C/n!, \qquad (1.4.2)$$

where the $\langle\langle\hat{A}^n\rangle\rangle_C$ are certain averages of the operator $\hat{A}$ called cumulant averages (Kubo, 1962), which are implicitly defined in terms of the moments by eqs. (1.4.1) and (1.4.2).

An explicit relation between a cumulant of a given order and the moments and cumulants of lower orders may be obtained by the following procedure (Munster, 1969). Differentiating eqs. (1.4.1) and (1.4.2) once with respect to x and equating their right hand sides yields

$$\sum_{n=1}^{\infty} x^{n-1}\langle\langle\hat{A}^n\rangle\rangle/(n-1)! = \sum_{n,j=1}^{\infty} x^{n-1}\langle\langle\hat{A}^{n-j}\rangle\rangle\langle\langle\hat{A}^j\rangle\rangle_C/[(n-j)!(j-1)!], \tag{1.4.3}$$

where the equality follows by changing the dummy index of summation n to $n \to n + j$. Comparing powers of x in the last equation and solving for $\langle\langle\hat{A}^n\rangle\rangle_C$ gives the desired relation,

$$\langle\langle\hat{A}^n\rangle\rangle_C = \langle\langle\hat{A}^n\rangle\rangle - \sum_{j=1}^{n-1}\binom{n-1}{j-1}\langle\langle\hat{A}^{n-j}\rangle\rangle\langle\langle\hat{A}^j\rangle\rangle_C. \tag{1.4.4}$$

For example, the first four cumulants are

$$\langle\langle\hat{A}\rangle\rangle_C = \langle\langle\hat{A}\rangle\rangle, \tag{1.4.5a}$$

$$\langle\langle\hat{A}^2\rangle\rangle_C = \langle\langle\hat{A}^2\rangle\rangle - \langle\langle\hat{A}\rangle\rangle^2, \tag{1.4.5b}$$

$$\langle\langle\hat{A}^3\rangle\rangle_C = \langle\langle\hat{A}^3\rangle\rangle - 3\langle\langle\hat{A}\rangle\rangle\langle\langle\hat{A}^2\rangle\rangle + 2\langle\langle\hat{A}\rangle\rangle^3, \tag{1.4.5c}$$

$$\langle\langle\hat{A}^4\rangle\rangle_C = \langle\langle\hat{A}^4\rangle\rangle - 4\langle\langle\hat{A}^3\rangle\rangle\langle\langle\hat{A}\rangle\rangle + 3\langle\langle\hat{A}^2\rangle\rangle(3\langle\langle\hat{A}\rangle\rangle^2 - \langle\langle\hat{A}^2\rangle\rangle) - 6\langle\langle\hat{A}\rangle\rangle^4. \tag{1.4.5d}$$

In particular, letting $x = it/\hbar$ and $\hat{A} = L_M$, we can express the correlation function of eq. (1.3.11) in terms of the cumulant averages of L_M, as follows:

$$C(t) = C(0)\exp\sum_{n=1}^{\infty}(it/\hbar)^n\langle\langle L_M^n\rangle\rangle_{CS}/n!. \tag{1.4.6}$$

In analogy with eq. (1.3.12) we define the cumulant averages of the energy transfer by $\langle\varepsilon^n\rangle_C = \langle\langle L_M^n\rangle\rangle_{CS}$, which are related to the moment averages as shown below

$$\langle\varepsilon^n\rangle_C = \langle\varepsilon^n\rangle - \sum_{j=1}^{n-1}\binom{n-1}{j-1}\langle\varepsilon^{n-j}\rangle\langle\varepsilon^j\rangle_C. \tag{1.4.7}$$

Finally, substituting eq. (1.4.6) into eq. (1.2.11), we obtain

$$\frac{d^2\sigma}{d\Omega d\varepsilon} = (2\pi/\hbar)^4 M^2 (k'/k) C(0) \int_{-\infty}^{\infty} \frac{dt}{2\pi\hbar} \exp[-i\varepsilon t/\hbar + \sum_{n=1}^{\infty} (i t/\hbar)^n \langle \varepsilon^n \rangle_c / n!]. \tag{1.4.8}$$

For given values of the initial and final momenta, this last equation provides a convenient parametrization of the cross section in terms of the averages of the energy transfer. As the cumulant averages correspond to differences between numbers of the same order of magnitude, the cumulant series will converge very rapidly. Furthermore, the above expression allows us to obtain well-behaved approximations to the cross section by truncating the series at any term of even order which is negative. The significance of these approximations is considered in the following section.

5. Short-Time Expansions

We now apply the techniques introduced above to systems in which the transfer of energy occurs in a time interval much smaller than the typical periods of the internal molecular motions. For example, even at collision energies below the threshold for vibrational excitation, the rotational motion of most molecules is much slower than the relative motion of the colliding partners (Micha, 1979b). This is also the case in atom-surface scattering at hyperthermal energies because the vibrational periods of phonons are much longer than collision times (Micha, 1981c). In these cases, the correlation between the two transition operators that determine the cross section is significant only during a short period of time. We are

then justified in retaining only the lowest powers of t in the cumulant expansion of the correlation function and writing

$$C(t) \approx C(0) \exp[i\langle\varepsilon\rangle t/\hbar - \langle\varepsilon^2\rangle_c t^2/(2\hbar^2)]. \qquad (1.5.1)$$

The applicability of the short-time approximation to a specific system can be judged by calculating or measuring the cumulants which have been omitted in the above equation. Alternatively, we can systematically develop improved approximations by including the higher order cumulants.

Substituting the correlation function of eq. (1.5.1) into eq. (1.2.11) and evaluating the Fourier transform (Churchill et al., 1974), we obtain the following expression for the cross section,

$$\frac{d^2\sigma}{d\Omega d\varepsilon} = I(\Omega)(2\pi\langle\varepsilon^2\rangle_c)^{-\frac{1}{2}} \exp[-(\varepsilon-\langle\varepsilon\rangle)^2/(2\langle\varepsilon^2\rangle_c)], \qquad (1.5.2a)$$

$$I(\Omega) = (2\pi/\hbar)^4 M^2 (k'/k) C(0). \qquad (1.5.2b)$$

This result shows that collisions in which the transfer of energy is much faster than the internal motions are characterized by a normalized Gaussian distribution in the energy transfer. This holds true for all scattering angles, regardless of the nature of the collision partners. The distribution is centered about the average energy transferred in the collision, $\langle\varepsilon\rangle$, and broadened by an amount $\langle\varepsilon^2\rangle_c^{\frac{1}{2}} = (\langle\varepsilon^2\rangle - \langle\varepsilon\rangle^2)^{\frac{1}{2}}$. The nature of the colliding species determines the values and the dependence on scattering angle of the intensity $I(\Omega)$ and of the location and width of the distribution. These conclusions are supported by several experimental measurements of atom-molecule (Bottner et al., 1976, Eastes et al., 1977 and 1979a,b) and atom-surface (Micha, 1981c) collisions.

We should emphasize the differences between the short-time and the various sudden approaches which have been widely used to describe molecular scattering. The latter are based on different approximations to the dynamics by which the energy is transferred. In contrast, throughout the present derivation, we have made no approximations to the dynamics of the collision. The intensity, location and width of the distribution of eqs. (1.5.2) depend on the exact transition operator. In particular, the coordinate-sudden approach (also called fixed-nuclei and adiabatic, see Chase, 1956) assumes that the internal degrees of freedom are frozen during the duration of the collision. In the short-time approximations these degrees of freedom evolve in time, albeit slowly, as can be seen in eq. (1.5.1). On the other hand, the energy-sudden (Khare, 1977 and 1978) and infinite-order-sudden (Secrest, 1975, Goldflam et al., 1977) methods fix the internal energy of the molecules throughout the collision; in the short-time approximation, the internal energy can and does change during the collision, as prescribed by the exact transition operator.

CHAPTER II
THE MANY-BODY CORRELATION FUNCTION APPROACH

In this chapter we develop and study the time-correlation functions that are appropriate to describe hyperthermal collisions in which a light projectile is deflected into large scattering angles. In order to maintain the formalism at the clearest level possible, we take the projectile A to be a structureless atom (neutral or ionized), while the target B remains a general N-atom polyatomic. Furthermore, we focus our attention on scattering processes in which the amount of energy transferred is considerably smaller than the relative collision energy.

The standard parameterization of atom-molecule potential energy surfaces is based on an expansion in a basis-set of functions of angles centered at the center of mass of the target (see Staemler, 1975, Parker et al., 1976 and Thomas et al., 1978 for examples). However, when the collision energy is much larger than the typical well-depths of the potential, large-angle scattering is due to the deflection of the projectile from the steeply repulsive inner region of the surface (McDowell and Coleman, 1970, Chap. 1), which is of a multicenter nature. In these cases, the potential is better represented by expanding about the atomic centers of the target, as follows (Micha, 1979a):

$$V(\vec{R},\vec{r}^{B}) = \sum_{a} v_a(\vec{R},\vec{r}_a). \qquad (2.1)$$

Here, $\vec{R}$ is the position of A with respect to the center of mass of the target and $\vec{r}^{B} = \{ \vec{r}_a, \ a = 1 \text{ to } N \}$ is the collection of the coordinate vectors of the atoms that constitute the polyatomic, referred to the center of mass of B. The two-body potential v_a represents the interaction between the (A,**a**) atom pair and depends on the electronic distribution of A and that of the valence state of atom **a** in the molecule. In general, at short distances, the pair potentials are steeply repulsive due to the overlapping of the electronic clouds, while in the long-range region they fall off as inverse powers of the relative distance between A and **a**. We postpone a detailed study of the pair potentials to a later chapter and concentrate here on the collision problem.

The many-body representation of the potential shown above suggests that atom-molecule scattering processes should be interpreted in terms of the dynamics of a many-body system; this approach has resulted in the recent development (Micha, 1979a) of a quantal many-body theory of atom-molecule collisions. Such a description, briefly reviewed in Sec. 1, leads to a simple model for vibrational and rotational energy transfer processes, in which the cross section is expressed in terms of atom-pair correlation functions of the isolated target molecule. These correlation functions can be readily evaluated for polyatomics whose vibrational motions arise from harmonic forces (Micha, 1979b). This model has been successful in describing the large-angle scattering of Li^+ from N_2 and CO (Micha et al., 1979) and from CO_2 (Vilallonga et al., 1979). However, recent quantal calculations for the system He/CO_2 indicate that

molecular anharmonicity may considerably influence vibrational energy transfers at thermal collision energies (Clary, 1980). Therefore, we extend the atom-pair correlation functions to encompass anharmonic force-fields, so that we can ascertain the effects of molecular anharmonicity in hyperthermal collisions. In order to focus our attention on the vibrational dynamics of the target, in Sec. 2 we decouple the vibrational and the rotational correlations from each other. By means of the cumulant expansion methods introduced in Chap. I, we express the vibrational correlation in terms of the displacement-displacement correlation functions, as shown in Sec. 3. These simpler functions are readily obtained from the corresponding double-time Green functions (Zubarev, 1960), which in turn may be evaluated from their hierarchy of equations of motion. In Sec. 4, this set of coupled differential equations, which is of infinite size, is decoupled by a linear procedure that contains anharmonic forces to infinite order. From this development, we conclude that anharmonic intramolecular forces cause a shift in the energy transfer spectrum and in the cross sections for vibrational excitation, as discussed in Sec. 5. Finally, in Sec. 6, we complete the evaluation of the atom-pair correlation function, by means of a short-time approximation to the rotational motions.

1. Outline of the Many-Body Approach

The many-body transition operator presented in eq. (1.2.2) can be expressed in terms of the two-body potentials v_a of eq. (2.1), by means of the formalism of multicenter scattering (Rodberg and Thaler, 1967, chap. 12). This leads to the final-channel decomposition

$$\hat{T} = \sum_a \hat{T}^{(a)} \quad , \tag{2.1.a}$$

$$\hat{T}^{(a)} = \hat{T}_a + \hat{T}_a \hat{G}_o \sum_{b \neq a} \hat{T}^{(b)} \quad , \tag{2.1.1b}$$

$$\hat{T}_a = \hat{v}_a + \hat{v}_a \hat{G}_o \hat{T}_a , \tag{2.1.1c}$$

where $\hat{T}^{(a)}$ describes the process in which the last interaction is mediated by v_a, while in $\hat{T}_a$ the only interaction is through v_a. In particular, iterating eq. (2.1.1) gives the multiple-collision expansion 2.1.2 that describes the operator $\hat{T}^{(a)}$ in terms of successive collisions between the projectile and each atom of the target.

Two assumptions (Micha, 1979a), that are appropriate to experimental conditions of high relative energies and large scattering angles, greatly simplify the evaluation of $\hat{T}^{(a)}$. When the wavelength for relative motion is much shorter than the distance between scattering centers, one may assume that only single collisions between the projectile and each atom of the target are significant, so that $\hat{T}^{(a)} \simeq \hat{T}_a$. In order to calculate $\hat{T}_a$, the N + 1 body problem must still be solved because the propagator $\hat{G}_o$ involves the motions of all the atoms of the target. However, substantial simplifications occur whenever the energy transfer is impulsive; this constitutes the second assumption.

In an impulsive collision between the projectile A and target atom a, a large force acts on a for a very short period of time. The position of a does not change but its kinetic energy in the initial state of B jumps to the new value that corresponds to the final state the molecule. Energy and momentum are transferred to the target through the interaction between the pair (A,a), while the remaining N-1 atoms only provide the restoring forces on a that determine its

momentum distribution within the polyatomic. When the collision energy E is much larger than the energy transferred ε, the part of $\hat{T}_a$ that acts on the internal coordinates of B is given by (Micha, 1979a)

$$\langle \vec{k}' | \hat{T}_a | \vec{k} \rangle = \tau_a(\vec{k}', \vec{k}) \exp(i\vec{\kappa} \cdot \hat{\vec{r}}_a), \tag{2.1.3a}$$

$$\tau_a(\vec{k}', \vec{k}) = \langle \vec{\kappa}_a | \hat{t}_a(E_a) | \vec{\kappa}_a \rangle . \tag{2.1.3b}$$

Here, τ_a is the transition amplitude for the collision of the atom pair (A,a) evaluated at their relative kinetic energy $E_a = m_a E/(M + m_a)$ and relative momentum $\hbar \vec{\kappa}_a = \hbar \vec{k} m_a/(M + m_a)$, and $\hat{t}_a$ is the two-body transition operator for the potential v_a; whenever $\varepsilon << E$, the τ_a are independent of the internal state of the polyatomic. As a result of the collision, atom a at position $\vec{r}_a$ absorbs an amount of momentum $\hbar \vec{\kappa} = \hbar(\vec{k} - \vec{k}')$.

Under these assumptions, the cross section of eq. (1.2.11) factors into quantities that depend on two different types of motion, as follows:

$$\frac{d^2\sigma}{d\Omega d\varepsilon} = (2\pi/\hbar)^4 M^2 (k'/k) \sum_{a,b} \tau_b^*(\vec{k}', \vec{k}) \tau_a(\vec{k}', \vec{k}) S^{(ba)}(\vec{\kappa}, \varepsilon), \tag{2.1.4a}$$

$$S^{(ba)}(\vec{\kappa}, \varepsilon) = \int_{-\infty}^{\infty} \frac{dt}{2\pi\hbar} \exp(-i\varepsilon t/\hbar) \langle\langle \exp[-i\vec{\kappa} \cdot \hat{\vec{r}}_b(0)] \exp[i\vec{\kappa} \cdot \hat{\vec{r}}_a(t)]_M \rangle\rangle . \tag{2.1.4b}$$

The first factor, $\tau_a(\vec{k}', \vec{k})$, involves only the relative motion of the pair (A,a). The second factor, $S^{(ba)}(\vec{\kappa}, \varepsilon)$, is the Fourier transform of the atom-pair time-correlation function (Van Hove, 1954) and depends only on the internal dynamics of the isolated target.

The correlation function for a pair of different atoms ($a \neq b$) contains phases that depend on the initial values of the internal dynamical variables of the target. Experimental measurements usually correspond

to initial averages over random phases so that the terms of eq. (2.1.4b) that have a≠b average to zero. In these cases, the cross section is given by

$$\frac{d^2\sigma}{d\Omega d\varepsilon} = \sum_a \sigma_a(\vec{k}',\vec{k})\ S^{(aa)}\ (\vec{\kappa},\varepsilon), \qquad (2.1.5a)$$

$$\sigma_a(\vec{k}',\vec{k}) = (2\pi/\hbar)^4\ M^2\ (k'/k)\,|\tau_a\ (\vec{k}',\vec{k})|^2, \qquad (2.1.5b)$$

where σ_a is an effective two-body cross section for the (A,a)-pair collision. Hence, the contribution of atom a to the overall cross section may be interpreted as the product of the probability that a will deflect the projectile from $\vec{k}$ to $\vec{k}'$, given by σ_a, multiplied by the probability that the molecule will absorb energy and momentum through this atom, given by $S^{(aa)}$. The self-correlation function $S^{(aa)}$ $(\vec{\kappa},\varepsilon)$ completely describes the response of the target atom a to the transfer of momentum $\hbar\vec{\kappa}$ and energy ε in the impulsive collision, regardless of the nature of the projectile atom.

The two-body cross-sections σ_a are, in principle, off-energy-shell quantities that must be obtained from the τ_a. These can be evaluated using any of several well-known techniques which need not be repeated here (see, for example, Brumer and Shapiro, 1975, Beard, 1979 and Kuruoglu and Micha, 1980). However, for the experimental conditions of quasielastic scattering, $|\vec{k}| \approx |\vec{k}'|$, so the σ_a can be obtained from standard two-body elastic cross sections.

Due to the factorization of internal from relation motion just described, from here on we need to consider only the internal dynamics of the target molecule. In order to focus our attention on the vibrational dynamics, it will prove convenient to decouple rotational and vibrational motions, as follows.

2. Vibrational and Rotational Correlations

Working in the center of mass of the isolated polyatomic, for each atom a of B we introduce its equilibrium position $\vec{d}_a$ and its displacement from equilibrium $\vec{u}_a$, so that $\vec{r}_a = \vec{d}_a + \vec{u}_a$. The conditions of zero total linear and angular momenta lead to the constraints (Wilson et al., 1955, Chap. 11)

$$\sum_a m_a \vec{r}_a = \vec{0}, \tag{2.2.1a}$$

$$\sum_a m_a \vec{u}_a \times \vec{d}_a = \vec{0}, \tag{2.2.1b}$$

which introduces N_{tr}=5 or 6 relationships among the vibrational displacements for linear and nonlinear molecules, respectively. This leaves $N_V = 3N-N_{tr}$ free vibrational coordinates in the body-fixed (BF) reference frame. The atom-pair correlation function (APCF) can now be written as

$$F^{(aa)}(\vec{\kappa},t) = \langle\langle \exp\{-i\vec{\kappa}\cdot[\hat{\vec{d}}_a(0) + \hat{\vec{u}}_a(0)]\} \exp\{i\vec{\kappa}\cdot[\hat{\vec{d}}_a(t)_R + \hat{\vec{u}}_a(t)_M]\}\rangle\rangle_{VR}. \tag{2.2.2}$$

For most polyatomics (except those that contain several hydrogen atoms), rotational motions are much slower than vibrational ones, indicating that the vibrational and the rotational correlations should be studied separately from one another (Micha, 1979b). This can be done by writing the internal Hamiltonian as $\hat{H}_M = \hat{H}_V + \hat{H}_R$ and requiring that the vibrational ($\hat{H}_V$) and rotational ($\hat{H}_R$) Hamiltonians satisfy $[\hat{H}_V, \hat{H}_R] = \hat{0}$. This means that $[\hat{H}_V, \hat{\vec{u}}_a] \neq \hat{0}$ because the $\vec{u}_a$ depend on the orientation of the molecule with respect to the

spaced-fixed (SF) coordinate system. These commutation relations cause the APCF to factor as follows,

$$F^{(aa)}(\vec{\kappa},t) = \langle\langle \exp[-i\vec{\kappa}\cdot\hat{\vec{d}}_a(0)]\ \hat{F}_V^{(aa)}(\vec{\kappa},t)\exp[i\vec{\kappa}\cdot\hat{\vec{d}}_a(t)_R]\rangle\rangle_R, \quad (2.2.3a)$$

$$\hat{F}^{(aa)}(\vec{\kappa},t) = \langle\langle \exp[-i\vec{\kappa}\cdot\hat{\vec{u}}_a(0)]\exp[-i\vec{\kappa}\cdot\hat{\vec{u}}_a(t)_M]\rangle\rangle_V. \quad (2.2.3b)$$

The vibrational correlation of $\hat{F}_V^{(aa)}$ can now be calculated in the BF frame, in which case it depends on the set of Euler angles $\Gamma = \{\alpha, \beta, \gamma\}$ that determine the orientation of this frame with respect to the SF one. These angles vary in time in accordance with the rotational Hamiltonian of the polyatomic. However, when this motion is much slower than the vibrational one, we need only consider the vibrational correlation for fixed orientation of the molecule. Hence, within the vibrational APCF of eq. (2.2.3b) we may approximate $\hat{\Gamma}(t)_R \approx \hat{\Gamma}(0)$, so that $\hat{\vec{u}}_a(t)_M \approx \hat{\vec{u}}_a(t)_V$. Evaluating the time derivatives of eq. (2.2.3b), one can easily show that this is equivalent to neglecting the rotational energy transferred through the torques that act on the vibrational displacements; this is justified whenever $|\vec{u}_a| << |\vec{d}_a|$, as is the case for vibrational excitations well below the dissociation thresholds.

The effects of anharmonic intramolecular forces are now entirely contained in the vibrational APCF of eq. (2.2.3b). For harmonic force-fields, this function may be readily evaluated by obtaining the $\hat{\vec{u}}_a(t)_V$ from second quantization methods (Micha, 1979b). In contrast, anharmonic forces introduce two main difficulties into the evaluation of the APCF. Firstly, the time-evolution of anharmonic motions

usually cannot be solved in a closed form. However, the evolution of the operators $\hat{\vec{u}}_a$ is of central importance, because they determine how energy is absorbed by and distributed within the polyatomic. Therefore, we must develop approximations to the vibrational dynamics that contain the features of the evolution of the $\hat{\vec{u}}_a$ which are most important to the collisions of interest; this is the subject of Sec. 4. The second difficulty resides in the calculation of quantal and statistical averages of the complicated exponential operators; however, these averages may be systematically approximated in the following way.

3. Cumulant Expansion of the Vibrational Correlation

In order to abbreviate the notation, let x_t be the component of $\vec{u}_a(t)_V$ in the direction of the momentum transfer $\vec{\kappa}$, so that $\vec{\kappa} \cdot \vec{u}_a(t) = \kappa x_t$, and omit the subscript V from the vibrational time dependence and from the average over initial states. The evaluation of $\langle\langle \exp(-i\kappa\hat{x}_0)\exp(i\kappa\hat{x}_t)\rangle\rangle$ is complicated by the fact that, in general,

$$\exp(-i\kappa\hat{x}_0)\exp(i\kappa\hat{x}_t) \neq \exp[-i\kappa(\hat{x}_0-\hat{x}_t)], \tag{2.3.1}$$

because $[\hat{\vec{u}}_a, \hat{H}_V] \neq \hat{0}$. We introduce the superoperator $\mathcal{O}$ which, when acting on a product of powers of $\hat{x}_0$ and $\hat{x}_t$, orders all the powers of $\hat{x}_0$ to the left of all the powers of $\hat{x}_t$, i. e. $\mathcal{O}\hat{x}_t\hat{x}_0 = \hat{x}_0\hat{x}_t$. The APCF may now be written as

$$F_V^{(aa)}(\vec{\kappa},t) = \langle\langle \mathcal{O}\exp[-i\kappa(\hat{x}_0-\hat{x}_t)]\rangle\rangle, \tag{2.3.2}$$

where the average of the ordered exponential operator is defined in terms of the moment-averages of the ordered exponent, as follows:

$$<<\mathcal{O}\exp[-i\kappa(\hat{x}_0-\hat{x}_t)]>> = \sum_{n=0}^{\infty}(-i\kappa)^n<<\mathcal{O}(\hat{x}_0-\hat{x}_t)^n>>/n!. \qquad (2.3.3)$$

From studies of the scattering of cold neutrons from crystals (Marshall and Lovesey, 1971), it is well known that the terms of eq. (2.3.3) which contain the product $\hat{x}_0^{\ell}\hat{x}_t^m$, with $\ell + m - 1 = n$, describe the simultaneous n-tuple excitation of the vibrational states of the target. In these cases, only single excitations are usually observed so the APCF is approximated by the second moment. However, in atom-polyatomic collisions, multiple excitations are readily observed in the experiments mentioned in the Introduction. Hence, it will prove more convenient to express the APCF in terms of the cumulant averages of the exponent, $<<(\hat{x}_0-\hat{x}_t)^n>>_C$, as follows

$$F_V^{(aa)}(\vec{\kappa},t) = \exp\sum_{n=1}^{\infty}(-i\kappa)^n<<(\hat{x}_0-\hat{x}_t)^n>>_C/n!. \qquad (2.3.4)$$

Comparing the coefficients of powers of $(-i\kappa)$ in eqs. (2.3.3,4), as done in Chap. I, Sec. 4, shows that the cumulants are related to the moment averages by

$$<<(\hat{x}_0-\hat{x}_t)^n>>_C = <<\mathcal{O}(\hat{x}_0-\hat{x}_t)^n>> - \sum_{j=1}^{n-1}<<\mathcal{O}(\hat{x}_0-\hat{x}_t)^{n-j}>><<(\hat{x}_0-\hat{x}_t)^j>>_C. \qquad (2.3.5)$$

Due to the invariance of the trace of a product of operators with respect to a cyclic permutation of their order, $<<\hat{x}_0^n>>=<<\hat{x}_t^n>>$, so the first few cumulants are

$$\langle\langle \hat{x}_0 - \hat{x}_t \rangle\rangle_C = 0, \tag{2.3.6a}$$

$$\langle\langle (\hat{x}_0 - \hat{x}_t)^2 \rangle\rangle_C = 2(\langle\langle \hat{x}_0^2 \rangle\rangle - \langle\langle \hat{x}_0 \hat{x}_t \rangle\rangle), \tag{2.3.6b}$$

$$\langle\langle (\hat{x}_0 - \hat{x}_t)^3 \rangle\rangle_C = 3(\langle\langle \hat{x}_0 \hat{x}_t^2 \rangle\rangle - \langle\langle \hat{x}_0^2 \hat{x}_t \rangle\rangle), \tag{2.3.6c}$$

$$\langle\langle (\hat{x}_0 - \hat{x}_t)^4 \rangle\rangle_C = \langle\langle \mathcal{O}(\hat{x}_0 \hat{x}_t)^4 \rangle\rangle - \langle\langle \mathcal{O}(\hat{x}_0 - \hat{x}_t)^2 \rangle\rangle^2. \tag{2.3.6d}$$

Equations (2.3.4,5) express the APCF in terms of the simpler displacement-displacement correlation functions (DDCF) of the type $\langle\langle \hat{x}_0^{\ell} \hat{x}_t^m \rangle\rangle$, with ℓ and m integers.

By means of a theorem due to Bloch (Messiah, 1961, Chap. 12), one can readily show that, for harmonic motions, all the cumulants of order higher than two are identically zero. Therefore, these cumulants are explicitly proportional to the strength of the anharmonic forces. However, in the usual experimental distributions of initial states, only the lowest vibrational states are significantly populated. In these cases, the displacements are small and vibrational motions are approximately harmonic, so that we may write

$$F_V^{(aa)}(\vec{\kappa},t) \approx \exp\{-\langle\langle [\vec{\kappa}\cdot\hat{\vec{u}}_a(0)]^2 \rangle\rangle + \langle\langle [\vec{\kappa}\cdot\hat{\vec{u}}_a(0)][\vec{\kappa}\cdot\hat{\vec{u}}_a(t)] \rangle\rangle\}. \tag{2.3.7}$$

If necessary for highly excited targets, this approximation may be systematically improved by including the higher order cumulants indicated in eq. (2.3.4). We note that the above equation still contains anharmonic forces to infinite order, within the time dependence of the $\vec{u}_a$ and within the average over initial states. Furthermore, eq. (2.3.7) includes multiple excitations, as can be seen from the power-series expansion of the exponential function.

We must now stress a very important point of the present development. The cumulant series of the APCF corresponds to an expansion of the operator $O\exp[-i\kappa(\hat{x}_0-\hat{x}_t)]$ in terms of its exponent; this is not equivalent to expanding the vibrational time-evolution operator $\exp(iL_V t/\hbar)$ in powers of time. Therefore, eq. (2.3.7) does not correspond to a short-time approximation to the vibrational motions. In this case, a short-time approximation would not be valid because vibrational periods are comparable to collision times; this is further confirmed by the rich vibrational structure observed in the experiments, which cannot be described by the Gaussian distributions characteristic of slow internal motions.

Before proceeding to the evaluation of the DDCF, the vibrational Hamiltonian must be specified. The potential is usually given in terms of the internal coordinates of the molecule s_i, i=1 to N_V (Wilson et al., 1955, Chap. 8), which are related to the cartesian displacements $(\vec{u}_a)_\xi$, ξ=x,y,z,by the linear transformation

$$(\vec{u}_a)_\xi = \sum_i c_{a\xi i}(\Gamma)s_i. \tag{2.3.8}$$

Here, the coefficients $c_{a\xi i}$ depend on the orientation of the BF frame with respect to the SF one. Using eq. (2.3.8), the kinetic energy of vibration can be expressed in terms of the internal coordinates, as follows:

$$K_V = \frac{1}{2}\sum_{i,j}\frac{\partial s}{\partial t}_i\ m_{ij}\frac{\partial s}{\partial t}_j\ , \tag{2.3.9a}$$

$$m_{ij} = \sum_a\sum_\xi m_a c_{a\xi i}c_{a\xi j}. \tag{2.3.9b}$$

We take the vibrational potential $V_V(\vec{s})$ to be a general function of the s_i which satisfies the conventions $V_V(\vec{0}) = 0$ and $(\partial V_V/\partial \vec{s})|_{\vec{0}} = \vec{0}$ Wilson et al., 1955, Chap. 2). In order to single out the effects of anharmonicity, we separate V_V into a harmonic part V_h and an anharmonic one V_{anh}, by writing

$$V_V = V_h + V_{anh}, \tag{2.3.10a}$$

$$V_h = \sum_{i,j} s_i k_{ij} s_j/2, \tag{2.3.10b}$$

$$k_{ij} = \frac{\partial^2 V}{\partial s_i \partial s_j}\Big|_{\vec{s}=\vec{0}}. \tag{2.3.10c}$$

Using eq. (2.3.8) we could express $\langle\langle[\vec{\kappa}\cdot\hat{\vec{u}}_a(0)][\vec{\kappa}\cdot\hat{\vec{u}}_a(t)]\rangle\rangle$ in terms of the correlation functions of the internal coordinates and then proceed to evaluate the latter. However, in order to facilitate a comparison of the results of this study with those of harmonic vibrations, it will prove convenient to work with the set of coordinates that diagonalize the harmonic part of the Hamiltonian. These coordinates, denoted by Q_j, j=1 to N_V, are defined by the orthogonal transformation (Marion 1971, Chap. 13)

$$s_i = \sum_j a_{ij} Q_j, \tag{2.3.11}$$

where the coefficients a_{ij} satisfy the set of linear equations

$$\sum_i (k_{\ell i} - \omega_j^2 m_{\ell i}) a_{ij} = 0, \tag{2.3.12}$$

with the normalization condition

$$\sum_{i,\ell} a_{ij}\, m_{i\ell}\, a_{\ell j} = 1, \tag{2.3.13}$$

and with the frequencies ω_j given by the roots of the characteristic equation

$$\det\{k_{i\ell} - \omega_j^2 \, m_{i\ell}\} = 0. \tag{2.3.14}$$

Substituting eq. (2.3.11) into eqs. (2.3.9,10) yields for the vibrational Hamiltonian

$$\hat{H}_V = \hat{H}_h + \hat{V}_{anh}(\vec{Q}), \tag{2.3.15a}$$

$$\hat{H}_h = \sum_i (\hat{P}_i^2 + \omega_i^2 \, \hat{Q}_i^2)/2, \tag{2.3.15b}$$

where $\hat{P}_i = -i\hbar\partial/\partial Q_i$ is the canonical momentum conjugate to the coordinate Q_i. Combining the transformations defined in eqs. (2.3.8,11) we write

$$\vec{u}_a = \sum_i \vec{C}_{ai}(\Gamma) Q_i, \tag{2.3.16a}$$

$$(\vec{C}_{ai})_\xi = \sum_\ell c_{a\xi\ell}(\Gamma) a_{\ell i}; \tag{2.3.16b}$$

hence, the APCF of eq. (2.3.7) becomes

$$F_V^{(aa)}(\vec{\kappa},t) = \exp\{\sum_{i,j} (\vec{\kappa}\cdot\vec{C}_{aj})(\vec{\kappa}\cdot\vec{C}_{ai})[-\langle\langle\hat{Q}_j(0)\hat{Q}_i(0)\rangle\rangle + \langle\langle\hat{Q}_j(0)\hat{Q}_i(t)\rangle\rangle]\}. \tag{2.3.17}$$

The evaluation of the displacement-displacement correlation functions $\langle\langle\hat{Q}_j(0)\hat{Q}_i(t)\rangle\rangle$ is the subject of the next section. We emphasize, however, that the methods presented below are applicable to the evaluation of correlation functions of any vibrational displacements that are related to the $\vec{u}_a$ by a linear transformation. The

present choice of the Q_i is based only on the desire to compare the results obtained from anharmonic force-fields with those of harmonic ones. From a practical point of view, the coordinates that diagonalize the harmonic part of the Hamiltonian are useful when anharmonic couplings between Q_i and Q_j with $i \neq j$ are small, and when breakup channels need not be considered. If the intercoordinate couplings are large, or if one is interested in dissociative processes, a description in terms of the correlation of the internal coordinates s_i is more appropriate. Furthermore, the following procedure may be readily extended to the evaluation of correlation functions of the type $\langle\langle \hat{x}_0^{\ell} \hat{x}_t^{m} \rangle\rangle$ with $\ell,m>1$.

4. Evaluation of the Displacement-Displacement Correlation Function

Heisenberg's equation of motion for the displacement Q_i,

$$\frac{\partial}{\partial t} \hat{Q}_i(t) = \frac{i}{\hbar} [\hat{H}_V , \hat{Q}_i(t)], \qquad (2.4.1)$$

leads to a second order inhomogeneous differential equation that describes the time evolution of the displacement-displacement correlation function (DDCF) $\langle\langle \hat{Q}_j(t') \hat{Q}_i(t) \rangle\rangle$ (in this section we continue to omit the subscript V from the vibrational time-dependence and from the average over initial states). In order to solve this equation, one would need to specify two boundary conditions (for example, the value of the correlation function and of its time derivative at t=t'), which require knowledge of averages of operators over the initial states. For anharmonic Hamiltonians, the calculation of these averages requires considerable computational effort; hence, we will obtain the DDCF from the correspcnding double-time Green functions, which already incorporate boundary conditions.

For any operators $\hat{A}$ and $\hat{B}$, the double-time retarded (+) and advanced (-) Green functions are defined by (Zubarev, 1960)

$$<<\hat{A}(t);\hat{B}(t')>>^{(\pm)} = \mp i\Theta[\pm(t-t')]<<[\hat{A}(t),\hat{B}(t')]>>, \qquad (2.4.2)$$

where Θ is the Heavyside unit step-function. Differentiating eq. (2.4.2) with respect to time using eq. (2.2.1), and evaluating the necessary commutators, yields the equation of motion for the displacement-displacement Green function (DDGF). This is

$$(\partial^2/\partial t^2 + \omega_i^2)<<\hat{Q}_i(t);\hat{Q}_j(t')>>^{(\pm)} - <<\hat{f}_i(t);\hat{Q}_j(t')>>^{(\pm)} =$$
$$= -\hbar\, \delta_{ij}\, \delta(t-t'), \qquad (2.4.3)$$

where $f_i = -\partial V_{anh}/\partial Q_i$ is the anharmonic force that acts on the coordinate Q_i. Following the same procedure, one can write an equation of motion for the Green function $<<\hat{f}_i(t);\hat{Q}_j(t')>>^{(\pm)}$, which in turn involves Green functions of higher derivatives of the anharmonic potential. One thus develops an infinite hierarchy of coupled differential equations which cannot be solved unless it is closed by a decoupling approximation.

In studies of anharmonic vibrations of crystals, several decoupling schemes have been proposed (for examples, see Kascheev and Krivoglaz, 1961, Thompson, 1963, Maradudin and Ambegaokar, 1964, Pathak, 1965). These are based on polynomial-type anharmonicities, so that the third term on the left of eq. (2.3.3) is a sum of higher order DDGF of the type $<<\hat{Q}_i(t)\hat{Q}_\ell(t)\hat{Q}_m(t)\ .\ .\ .;\hat{Q}_j(t')>>^{(\pm)}$. One then develops the hierarchy of equations of motion for these functions,

which in turn involve DDGF of even higher order. At some level, the hierarchy is decoupled by either neglecting the high-order DDGF, or approximating them by products of time-independent averages multiplied by DDGF of lower order. For molecular vibrations, these procedures have the following disadvantages: 1) many anharmonic potentials of interest (eg. Morse-type) cannot be expressed as a finite-degree polynomial in the displacements, 2) even for polynomial anharmonicities, the factorization of the high-order Green functions is not uniquely defined, so that different factorization prescriptions lead to different results, 3) on the other hand, the neglect of higher-order DDGF introduces dynamical approximations that are not well understood. However, we can develop an alternative decoupling procedure that does not suffer from these drawbacks, as follows.

As discussed in the previous section, in the usual experimental distributions, the vibrational displacements are small. In these cases, we may approximate their dynamical correlation with an effective harmonic one, by means of the linearization

$$\langle\langle \hat{f}_i(t);\hat{Q}_j(t')\rangle\rangle^{(\pm)} \approx \sum_{\ell} b_{i\ell}\langle\langle \hat{Q}_\ell(t);\hat{Q}_j(t')\rangle\rangle^{(\pm)}; \qquad (2.4.4)$$

hence, all the dynamical effects of the anharmonic forces are contained in the decoupling parameters $b_{i\ell}$. Further on we will fix the $b_{i\ell}$ to reproduce the dynamical features of the exact DDCF during the brief collision times characteristic of impulsive energy transfer. On the other hand, when the population of excited initial states is large, eq. (2.4.4) may be generalized to

$$<<\hat{f}_i(t);\hat{Q}_j(t')>>^{(\pm)} \simeq \sum_{\ell} b^{(2)}_{i\ell} <<\hat{Q}_\ell(t);\hat{Q}_j(t')>>^{(\pm)} +$$

$$+ \sum_{\ell m} b^{(3)}_{i\ell m} <<\hat{Q}_\ell(t)\hat{Q}_m(t);\hat{Q}_j(t')>>^{(\pm)} +$$

$$+ \sum_{\ell mn} b^{(4)}_{i\ell mn} <<\hat{Q}_\ell(t)\hat{Q}_m(t)\hat{Q}_n(t);\hat{Q}_j(t')>>^{(\pm)} + \ldots , \tag{2.4.5}$$

which corresponds to approximating the anharmonic correlation by means of effective harmonic, cubic, quartic, and so on, correlations. The decoupling parameters $b^{(n)}_{i\ell m\ldots}$ may then be fixed to reproduce the exact values of the dynamical properties of the DDCF that are most relevant to the collisions of interest.

In order to maintain the formalism at the clearest level possible, from here on we consider the case of zero anharmonic couplings between Q_i and Q_j for $i \neq j$, so that $b_{ij}=\delta_{ij}b_i$. We discuss the effects of nonzero intercoordinate couplings, at the end of this section. Introducing the Fourier transform of the DDGF, defined by

$$<<\hat{Q}_i(t);\hat{Q}_j(t')>>^{(\pm)} = \int_{-\infty}^{\infty} d\omega\, e^{-i\omega(t-t')}\, G^{(\pm)}_{ij}(\omega), \tag{2.4.6}$$

the linearized equation of motion is readily solved for $G^{(\pm)}_{ij}(\omega)$, giving

$$G^{(\pm)}_{ij}(\omega) = \hbar\delta_{ij}/[2\pi(\omega^2 - \bar{\omega}_i^2)], \tag{2.4.7}$$

where $\bar{\omega}_i=(\omega_i^2 - b_i)^{\frac{1}{2}}$ is the effective vibrational frequency of the coordinate Q_i. For a Boltzmann distribution of initial states, the Fourier transform $J_{ij}(\omega)$ of $<<\hat{Q}_j(t')\hat{Q}_i(t)>>$, defined by

$$\langle\langle \hat{Q}_j(t')\hat{Q}_i(t)\rangle\rangle = \int_{-\infty}^{\infty} d\omega\, e^{-i\omega(t-t')}\, J_{ij}(\omega), \qquad (2.4.8)$$

may be obtained from $G_{ij}^{(\pm)}(\omega)$ by means of the relation (Zubarev, 1960)

$$J_{ij}(\omega) = \frac{i\, e^{-\alpha(\omega)}}{2\sinh\alpha(\omega)} \lim_{\eta\to 0^+} [G_{ij}^{(+)}(\omega + i\eta) - G_{ij}^{(-)}(\omega - i\eta)]. \qquad (2.4.9)$$

Here, $\alpha(\omega) = \hbar\omega/(2k_B T_V)$, k_B is Boltzmann's constant and T_V the temperature of the distribution. Substituting eq. (2.4.7) into (2.4.9) and using the expression

$$\lim_{\eta\to 0^+} (y \pm i\eta)^{-1} = \mathcal{P} y^{-1} \mp i\pi\delta(y), \qquad (2.4.10)$$

where $\mathcal{P}$ denotes the principal value, we find that the spectral function $J_{ij}(\omega)$ is given by

$$J_{ij}(\omega) = \hbar\delta_{ij}[e^{-\bar{\alpha}_i}\delta(\omega-\bar{\omega}_i) + e^{\bar{\alpha}_i}\delta(\omega+\bar{\omega}_i)]/(4\bar{\omega}_i\sinh\bar{\alpha}_i), \qquad (2.4.11)$$

in which $\bar{\alpha}_i = \hbar\bar{\omega}_i/(2k_B T_V)$. Finally, evaluating the Fourier transform indicated in eq. (2.4.8), we arrive at the following expression for the DDCF,

$$\langle\langle \hat{Q}_j(0)\hat{Q}_i(t)\rangle\rangle = \hbar\delta_{ij}[\exp(-\bar{\alpha}_i - i\bar{\omega}_i t) + \exp(\bar{\alpha}_i + i\bar{\omega}_i t)]/(4\bar{\omega}_i\sinh\bar{\alpha}_i). \qquad (2.4.12)$$

The decoupling coefficients may now be fixed to reproduce the dynamical properties of the exact DDCF that are most relevant to the collisions of interest. In the present case, impulsive energy transfer occurs during a brief period of time centered about t=0. Hence, we choose the b_i, or equivalently the $\bar{\omega}_i$, to yield the exact values

of the first few time-derivatives of the DDCF at the instant of collision. Differentiating eq. (2.4.8) with respect to time. shows that the b_i thus chosen will conserve the first few frequency-moments of the spectral function. From eq. (2.4.1) we see that the exact derivatives are given by

$$\frac{\partial^n}{\partial t^n} \langle\langle \hat{Q}_j(0)\hat{Q}_i(t)\rangle\rangle \Big|_{t=0} = (i/\hbar)^n \langle\langle \hat{Q}_j([\hat{H}_V,)^n \hat{Q}_i]\rangle\rangle. \tag{2.4.13}$$

Evaluation of the necessary commutators yields an expression for the first derivative that, at t=0, is independent of the dynamics of the anharmonic forces; this is

$$\frac{\partial}{\partial t} \langle\langle \hat{Q}_j(0)\hat{Q}_i(t)\rangle\rangle \Big|_{t=0} = i\hbar\delta_{ij}/2, \tag{2.4.14}$$

which coincides with the expression obtained by differentiating the approximate DDCF of eq. (2.4.12). However, the second derivative is exactly given by

$$\frac{\partial^2}{\partial t^2} \langle\langle \hat{Q}_j(0)\hat{Q}_i(t)\rangle\rangle \Big|_{t=0} = \delta_{ij}(\langle\langle \hat{Q}_j \hat{f}_i\rangle\rangle - \omega_i^2 \langle\langle \hat{Q}_j \hat{Q}_i\rangle\rangle), \tag{2.4.15}$$

which depends explicitly on the anharmonic forces. On the other hand, a second differentiation of eq. (2.4.12) yields

$$\frac{\partial^2}{\partial t^2} \langle\langle \hat{Q}_j(0)\hat{Q}_i(t)\rangle\rangle \Big|_{t=0} = -\delta_{ij} \frac{\hbar \bar{\omega}_i}{2} \coth \bar{\alpha}_i. \tag{2.4.16}$$

Hence, equating the right hand sides of eqs. (2.4.15,16) defines the effective frequencies $\bar{\omega}_i$ by the relation

$$\hbar\bar{\omega}_i \coth\bar{\alpha}_i = 2(\omega_i^2 \langle\langle \hat{Q}_i^2 \rangle\rangle - \langle\langle \hat{Q}_i \hat{f}_i \rangle\rangle). \tag{2.4.17}$$

Substituting into eq. (2.4.12) the $\bar{\omega}_i$ thus obtained, we find that the approximate DDCF contains the dynamical effects of the anharmonic forces to infinite order. Furthermore, for harmonic motions $\langle\langle \hat{Q}_i^2 \rangle\rangle = (\hbar\omega_i/4)\coth\alpha_i$ and $f_i = 0$, so the present development includes harmonic vibrations as a specific case.

Replacing eq. (2.4.12) into eq. (2.3.13) and rearranging terms, we obtain the following expression for the APCF.

$$F_V^{(aa)}(\vec{\kappa},t) = \prod_i \exp\{-\hbar(\vec{\kappa}\cdot\vec{C}_{ai})^2 [\cosh\bar{\alpha}_i + (e^{-\bar{\alpha}_i - i\bar{\omega}_i t} + e^{\bar{\alpha}_i + i\bar{\omega}_i t})/2]/(2\bar{\omega}_i \sinh\bar{\alpha}_i)\}. \tag{2.4.18}$$

Using the generating function of the modified Bessel functions of the first kind (I_n) (Abramowitz and Stegun, 1972),

$$\exp[x(y + 1/y)/2] = \sum_{n=-\infty}^{\infty} y^n I_n(x), \tag{2.4.19}$$

we finally arrive at

$$F_V^{(aa)}(\vec{\kappa},t) = \sum_{\vec{n}} p_{\vec{n}}^{(aa)}(\kappa;\Gamma)\exp(-i\vec{n}\cdot\vec{\omega}_V t), \tag{2.4.20a}$$

$$p^{(aa)}_{\vec{n}}(\vec{\kappa};\Gamma) = \prod_i I_{n_i}(X_{ai})\exp(-n_i\bar{\alpha}_i - X_{ai}\cosh\bar{\alpha}_i), \qquad (2.4.20b)$$

$$X_{ai} = \hbar[\vec{\kappa}\cdot\vec{C}_{ai}(\Gamma)]^2/(2\bar{\omega}_i\sinh\bar{\alpha}_i), \qquad (2.4.20c)$$

in which we have introduced the abbreviations $\vec{n}=\{n_i\}$ and $\vec{\omega}_V=\{\bar{\omega}_i\}$. Comparing these last equations with the ones corresponding to harmonic vibrations (eq. (4.16) in Micha, 1979b), we find that the APCF for harmonic and anharmonic motions coincide in form; however, for anharmonic molecules, the normal frequencies ω_i must be replaced by the effective ones $\bar{\omega}_i$ obtained from eq. (2.4.17).

Nonzero intercoordinate anharmonic couplings cause mixing of the normal coordinates Q_i, which is reflected in the off diagonal parameters $b_{i\ell}$ of eq. (2.4.4). In this case, the linearized equations of motion for the DDGF lead to the following matrix equation for their Fourier transforms.

$$(\omega^2\,\underset{\sim}{1} - \underset{\sim}{\Omega}_V^2 + \underset{\sim}{b})\,\underset{\sim}{G}^{(\pm)}(\omega) = \hbar\,\underset{\sim}{1}/(2\pi), \qquad (2.4.21)$$

where $\underset{\sim}{G}^{(\pm)}(\omega) = \{G^{(\pm)}_{ij}(\omega)\}$, $\underset{\sim}{b}=\{b_{ij}\}$ and $\underset{\sim}{\Omega}_V = \{\delta_{ij}\omega_i\}$. Solving for $\underset{\sim}{G}^{(\pm)}(\omega)$, shows that the effective frequencies are given by the roots of the determinant of $(\omega^2\underset{\sim}{1}-\underset{\sim}{\Omega}_V^2+\underset{\sim}{b})$. Hence, choosing the b_{ij} to reproduce the exact second derivative of the DDCF at t=0 leads to a matrix equation for $\underset{\sim}{b}$ analogous to eq. (2.4.17). Based on the present development, the effects of molecular anharmonicity in hyperthermal collisions may be interpreted in the following way.

5. Effects of Molecular Anharmonicity in Hyperthermal Collisions

In analogy to eq. (2.1.4b), the Fourier transform of the vibrational APCF,

$$S_V^{(aa)}(\vec{\kappa};\Gamma) = \int_{-\infty}^{\infty} \frac{dt}{2\pi\hbar} \exp(-i\varepsilon t/\hbar)\, F_V^{(aa)}(\vec{\kappa},t) = \tag{2.5.1a}$$

$$= \sum_{\vec{n}} p_{\vec{n}}^{(aa)}(\vec{\kappa};\Gamma)\, \delta(\hbar\vec{n}\cdot\vec{\omega}_V + \varepsilon), \tag{2.5.1b}$$

corresponds to the probability that the molecule will absorb vibrational energy and momentum in a collision involving atom a, for the fixed orientation of the principal axes of the polyatomic indicated by Γ. This has the form of δ-function peaks, located at the vibrational energy transfer $\varepsilon_V = -\vec{n}\cdot\vec{\omega}_V$, where n_i is the change in quantum number (initial minus final) of the ith effective normal mode; the probability for the transition $\vec{n}$ is given by $p_{\vec{n}}^{(aa)}(\vec{\kappa};\Gamma)$. In practice, these peaks are broadened into Gaussian functions by the rotational correlation, as is shown in the following section. In light of this analysis, the effects of molecular anharmonicity in hyperthermal atom-polyatomic collisions may be summarized as follows.

1) Anharmonic forces cause a shift in the spectrum of the vibrational energy transfer, from the set of harmonic frequencies ω_i to the effective ones $\bar{\omega}_i$.

2) Equation (2.4.17) shows that this shift is related to the work done by the anharmonic forces on the vibrational displacements.

3) The change in the vibrational frequencies is accompanied by a corresponding change in the probabilities for vibrational excitation, as indicated in eqs. (2.4.20b,c).

4) In contrast to the harmonic case, the effective frequencies depend on the temperature of the distribution of initial states. This is due to the fact that the anharmonic forces affect all the states that are present in the distribution.

The magnitudes of the effects depend on the specific nature and strength of the intramolecular forces of the target and require the evaluation of the averages indicated in eq. (2.4.17). These may be calculated by standard numerical procedures, or by finite-temperature perturbation theory, when the temperature of the initial distribution is sufficiently low. The application of this development to specific targets will be presented in Chap. IV. We now proceed to consider the rotational correlation, in order to complete the evaluation of the APCF.

6. Short-Time Approximation to the Rotational Correlation

The rotational correlation of heavy molecules has been previously evaluated by means of a Taylor-series expansion of the logarithm of the APCF (Micha, 1979b). In this section, we present an alternative approach to the evaluation of rotational correlation, which is based on the cumulant expansion techniques developed in Chap. I. Although the two approaches are completely equivalent, we feel that the present one allows a more unified understanding of the role of correlation functions in the description of many-body collisions.

Substition of eqs. (2.4.20) into eq. (2.2.3) gives the following expression for the complete self-correlation function

$$F^{(aa)}(\vec{\kappa},t) = \sum_{\vec{n}} F^{(aa)}_{\vec{n}}(\vec{\kappa},t)\ \exp(-i\vec{n}\cdot\vec{\omega}_V\, t), \tag{2.6.1a}$$

$$F^{(aa)}_{\vec{n}}(\vec{\kappa},t) = \langle\langle p^{(aa)}_{\vec{n}}(\vec{\kappa};\hat{\Gamma}(0))\ \exp[-i\vec{\kappa}\cdot\hat{\vec{d}}_a(0)]\ \exp[i\vec{\kappa}\cdot\hat{\vec{d}}_a(t)_R]\rangle\rangle_R, \tag{2.6.1b}$$

where the time dependence of $F^{(aa)}_{\vec{n}}$ is due only to the rotational motion of the molecule. Following the procedure described in Chap. I, Sec. 3, we find that the time evolution of $\exp(-i\vec{\kappa}\cdot\hat{\vec{d}}_a)$ is given by

$$\exp[i\vec{\kappa}\cdot\hat{\vec{d}}_a(t)_R] = \exp(itL_R/\hbar)\ \exp[i\vec{\kappa}\cdot\hat{\vec{d}}_a(0)]. \tag{2.6.2}$$

Here, L_R is the Liouville superoperator for rotational motions, which is defined by its action on an arbitrary operator $\hat{A}$, as follows

$$L_R^n \hat{A} = ([\hat{H}_R,)^n\hat{A}]. \tag{2.6.3}$$

Equation (2.6.1b) can now be rewritten as

$$F^{(aa)}_{\vec{n}}(\vec{\kappa},t) = P^{(aa)}_{\vec{n}}(\kappa)\ \{\langle\langle p^{(aa)}_{\vec{n}}(\vec{\kappa};\hat{\Gamma}(0))\exp[-i\vec{\kappa}\cdot\hat{\vec{d}}_a(0)]\exp(itL_R/\hbar)\ \times$$

$$\times\ \exp[-i\vec{\kappa}\cdot\hat{\vec{d}}_a(0)]\rangle\rangle_R/\langle\langle p^{(aa)}_{\vec{n}}(\vec{\kappa};\hat{\Gamma}\ (0))\rangle\rangle_R\}, \tag{2.6.4a}$$

$$P^{(aa)}_{\vec{n}}(\kappa) \doteq \langle\langle \bar{p}^{(aa)}_{n}(\vec{\kappa};\hat{\Gamma})\rangle\rangle_R. \tag{2.6.4b}$$

Whenever the rotational motion of the molecule is much slower than its vibrational one, we perform a short-time approximation to the rotational correlation of each vibrational transition. As discussed in Chap. I, Secs. 4,5, this corresponds to expanding the second factor of eq. (2.6.4) in terms of the cumulant rotational averages of L_R and retaining only the first two cumulants, so that

$$F_{\vec{n}}^{(aa)}(\vec{\kappa},t) \simeq P_{\vec{n}}^{(aa)}(\kappa)\exp\left[it\langle\langle L_R\rangle\rangle_{CR}/\hbar - t^2\langle\langle L_R^2\rangle\rangle_{CR}/(2\hbar^2)\right]. \quad (2.6.5)$$

The lowest-order cumulants are determined from eq. (1.3.5) to be

$$\langle\langle L_R\rangle\rangle_{CR} = \langle\langle p_{\vec{n}}^{(aa)}(\vec{\kappa};\hat{\Gamma})\exp(-i\vec{\kappa}\cdot\hat{\vec{d}}_a)[\hat{H}_R,\exp(i\vec{\kappa}\cdot\hat{\vec{d}}_a)]\rangle\rangle_R/P_{\vec{n}}^{(aa)}(\kappa), \quad (2.6.6a)$$

$$\langle\langle L_R^2\rangle\rangle_{CR} = \langle\langle p_{\vec{n}}^{(aa)}(\vec{\kappa};\hat{\Gamma})\exp(-i\vec{\kappa}\cdot\hat{\vec{d}}_a)[\hat{H}_R,[\hat{H}_R,\exp(i\vec{\kappa}\cdot\hat{\vec{d}}_a)]]\rangle\rangle_R/P_{\vec{n}}^{(aa)}(\kappa) - $$

$$- \langle\langle L_R\rangle\rangle_{CR}^2. \quad (2.6.6b)$$

Replacing eq. (2.6.5) into eqs. (2.6.1) we obtain the following expression for the APCF,

$$F^{(aa)}(\vec{\kappa},t) = \sum_{\vec{n}} P_{\vec{n}}^{(aa)}(\kappa)\exp\left[i(\langle\langle L_R\rangle\rangle_{CR} - \hbar\vec{n}\cdot\vec{\omega}_V)t/\hbar - \langle\langle L_R^2\rangle\rangle_{CR}t^2/(2\hbar^2)\right]. \quad (2.6.7)$$

Finally, evaluating its Fourier transform, as indicated in eq. (2.1.4b), we arrive at

$$S^{(aa)}(\vec{\kappa},\varepsilon) = \frac{1}{4\sqrt{\pi}}\sum_{\vec{n}} P_{\vec{n}}^{(aa)}(\kappa)\exp\{-[(\langle\langle L_R\rangle\rangle_{CR} - \hbar\vec{n}\cdot\vec{\omega}_V - $$

$$- \varepsilon)/(2\langle\langle L_R^2\rangle\rangle_{CR}^{1/2})]^2\}/(2\langle\langle L_R^2\rangle\rangle_{CR}). \quad (2.6.8)$$

Examining this last equation we find that, for a given value of the momentum transfer $\vec{\kappa}$, each atom of the target contributes a group of

normalized Gaussian peaks to the differential cross section. Each peak corresponds to the vibrational excitation indicated by the set of changes in quantum numbers $\vec{n}$, and is centered at the vibrational energy transferred $\hbar\vec{n}\cdot\vec{\omega}_V$ plus the average rotational energy transferred to this vibrational transition $\langle\langle L_R \rangle\rangle_{CR}$; furthermore, each peak is rotationally broadened by an amount $2\langle\langle L_R^2 \rangle\rangle_{CR}^{\frac{1}{2}}$. Equations (2.6.6) show that the rotational energy transfer and the width contributed by each atom are functions of the momentum transfer (hence of collision energy and scattering angle) and depend on the vibrational transition indicated by $\vec{n}$. The probability that a collision involving atom a will excite the vibrational transition $\vec{n}$ is given by $P_{\vec{n}}^{(aa)}$, which is also a function of the momentum transfer.

However, if atom a is at the center of mass of the molecule, so that $\vec{d}_a=\vec{0}$, then instead of eqs. (2.6.7) and (2.6.8), we have

$$F^{(aa)}(\vec{\kappa},t) = \sum_{\vec{n}} P_{\vec{n}}^{(aa)}(\kappa) \exp(-i\vec{n}\cdot\vec{\omega}_V t), \tag{2.6.9a}$$

$$S^{(aa)}(\vec{\kappa},\varepsilon) = \sum_{\vec{n}} P_{\vec{n}}^{(aa)}(\kappa)\, \delta(\varepsilon+\hbar\vec{n}\cdot\vec{\omega}_V), \tag{2.6.9b}$$

which shows that such an atom does not absorb rotational energy but does contribute to the vibrational excitation.

As discussed in Sec. 1, the correlation functions given by eqs. (2.6.8,10) together with eqs. (2.4.20b,c) and (2.6.6) completely describe the response of the target to an impulsive collision, regardless of the nature of the projectile. The nature of the projectile atom determines the two-body cross sections of eq. (2.1.5), in accordance with the atom-pair potentials. Therefore, before

proceeding to the applications of the many-body theory, we must construct the multicenter representation of the intermolecular potential for the collision systems of interest; this is the subject of the following chapter.

CHAPTER III
MULTICENTER POTENTIAL ENERGY SURFACES

In this chapter we investigate the multicenter representation of the intermolecular potential energy surface (PES) for nonreactive atom-molecule systems. Our aim is to develop a parametrization of the PES which is appropriate for the study of hyperthermal molecular collisions. In the first section, we weigh the relative advantages of the single-center and multicenter representations. In the second section, we develop a parametrization for ion/linear molecule surfaces in terms of atom-pair potentials that are based on the known general properties of intermolecular forces. Next, we evaluate the atom-pair potentials that reproduce the quantum chemical PES of the system Li^+/CO. In the final section, we study the system Li^+/CO_2, for which no quantum chemical information is yet available. Using a simple model of short-range forces plus experimental information on the molecular properties of CO_2, we construct a model PES for this system. Both surfaces developed here will be used in subsequent atom-molecule scattering calculations.

1. Single-Center vs. Multicenter Expansion

The standard procedure used to describe the interaction between an atom A and a molecule B consists of assuming the Born-Oppenheimer separation of nuclear and electronic motions (Tully, 1976) and then calculating the lowest PES for a set of conformations, by means of more or less accurate quantum-chemical methods; for examples see

Staemmler,1975, Parker et al., 1976 and Thomas et al., 1978. Working in the body-fixed (BF) coordinate system determined by the principal axes of B, one thus obtains a table of the intermolecular potential V for several values of the relative position of A, denoted by $\vec{R}$, and of the positions of the constituent atoms of B, which we indicate with $\vec{r}^{B} = \{\vec{r}_a, a \in B\}$. In order to facilitate scattering calculations, one must usually construct a functional representation for the surface. The most common of these is the single-center expansion, in which the dependence on the orientation of $\vec{R}$ is described in terms of a set of basis functions of angles, centered at the center of mass of the molecule, as follows:

$$V(\vec{R},\vec{r}^{B}) = \sum_n V_n(R,\vec{r}^{B}) Y_n(\eta,\xi). \qquad (3.1.1)$$

Here, η,ξ are the polar and azimuthal angles of $\vec{R}$ in the BF system, respectively, and the Y_n are the elements of the basis set. The radial coefficients V_n are fitted to reproduce the values of the PES at the tabulated configurations.

For atom-molecule scattering in the thermal collision energy regime, such a single-center expansion has several advantages. Since low energy scattering is mediated by long-range forces (McDowell and Coleman, 1970) and these forces vary slowly with the orientation of $\vec{R}$, usually only the first few terms of eq. (3.1.1) need be included in scattering calculations. On the other hand, the PES can be represented to any arbitrary degree of accuracy by increasing the size of the angular basis set. Furthermore, if the radial dependence of the coefficients V_n is judiciously chosen, these can be related to molecular properties (electrostatic moments, polarizabilities, etc.)

of the isolated collision partners (Hirschfelder et al., 1967), this can be used to check the accuracy of the fitting procedure, or to supplement the quantum-chemical information when only a few points of the surface are available.

However, as the collision energy increases above a few hundredths of an electron volt, the single-center expansion, although accurate in principle, presents rather serious disadvantages. At hyperthermal energies and for small impact parameters, the projectile probes the inner region of the PES which is of a multicenter nature, so the single-center representation loses physical meaning. Furthermore, as the short-range intermolecular forces depend strongly on the orientation of $\vec{R}$, a very large number of terms are necessary for eq. (3.1.1) to converge. These drawbacks will be further clarified by the example presented in the next section.

Alternatively, the multicenter nature of the intermolecular forces can be better represented by expanding the potential about each atom of the target, as follows:

$$V(\vec{R},\vec{r}^{B}) = \sum_{a} v_a(\vec{R},\vec{r}_a), \qquad (3.1.2)$$

where the sum runs over the N atoms the polyatomic. Here, v_a corresponds to the interaction between the (A,a) atom-pair which depends on the electronic distribution of A and on that of atom a in the valence state of the target. Hence, v_a is a function of the orientation of $\vec{R}$ with respect to $\vec{r}_a$ and of the magnitude of $\vec{R}-\vec{r}_a$. In general, for small A-a separation, the atom-pair potentials are steeply repulsive due to the overlapping of the electronic clouds

of A and a; in the long-range region, the v_a fall off as inverse powers of the A-a distance due to the interactions of the charge distributions of A and a. For example, the PES corresponding to an atomic ion with charge q_A and a molecule could be modeled, most simply, by the sum of the pair potentials

$$v_a(\vec{R},\vec{r}_a) = A_a \exp(-B_a|\vec{R}-\vec{r}_a|) + q_A q_a/|\vec{R}-\vec{r}_a|, \qquad (3.1.3)$$

in which the fractional atomic charges q_a reproduce the experimental values of the N-lowest electrostatic multipole moments of B. The coefficients A_a and B_a (both positive) can be obtained by fitting to a previously calculated PES or from combination rules (Gaydaenko and Nikulin, 1970).

More, generally, eq. (3.1.2) is the leading term obtained by expanding the potential in contributions from two atom, three atom, and so on, atom-clusters as indicated below (Micha, 1979a)

$$V(\vec{R},\vec{r}^B) = \sum_a v_a^{(2)}(\vec{R},\vec{r}_a) + \sum_{a<b} v_{ab}^{(3)}(\vec{R},\vec{r}_a,\vec{r}_b) + \ldots, \qquad (3.1.4)$$

Recent attempts have been made at understanding the properties of large polyatomic systems in terms of contributions of the constituent atomic centers (Bader, 1980). We hope that, in the future, such studies would allow the determination of the atom-cluster potentials from first principles. However, for our present purposes, we will consider the atom-pair potentials to be functions of $\vec{R}$ and $\vec{r}_a$, with parameters that will be adjusted to reproduce a previously calculated PES and/or the known molecular properties of the separated collision partners. As we shall see in the following section, by judiciously choosing the form of the v_a, the contributions of the higher-order cluster potentials can be made negligibly small.

2. Atom-Pair Potentials for Ion/Linear Molecule Interactions

As with any other fitting procedure, the functional form of the v_a greatly influences the accuracy of the representation and the number of parameters required. In order to allow for a physically meaningful interpretation of the pair potentials and to reduce the number of parameters to a minimum, the v_a should be chosen in accordance with the known general properties of intermolecular forces (Hirschfelder et al., 1967, Margenau and Kestner, 1971). For the interaction between two closed-shell molecules, these properties may be summarized as follows.

When the relative distance R is much greater than the lengths over which the electronic clouds of each species are appreciable, the intermolecular potential can be written as a sum of the following three contributions:

1) the electrostatic interaction between the permanent multipole moments of the charge distributions of each molecule,

2) the induction contribution, due to the interaction between the permanent moments of one species and those induced in the other one, and

3) the dispersion or Van-der-Waals forces, which may be interpreted as arising from the interactions between the induced moments of each species. However, when at least one of the molecules has a net permanent charge, the magnitudes of the dispersion terms are much smaller than the electrostatic and induction ones, so that dispersion forces may be neglected.

In order to maintain the notation at the clearest level possible, from here on we take B to be a linear polyatomic at its equilibrium configuration ($\vec{r}^B = \vec{d}^B$). Hence, the long-range potential for an atomic ion A and B is given by the following single center expression,

$$V(\vec{R},\vec{r}^B) \underset{R\to\infty}{\sim} q_A q_B/R + q_A \mu_B(\cos\eta)/R^2 + q_A Q_B P_2(\cos\eta)/R^3 - \\ - q_A^2[\alpha_B/2 + \Delta_B P_2(\cos\eta)]/R^4 + \ldots \quad , \qquad (3.2.1)$$

in which we have explicitly indicated the first three leading terms of the electrostatic forces, the leading induction contribution (of order R^{-4}), and we have neglected the dispersion forces that are of order R^{-6} and smaller. Here, $P_2(x) = (3x^2 - 1)/2$ is the second order Legendre polynomial, q_A is the charge of the ion, while the molecular properties of B are the net charge q_B, the electrostatic dipole μ_B and quadrupole Q_B moments, and the isotropic $\alpha_B = (\alpha_{zz} + 2\alpha_{xx})/3$ and anisotropic $\Delta_B = (\alpha_{zz} - \alpha_{xx})/3$ polarizabilities; α_{zz} and α_{xx} are the components of the static dipole-polarizability tensor parallel and perpendicular to the molecular axis, respectively. Equation (3.2.1) follows from a perturbation-theoretical approach, in which the electrostatic interaction between the charge distributions of each species is expressed in terms of a multipole expansion (Margenau and Kestner, 1971, Chap. 2). Such an expansion is valid only when the distance between the centers of charge of each distribution is much larger than the range of the individual densities (Jackson, 1975, Chap. 4). Therefore, eq. (3.2.1) loses physical meaning whenever $\vec{R} \to \vec{r}_a$; this is reflected in the unphysical divergence for small R.

When the relative distance decreases, the overlap of the electronic clouds of each species causes the intermolecular forces to become steeply repulsive. Hence, the small R behavior of the potential depends very strongly on the details of the electronic distributions. However, when the molecular orbitals of each species are described in terms of Slater-type orbitals centered on each nucleus, the overlap will be an approximately exponential function of the A-a internuclear distance. Slater-type bases are most commonly used in quantum-chemical calculations for atoms and for linear molecules (Pople and Beveridge, 1970); in these cases, the short-range behaviour of the potential is of the form

$$V(\vec{R},\vec{r}^{B}) \underset{\vec{R} \to \vec{r}_a}{\sim} A_a \exp(-B_a |\vec{R}-\vec{r}_a|). \qquad (3.2.2)$$

Here A_a and B_a are positive coefficients that are independent of the magnitude of $\vec{R}$, but they may be functions of the orientation of $\vec{R}$ with respect to $\vec{r}_a$.

We thus find that the single-center representation of eq. (3.2.1) must be smoothly transformed into a multicenter one, as the relative distance decreases. The transformation must avoid the unphysical divergences of the multipole expansion and must accurately reproduce the intermediate region of the surface which includes the potential wells. One might attempt to carry out this transformation by multiplying the right-hand side of eq. (3.2.1) by a switching function that tends to one for large R, and to zero whenever $\vec{R} \to \vec{r}_a$. Unfortunately, the second requirement would force the switching function to have an extremely complicated dependence on the orientation

of $\vec{R}$. However, this difficulty may be readily avoided by extending the multicenter representation to large R, as follows.

Assuming that the molecular properties of B can be expressed in terms of the individual contributions of each atom, we expand the long-range region of the potential about the atomic centers and write

$$V(\vec{R},\vec{r}^{B}) = \sum_a v_a(\vec{R},\vec{r}_a), \tag{3.2.3a}$$

$$v_a(\vec{R},\vec{r}_a) = v_a^{(SR)}(\vec{R},\vec{r}_a) + f_a(\vec{R},\vec{r}_a)v_a^{(LR)}(\vec{R},\vec{r}_a), \tag{3.2.3b}$$

$$v_a^{(LR)}(\vec{R},\vec{r}_a) = C_{10a}/R_a + C_{21a}(\cos\eta_a)/R_a + C_{32a}P_2(\cos\eta_a)/R_a^3 + \\ + [C_{40a} + C_{42a}P_2(\cos\eta_a)]/R_a^4, \tag{3.2.3c}$$

where $\vec{R}_a = \vec{R}-\vec{r}_a$ is the position of the ion with respect to target atom a and $\eta_a = \arccos[\vec{R}_a\cdot\vec{r}_a/(R_a r_a)]$ is the angle between $\vec{R}_a$ and $\vec{r}_a$. The terms of $v_a^{(LR)}$ represent the interaction of the charge of A with the first three electrostatic moments and polarization of the electronic distribution about center **a**, respectively. In eq. (3.2.3b), $v_a^{(SR)}$ corresponds to the short-range repulsive forces and f_a is a switching function that eliminates the singularity of $v_a^{(LR)}$ at $\vec{R} = \vec{r}_a$. The detailed form of f_a is not crucial, provided it satisfies the following requirements: 1) f_a and its gradient with respect to $\vec{R}$ must be continuous, 2) $f_a \underset{\vec{R}\to\vec{r}_a}{\sim} 0$ and 3) $f_a \underset{\vec{R}\to\infty}{\sim} 1$. One such function is, for example,

$$f_a(\vec{R},\vec{r}_a) = \theta(R_a - c_a)\exp[-\gamma_a(R_a - c_a)^2], \tag{3.2.4}$$

where θ is the Heavyside unit step-function. Here, c_a is a radius

about atom a within which the long-range pair potential is zero, while γ_a determines how fast $v_a^{(LR)}$ is turned off as the A-a distance decreases. We may complete the representation by taking the repulsive potentials to be

$$v_a^{(SR)}(\vec{R},\vec{r}_a) = A_a \exp(-B_a R_a), \tag{3.2.5}$$

with A_a and B_a positive and independent of $\vec{R}$. If necessary for a specific system, the $v_a^{(SR)}$ may be rendered more flexible by letting A_a and B_a depend on η_a, or by expanding $v_a^{(SR)}$ is a basis-set of functions of the orientation of $\vec{R}_a$.

Expressing $|\vec{R}-\vec{r}_a|$ in a Taylor series in $\vec{r}_a$ about $\vec{R}$, we find that eqs. (3.2.3) and (3.2.1) coincide as $R \to \infty$, whenever the coefficients $C_{n\ell a}$ satisfy

$$q_A q_B = \sum_a C_{10a}, \tag{3.2.6a}$$

$$q_A \vec{\mu}_B = \sum_a (C_{10a}\vec{r}_a + C_{21a}\vec{r}_a/r_a), \tag{3.2.6b}$$

$$q_a Q_B = \sum_a (C_{10a} r_a^2 + 2C_{21a} r_a + C_{32a}), \tag{3.2.6c}$$

$$q_a^2 \alpha_B/2 = -\sum_a C_{40a}, \tag{3.2.6d}$$

$$q_a^2 \Delta_B = -\sum_a C_{42a}. \tag{3.2.6e}$$

If the $C_{n\ell a}$ are fit to a previously calculated PES, these equations provide us with an independent check of the fit, as the $C_{n\ell a}$ should yield the correct values of the molecular properties of B. On the other hand, if a quantum-chemical PES is not available, eqs. (3.2.6) together with experimental values of the molecular properties may be used to partly determine the atom-pair potentials.

In the multicenter representation defined by eqs. (3.2.3-5), the set of parameters that must be adjusted to reproduce the tabulated PES is $\{p_i\} = \{A_a, B_a, c_a, \gamma_a, C_{10a}, C_{21a}, C_{32a}, C_{40a}, C_{42a}$ for a=1 to N$\}$. Although at first sight this set seems rather large, the above analysis shows that this is the smallest possible set that is required by the physical nature of ion/linear molecule forces. Furthermore, the p_i generally depend on the internal configuration of the polyatomic, and hence on $\vec{r}^B$. However, for a specific molecule, some of the long-range parameters $C_{n\ell a}$ may be negligibly small. In particular, the electrostatic interaction between the charge of A and a permanent multipole moment of B may be represented, at large R, as the sum of the forces between the charge of A and the lower-order multipoles of the target atoms, as shown in eqs. (3.2.6a-c); this usually involves cancellations between the terms contributed by each center. As the A-a distance decreases, the atomic contributions become large, due to the $1/R_a^n$ dependence, and may not cancel to yield a correct description of the intermediate region; this indicates that such atomic multipoles should be made vanishingly small. We will encounter examples of this phenomenon in the following sections.

3. Multicenter Potential for the System Li^+/CO

We now develop the multicenter representation of the intermolecular potential for the Li^+/CO system. This is one of the few many-electron systems for which a detailed PES has been calculated quantum chemically, at the configuration-interaction level of accuracy (Thomas et al., 1978). This surface has been tabulated for a wide

range of values of $\vec{R}$, at the equilibrium configuration of CO ($|\vec{r}_a - \vec{r}_b| = 1.224$ Å); this will allow us to judge the applicability of the multicenter expansion for small and large R. Unfortunately, only a few points have been calculated for nonequilibrium configurations of the molecule; therefore, throughout this section, we fix the target atoms at their equilibrium positions and take the potential parameters to be independent of $\vec{r}^B$.

Due to the nonlinear dependence of the potential on several of the parameters, the usual least-squares optimization (Doren and McCracken, 1972, Chap. 7) would lead to a system of sixteen coupled transcendental equations in the p_i whose solution represents the best values of the parameters. However, such a system can only be solved by iterative methods (Ostrowski, 1966, Sec. 25) whose convergence is impracticably slow due to the large dimensionality of the problem. In order to avoid this inconvenience, we optimize the linear ($C_{n\ell a}$) and nonlinear (B_a, α_a, γ_a) parameters in two separate steps, as follows.

In the first step, the $C_{n\ell a}$ are obtained by a linear least-squares fit to the long-range region of the PES. In order to test the correctness of the functional representation chosen for the $v_a^{(LR)}$, we do not a priori constrain the $C_{n\ell a}$ to reproduce the known molecular properties of CO. Hence, we allow the $C_{n\ell a}$ to vary freely in order to minimize the root-mean-squared relative error of the representation; for large R, this error is given by

$$\bar{e}^2 = \sum_{\vec{R}} \{[V_T(\vec{R},\vec{r}^B) - V_F(\vec{R},\vec{r}^B)]/[N_{\vec{R}} V_T(\vec{R},\vec{r}^B)]\}^2. \qquad (3.3.1)$$

Here, the sum runs over the $N_{\vec{R}}$ points of the surface for which $R > 3.7$ Å, V_T is the tabulated value and $V_F = \sum_a v_a^{(LR)}$. The optimum values of the $C_{n\ell a}$ are those that satisfy the system of linear equations

$$\partial \bar{e}^{\,2}/\partial C_{n\ell a} = 0, \qquad (3.3.2)$$

together with the conditions $\partial^2 \bar{e}^{\,2}/\partial C_{n\ell a}^2 > 0$.

Solving eqs . (3.3.1) for all the $C_{n\ell a}$ indicated in eq. (3.2.3c) gave C_{10a}, C_{21a}, and C_{32a} of the order of $\pm 6\ e^2\ \text{Å}^n$, n=0,1,2, respectively, with opposite signs for each atom. These values, although of unphysically large magnitudes, lead the $v_a^{(LR)}$ to cancel each other in order to reproduce the tabluated PES. Examining the resulting fit, we concluded that, for the Li^+/CO system, the long-range potential could be reproduced with fewer parameters than those indicated in eq. (3.2.3c). Repeating the fitting procedure while omitting each time one pair of the C_{10a}, C_{21a}, and C_{32a}, we found that the C_{21a} were redundant. The optimum values of the parameters are shown in table 3.1. These reproduce the long range region of the PES with an r. m. s. error $\bar{e} = 0.85\%$ over the 25 points available (four equally-spaced values of R from 3.7 Å to 5.3 Å and one at R = 7.9 Å, each for the five orientations η= 0, 45, 90, 135 and 180 deg). Throughout the remainder of the optimization procedure, the $C_{n\ell a}$ were kept fixed.

In the second step, using the full multicenter potential of eqs. (3.2.3-5), for a given set of values of the nonlinear parameters B_a, c_a, and γ_a, we least-squares fitted the A_a to the short-range region of the tabluated surface for which $V_T > 0$. This fit was

repeated for several sets of B_a, c_a, and γ_a, each time obtaining a new A_a. Finally, we chose the B_a, c_a, γ_a and the corresponding A_a that yielded the smallest r. m. s. error in the short and intermediate ranges; these values are also shown in the table below.

Table 3.1. Ion/atom potential parameters for Li^+/CO

	Li^+/C	Li^+/O
$\vec{d}_a$(Å)	$0.6447\vec{z}$	$-0.4835\vec{z}$
A_a(eV)	1086.33	1191.92
B_a(Å^{-1})	4.25	4.63
c_a(Å)	1.38	1.48
γ_a(Å^{-1})	1.38	2.27
C_{10a}(eVÅ)	-0.189892	0.193190
C_{21a}(eVÅ^2)	0	0
C_{32a}(eVÅ^3)	-5.70326	-0.951450
C_{40a}(eVÅ^4)	-11.4071	-2.54812
C_{42a}(eVÅ^4)	-1.07765	-4.90754

Substituting the $C_{n\ell a}$ into eqs. (3.2.6) yields the molecular properties of CO that correspond to the present representation; these are in good agreement with the experimental ones (Thomas et al., 1978), as is seen in table 3.2. This comparison further confirms the validity of the multicenter expansion for large R.

Table 3.2 Molecular properties of CO_2

	Present Fit	Exact
q_B(e)	2.3×10^{-4}	0
μ_B(eÅ)	-0.0150	-0.0236
Q_B(eÅ^2)	-0.4646	-0.4666
α_B(Å^3)	1.939	1.947
Δ_B(Å^3)	0.415	0.325

Figures 3.1 and 3.2 show the full multicenter potential (eqs. (3.2.3-5) together with the parameters of table 3.1) and the quantum-chemical values. We find that the multicenter representation reproduces the tabulated values with an r. m. s. error $\bar{e}$ = 4.4% over the 55 points available. The largest errors occur near the zeroes of the potential where its absolute value is less than 0.03eV. We also find a small discrepancy (15%) near the bottom of the potential wells at the two orientations η=0 and 180 deg. This discrepancy is most probably due to the simple angular dependence (isotropic) that we have chosen for the $v_a^{(SR)}$. The errors could be greatly reduced by expanding $v_a^{(SR)}$ in a basis of functions of η_a. However, we feel that the increase in computational effort resulting from a larger set of parameters is not justified for the description of hyperthermal collisions.

Figure 3.1 Comparison of the multicenter representation (curves) of the Li^+/CO potential with the quantum chemical values (points).

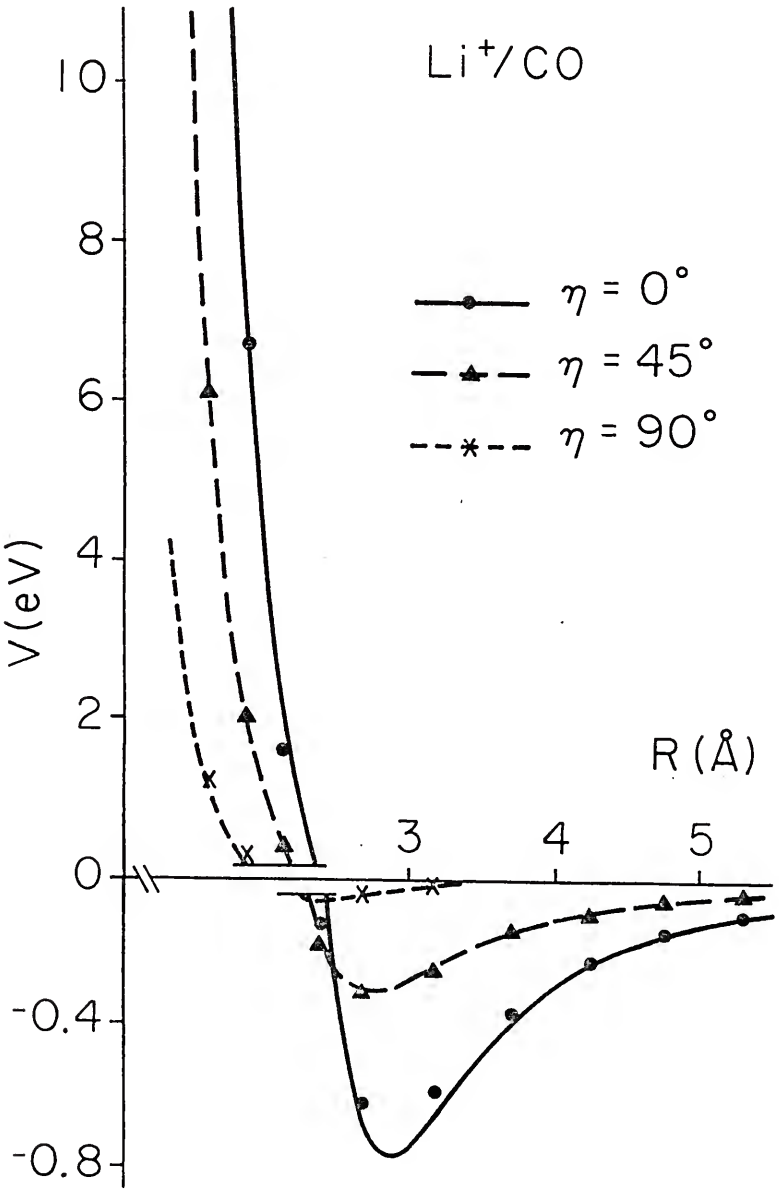
Li+/CO
η = 0°
η = 45°
η = 90°
V(eV)
R(Å)
10
8
6
4
2
0
-0.4
-0.8
3
4
5

Figure 3.2 Comparison of the multicenter representation (curves) of the Li^+/CO potential with the quantum chemical values (points).

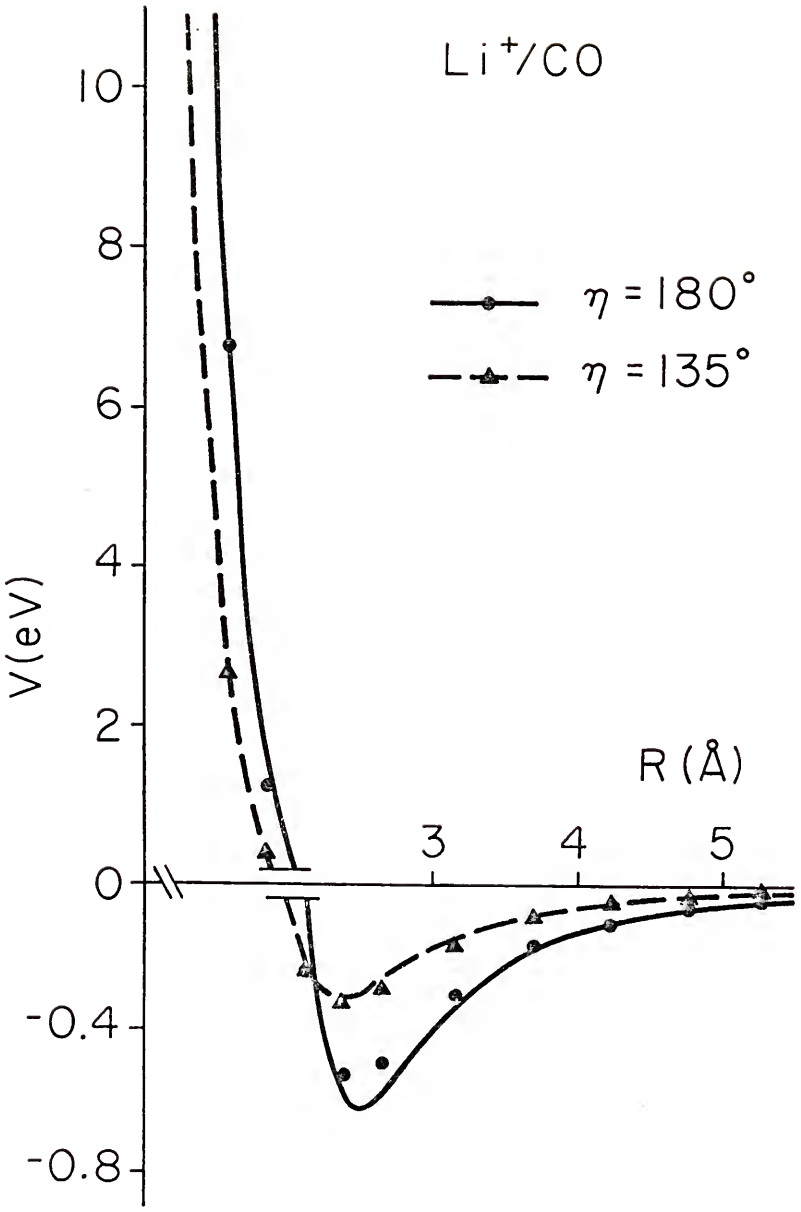
Li+/CO
η = 180°
η = 135°
V(eV)
R (Å)
10
8
6
4
2
0
-0.4
-0.8
3
4
5

Excepting the two regions just mentioned, the multicenter representation gives a very accurate description of the Li^+/CO surface over the four-decade range of magnitudes of the potential, with a minimum of adjustable parameters. The single-center expansion developed by Thomas et al., which is of comparable accuracy, required fifty parameters, in contrast to the sixteen used in the present one. Furthermore, the multicenter representation allows us to understand the physical origin of the parameters, even in the short-range regions. On the other hand, the ion/atom potentials just obtained may be utilized to gain insight into the physical structure of the CO molecule. Recognizing the dangers of extrapolating excessively from indirect results, we propose the following interpretation to the differences between the Li^+/C and Li^+/O potentials.

A comparison of the short-range regions of the v_a, shown in fig. 3.3, suggests that the electronic density about carbon extends farther from its nucleus than does that of oxygen. This observation is consistent with the signs of the C_{10a} which indicate a slight excess of electrons on the C-center and a corresponding deficit on the O-one. This causes the Li^+/O interaction to be repulsive at large R_a, while the Li^+/C potential is attractive for large distances, as is seen if figs. 3.4 and 3.5, respectively. Comparing the magnitudes of the C_{32a}, we conclude that the charge distribution about C is more anisotropic than the one about O, and that both distributions are prolate spheroidal. Finally, the C_{40a} indicate that the electrons around C are more polarizable than those about O; however, the anisotropy of the polarizability of O is quite large, so that, at

Figure 3.3 Short-range region of the ion/atom potentials of Li^+/CO.

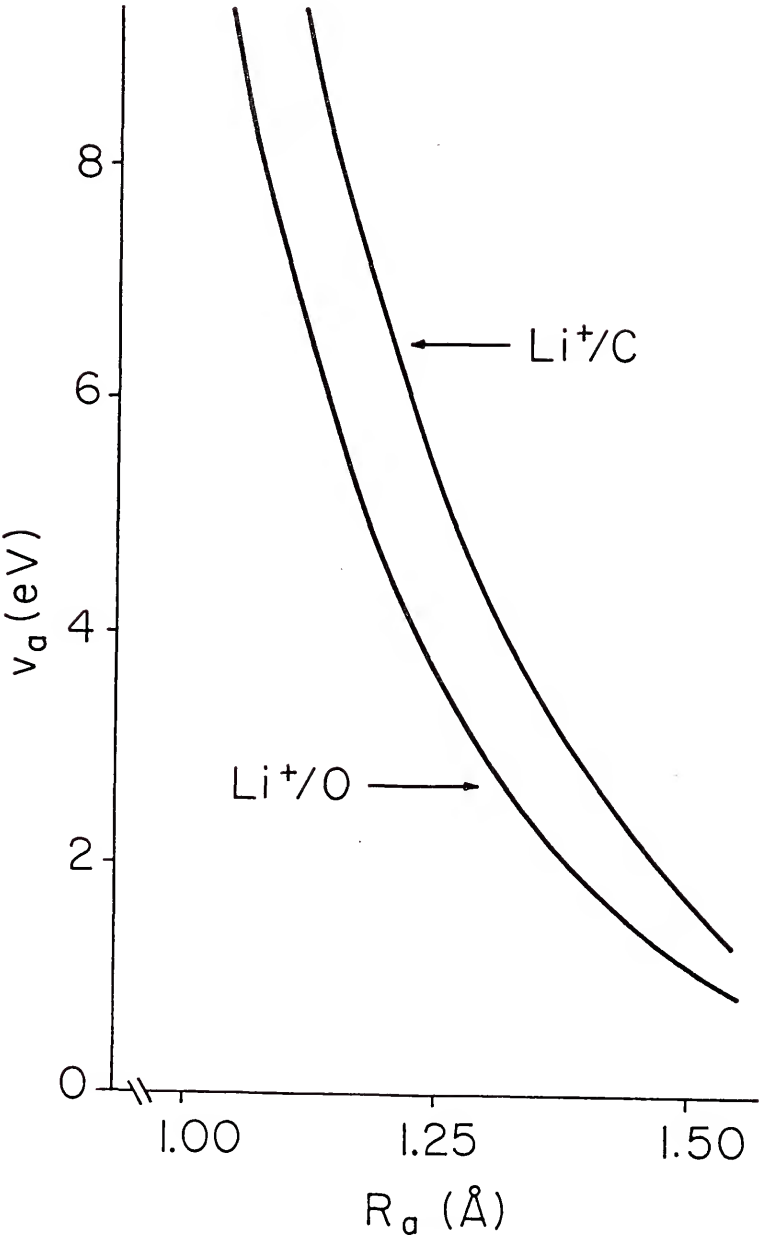
8
6
4
2
0
v_a (eV)
Li+/C
Li+/O
1.00
1.25
1.50
R_a (Å)

Figure 3.4 Intermediate- and long-range regions of the Li^+/C potential of Li^+/CO.

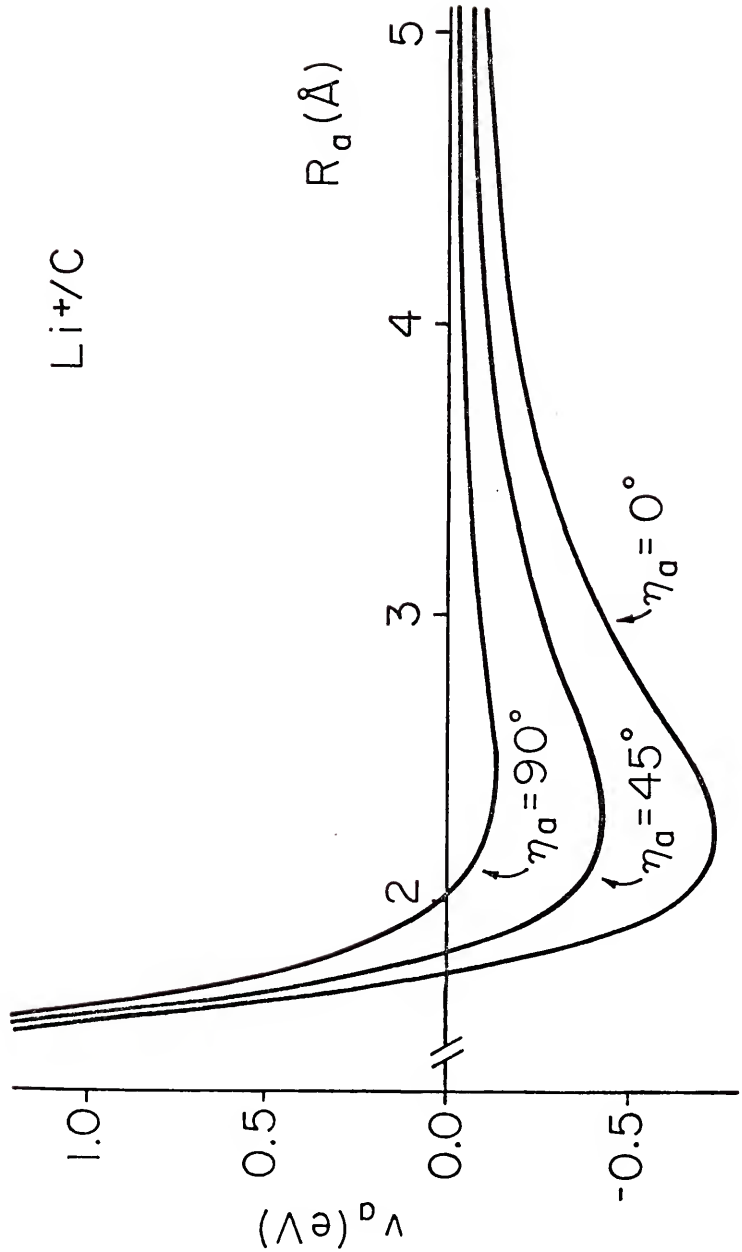
Li+/C
R_a(Å)
2
3
4
5
η_a=90°
η_a=45°
η_a=0°
1.0
0.5
0.0
-0.5
v_a(eV)

Figure 3.5 Intermediate- and long-range regions of the Li^+/O potential of Li^+/CO.

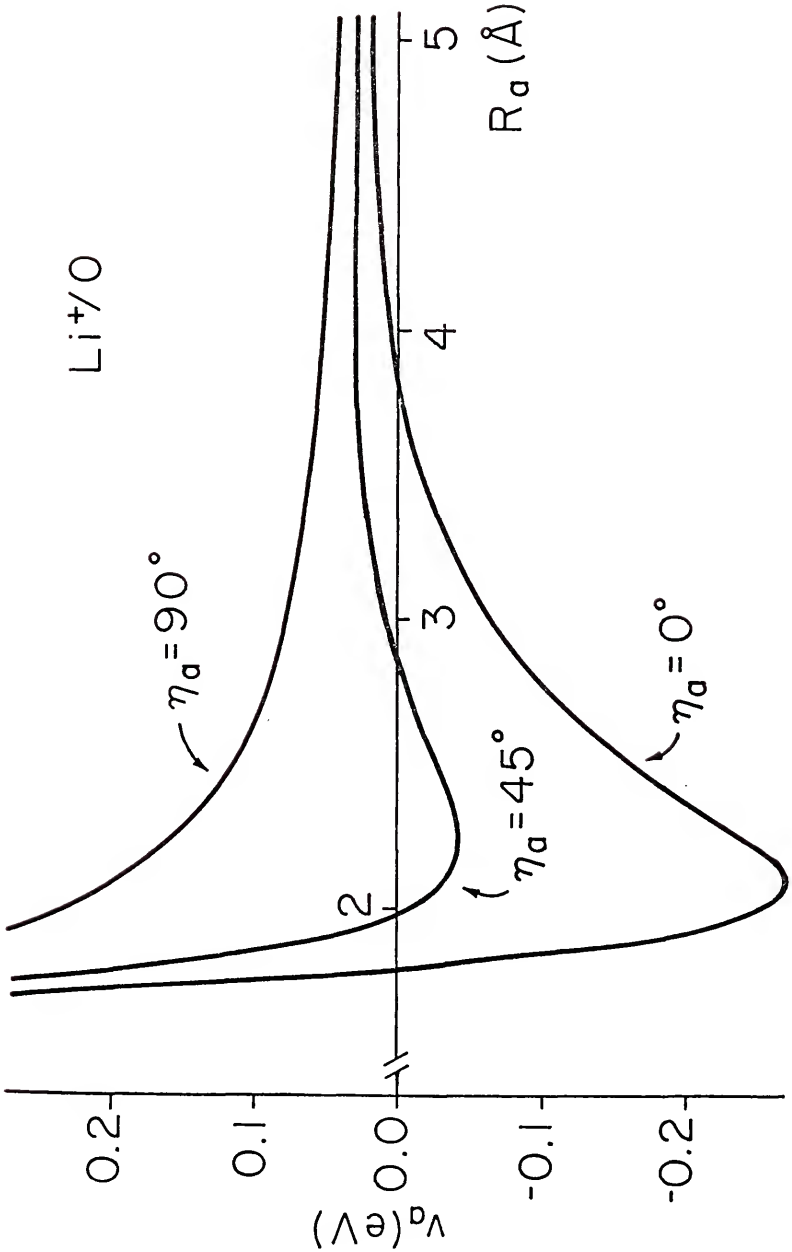
Li+/O
η_a=90°
η_a=45°
η_a=0°
R_a (Å)
V_a(eV)
0.2
0.1
0.0
-0.1
-0.2
2
3
4
5

η_a=90 deg. the Li^+/O potential is repulsive at all distances. We expect that these conclusions would be confirmed by the configuration-interaction charge density of the isolated CO molecule; unfortunately, the wave-function of CO is not available to us at the present time.

4. Multicenter Potential for the System Li^+/CO_2

Due to the large computational effort required by the number of electrons in CO_2, a quantum chemical PES for the Li^+/CO_2 system has not been calculated. Until such a surface becomes available, we propose a multicenter potential which is based on the electron-gas model of short-range forces (Gordon and Kim, 1972) and on the long-range interaction between the charge of Li^+ and the known electrostatic multipoles and polarization of CO_2.

Briefly, the uniform-electron-gas model of the interaction between two closed-shell atoms and/or molecules A and B is based on the following assumptions. Firstly, the potential is written as the sum of four terms that represent the kinetic energy of the electrons, the electrostatic interactions between the charge distributions of A and B, the electron exchange and correlation effects, respectively. Each term is separately calculated as an integral over all space of the corresponding energy density, which is a functional of the electronic density of the system. The electrostatic energy-density functional may be readily obtained by considering the Coulombic interactions between the charge distribtuions. However, the kinetic, exchange and correlation density functionals are taken to be those of a uniform gas of electrons (Slater, 1968, Carr et al., 1961,

Carr and Maradudin, 1964). Furthermore, the electronic density of the A-B system is approximated by the sum of the densities of the isolated partners, regardless of their separation. Hence, if the density of each species is known, the calculation of the PES is reduced to the numerical evaluation of the integrals of the energy-density functionals.

This model has been found to provide a reasonably accurate description of the short-range repulsive forces in atom-atom (Kim and Gordon, 1974a, b) atom-molecule (Green et al., 1975, Parker et al., 1976, Davies et al., 1979) and molecule-molecule (Parker et al., 1975) systems, at a small fraction of the computational cost of even the most approximate quantum-chemical methods. Unfortunately, the model does not correctly describe the long-range forces, for the following reasons. Due to the additive nature of the approximate total density, the correlation effects depend on the overlap between the individual densities. Hence, for large R, the correlation contribution decreases exponentially and does not reproduce the Van-der-Waals potential which is of order R^{-2n}, $n \geq 3$. This deficiency may be remedied by smoothly switching from the electron-gas correlation potential to the dispersion one, as R increases (Parker et al., 1976). In the Li^+/CO system, we expect that the dispersion forces are much smaller than the induction ones, due to the net charge of the ion. However, by assuming that the electronic densities of each species remain unchanged for all distances, the model excludes the rearrangement of the charge distribution of CO_2 caused by the charge of Li^+, and hence the induction forces.

Nevertheless, we may obtain a realistic model of the Li^+/CO_2 PES by combining the short-range results of the electron-gas method with the long-range multicenter expansion studied in the previous section, as shown below.

Electron-gas calculations were performed for the collinear (η= 0 deg) and perpendicular (η = 90 deg) configurations of Li^+/CO_2, using the program developed by Green and Gordon, 1974. These calculations incorporated the correction due to Rae, 1973, that avoids overcounting of the electrons in the density functionals. The electronic density of CO_2 was approximated by that of the self-consistent-field (SCF) molecular wave-function calculated by McClean and Yoshimine, 1967, p. 192. The equilibrium C-O bond distance was fixed at the value that corresponds to the SCF wave-function (1.1348 Å) instead of the experimental one (1.161 Å, in Eastes et al., 1977), because the experimental bond-length represents a slightly stretched CO_2 molecule in the SCF approximation. The Li^+ ion was also described by an SFC wave-function (Clementi, 1965, table 03-01). The numerical integration of the energy density functionals was carried out by means of three-dimensional Gaussian quadratures, the number of quadrature points was gradually increased until the calculated potential converged to 1%, at all the values of $\vec{R}$. Due to the approximate nature of the model, we felt that the increase in computational cost required for a greater accuracy was not justified. Hence, the number of points ranged from (56, 80, 1), at η=0 deg, to (24, 40, 24), at η=90 deg, for the (λ, μ, Φ) spheroidal coordinates, respectively.

Table 3.3 Electron-gas Li^+/CO_2 potential.

R (Bohr)	V(R,0 deg) (Hartree)	R (Bohr)	V(R,90 deg) (Hartree)
3.7444	0.81826	1.60	0.87678
3.8444	0.63961	1.80	0.62150
3.9444	0.52927	2.00	0.44061
4.0444	0.40132	2.20	0.31309
4.1444	0.32335	2.40	0.22474
4.2444	0.25550	2.60	0.16382
4.3444	0.20132	2.80	0.12175
4.4444	0.15878	3.00	0.09251
4.5444	0.12499	3.20	0.07347
4.6444	0.09931	3.40	0.05994
4.7444	0.07718	3.60	0.04937
4.8444	0.01634	3.80	0.04059
		4.00	0.03335

The results of the above calculations are shown in table 3.3 (the odd-looking scale chosen for R at $\eta = 0$ is due to the face that the coordinate most appropriate to short-range interactions is the separation between the ion and the nearest atom of CO_2). These results correspond to the so called Hartree-Fock model potential, which is the sum of the kinetic, electrostatic and exchange contributions.

The electron-gas correlation is not presented here, due to the inaccuracies of the model previously discussed. However, the correlation effects were calculated to be of the order of 1% of the "Hartree-Fock" potential, and hence comparable to the numerical errors of the quadratures. In order to facilitate future scattering calculations, the short-range potential was fitted to a multicenter expansion, as follows.

A plot of the logarithm of the potential versus the distance between Li^+ and the nearest molecular atom yielded an approximately straight line, for the collinear configuration. This indicated that the Li^+/O potentials, v_1 and v_3, could be represented by the single exponential of eq. (3.2.5). However, an analogous plot for the perpendicular configuration showed a steep straight line for small R, that smoothly changed to a shallower slope for larger distances. This graph suggested that two exponential terms were required for the Li^+/C potential. The parameters of the ion/atom potentials were adjusted to reproduced the tabulated electron-gas surface, by a procedure analogous to the second step described in Sec. 3.3. Briefly, for fixed values of the exponential coefficients $B_1 = B_3$, B_2 and B_2', the preexponential factors $A_1 = A_3$, A_2 and A_2', were simultaneously least-squares fitted to all the points of the tabulated surface. This fitting was repeated for several sets of values of $B_1 = B_3$, B_2 and B_2', finally selecting the exponential coefficients and corresponding preexponential ones that yielded the lowest r. m. s. relative error. These are shown in table 3.4 (below), and they reproduced the surface with an r. m. s. error $\bar{e}$ = 0.43% over the 25

tabulated points; the largest error (3.6%) occurred at $\vec{R} = (4.8444\ a_o, \eta = 0\ \text{deg})$. These short range ion/atom potentials may now be combined with the known long-range forces of the Li^+/CO_2 system, as follows.

Without further knowledge of the properties of the exact charge distribution of CO_2, there is some ambiguity in the determination of the $v_a^{(LR)}$, because only $\lim_{R\to\infty} \sum_a v_a^{(LR)}$ may be determined from experimental measurements of CO_2. In particular, the Li^+-charge/CO_2-quadrupole interaction, may be represented in several different ways that are in accordance with eq. (3.2.6c). For example, Eastes et al., 1977, assumed fractional charges q_a located on the atomic centers of the molecule. The values $q_1 = q_3 = -0.331$ e and $q_2 = +0.662$ e reproduce the experimental quadrupole moment $Q_B = -0.90\ e\text{Å}^2$, at large distances. However, for small R, these charges yield values for the perpendicular Li^+/CO_2 interaction that are much larger than those calculated above, because the Coulomb potentials $q_A\, q_a/R_a$ do not cancel in the appropriate way. Similarly, one may set the q_a equal to zero, and consider fractional atomic dipoles μ_a (note that $\vec{\mu}_2 = \vec{0}$ due to the symmetry of oxygen); however, such a model is also in disagreement with the above short-range results. Therefore, we presently assume that $q_a = 0$ and $\vec{\mu}_a = \vec{0}$, for all a, and take nonzero atomic quadrupoles Q_a, such that $\sum_a Q_a = Q_B$. We must emphasize that this choice is not unique; a combination of small atomic charges, dipoles and quadrupoles may not be excluded as a possibility. On the other hand, the electronic clouds about each of the atomic centers are polarized by the net charge of the ion; hence, we represent the isotropic and

and anisotropic polarizabilities of CO_2 by the sum of the atomic polarizabilities α_a and Δ_a, respectively. Furthermore, since the number of electrons in C and in O are comparable, we let $Q_a = Q_B/3$, $\alpha_a = \alpha_B/3$ and $\Delta_a = \Delta_B/3$, with $\alpha_B = 2.602$ Å^3 and $\Delta_B = 0.6931$ Å^3 (Buckingham and Orr, 1967). Finally, the resulting $v_a^{(LR)}$ are switched off at small A-a distances as in eqs. (3.2.3b,4) using the switching parameters c_a and γ_a of C and of O determined in the previous section. The parameters for the long range ion/atom potentials of Li^+/CO_2 are also included in the table below.

Table 3.4 Ion/atom potential parameters for Li^+/CO_2.

	Li^+/C	Li^+/O
A_a(eV)	650.697	1340.16
A_2'(eV)	17.5648	———
B_a(Å^{-1})	4.346	4.856
B_2'(Å^{-1})	1.455	———
c_a(Å)	1.38	1.48
α_a(Å^{-1})	1.38	2.27
C_{10a}(eVÅ)	0	0
C_{21a}(eVÅ^2)	0	0
C_{32a}(eVÅ^3)	-4.32	-4.32
C_{40a}(eVÅ^4)	-6.246	-6.246
C_{42a}(eVÅ^4)	-3.327	-3.327

The complete model potential (eqs. (3.2.3-5) together with table 3.4) is presented in figs. 3.6,7. Examination of the short-range region shows the large anisotropy of the repulsive forces, which is due to the many-body nature of the target. In this region, the accuracy of the model is determined only by that of the electron-gas approximation because the $v_a^{(LR)}$ are switched off. By design, the present model reproduces the exact long-range forces, as determined by the properties of CO_2. A judgement of the validity of this surface in the intermediate regions must be postponed until a quantum-chemical PES becomes available. The latter region includes the potential wells and is thus sensitive to the atomic quardupoles and polarizabilities, which are not uniquely defined by Q_B, α_B and Δ_B. However, we expect this model to provide at least a qualitative description of the eact PES for intermediate R; in particular, the disappearance of the well at $\eta = 0$ deg as $\eta \to 90$ deg, seen in fig. 3.7, clearly reflects the change in sign of the Li^+ charge/CO_2-polarization interactions. Finally, in figs. 3.8-10 we present the ion/atom potentials. Examination of their short-range behaviour (fig. 3.8) indicates that the charge distribution about the C-center extends farther away from its nucleus than do those of the O-centers. Consequently, the larger extent of the Li^+/C repulsion causes the wells of v_2 to be much shallower than those of v_1 and v_3, as is seen in figs. 3.9,10.

Having determined multicenter potentials for Li^+/CO and Li^+/CO_2, we may now proceed to study energy transfer processes in these systems by means of the many-body theory developed in Chap. II.

Figure 3.6 Short-range region of the Li^+/CO_2 model potential.

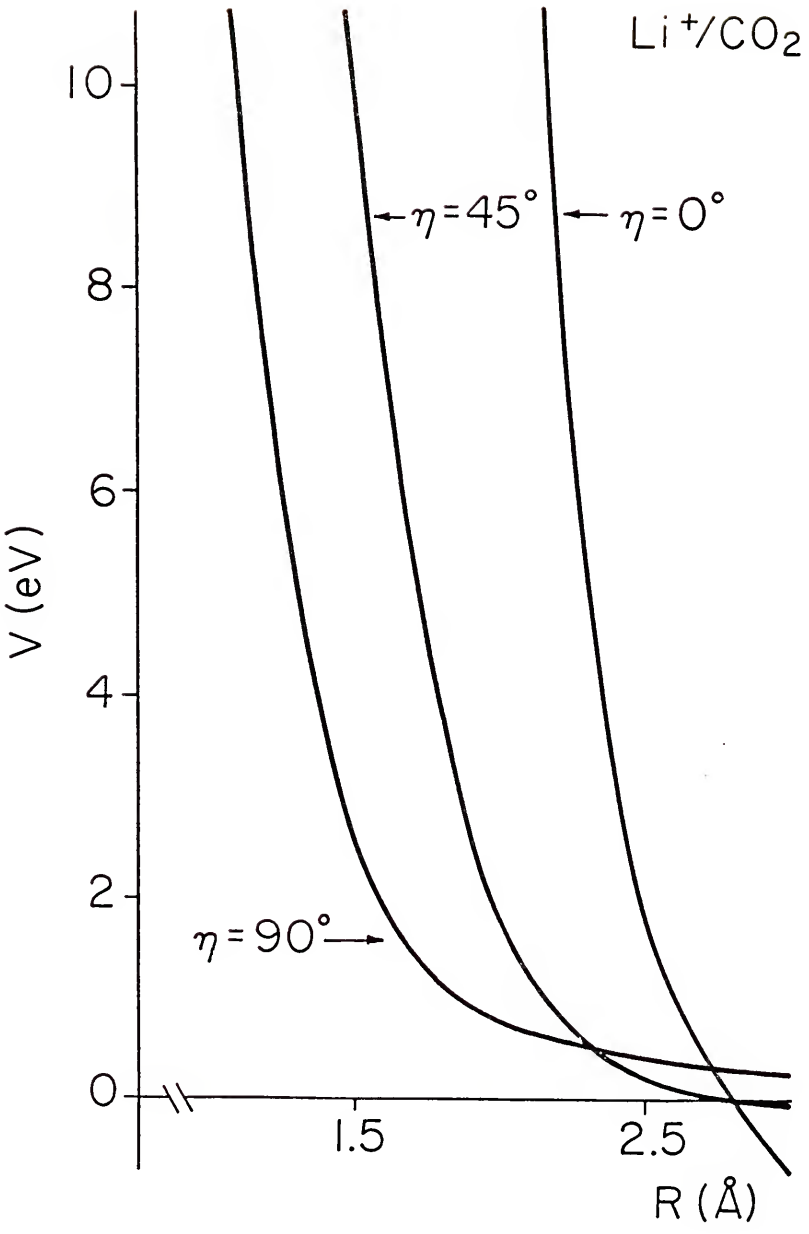
Li+/CO2
10
8
6
4
2
0
V (eV)
η=45°
η=0°
η=90°
1.5
2.5
R (Å)

Figure 3.7 Intermediate- and long-range regions of the Li^+/CO_2 model potential.

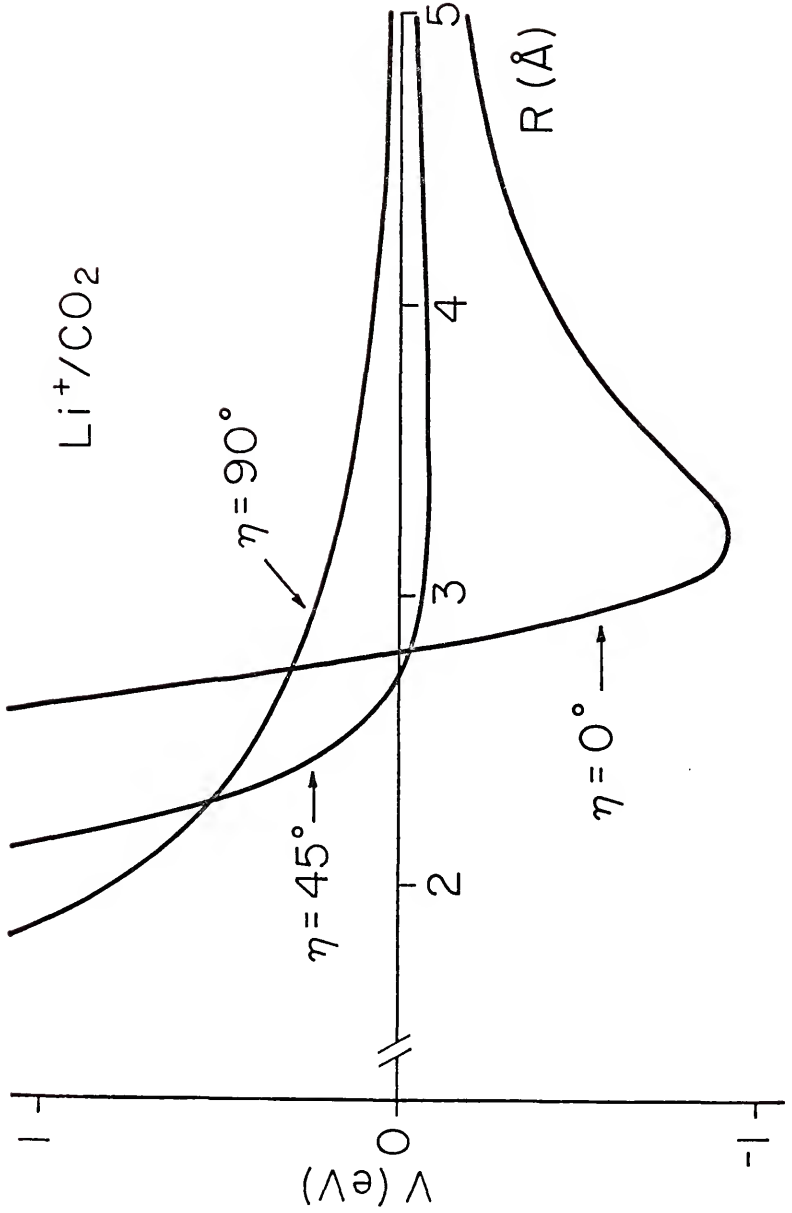
Li+/CO2
η=90°
η=45°
η=0°
R (Å)
5
4
3
2
1
0
-1
V (eV)

Figure 3.8 Short-range region of the ion/atom potentials of the Li^+/CO_2 model surface.

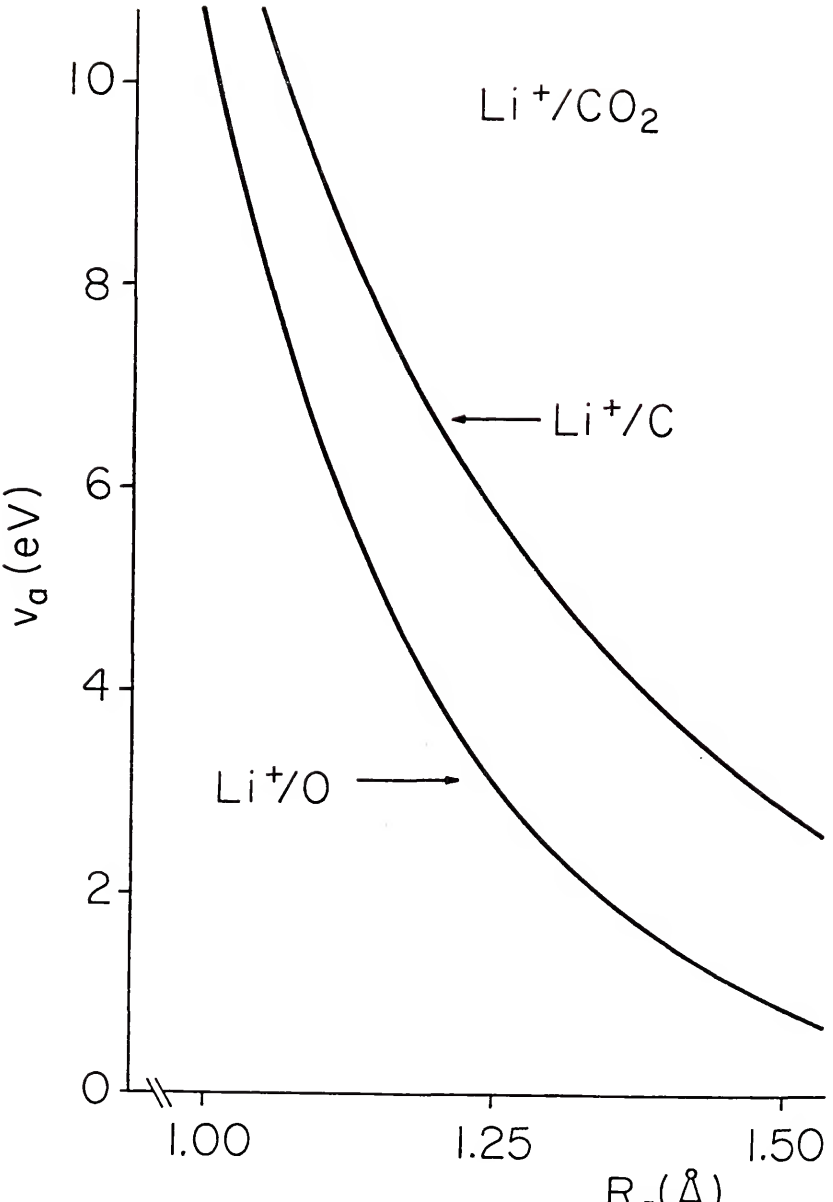
10
8
6
4
2
0
V_a (eV)
Li^+/CO_2
Li^+/C
Li^+/O
1.00
1.25
1.50
R_a(Å)

Figure 3.9 Intermediate- and long-range regions of the Li^+/C potential of the Li^+/CO_2 model surface.

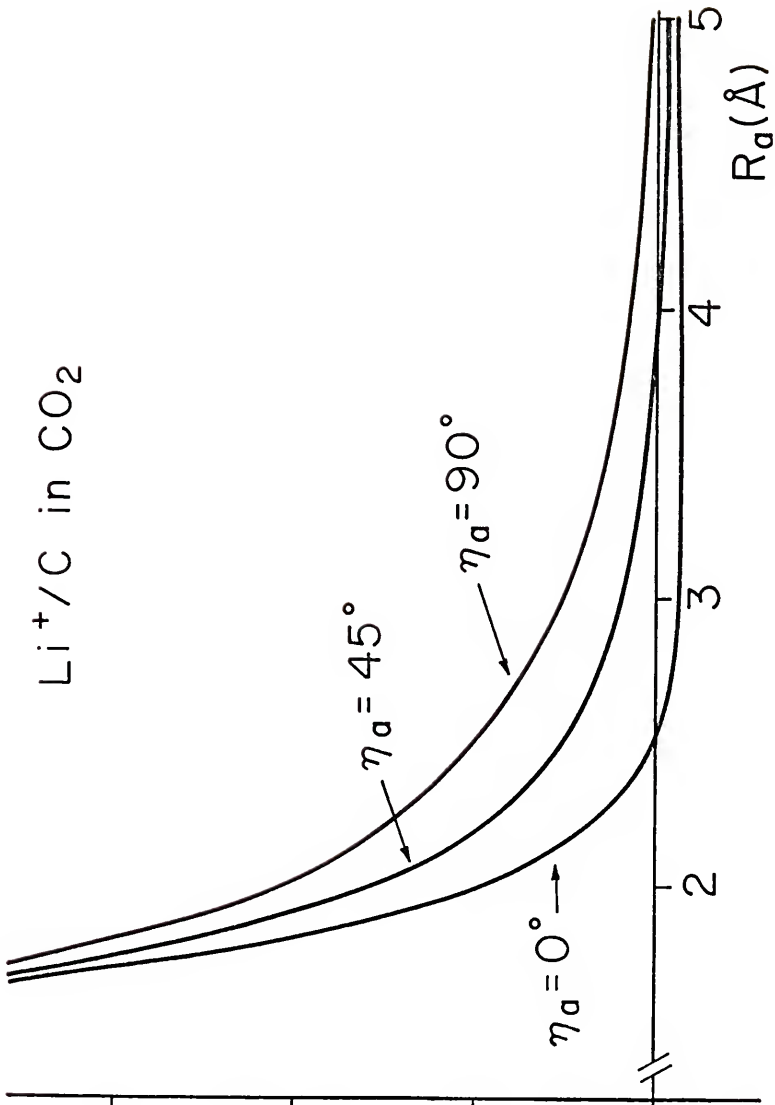
Li+/C in CO2
ηa= 45°
ηa=90°
ηa=0°
Va (eV)
1.5
1.0
0.5
0.0
2
3
4
5
Ra(Å)

Figure 3.10 Intermediate- and long-range regions of the Li^+/O potential of the Li^+/CO_2 model surface.

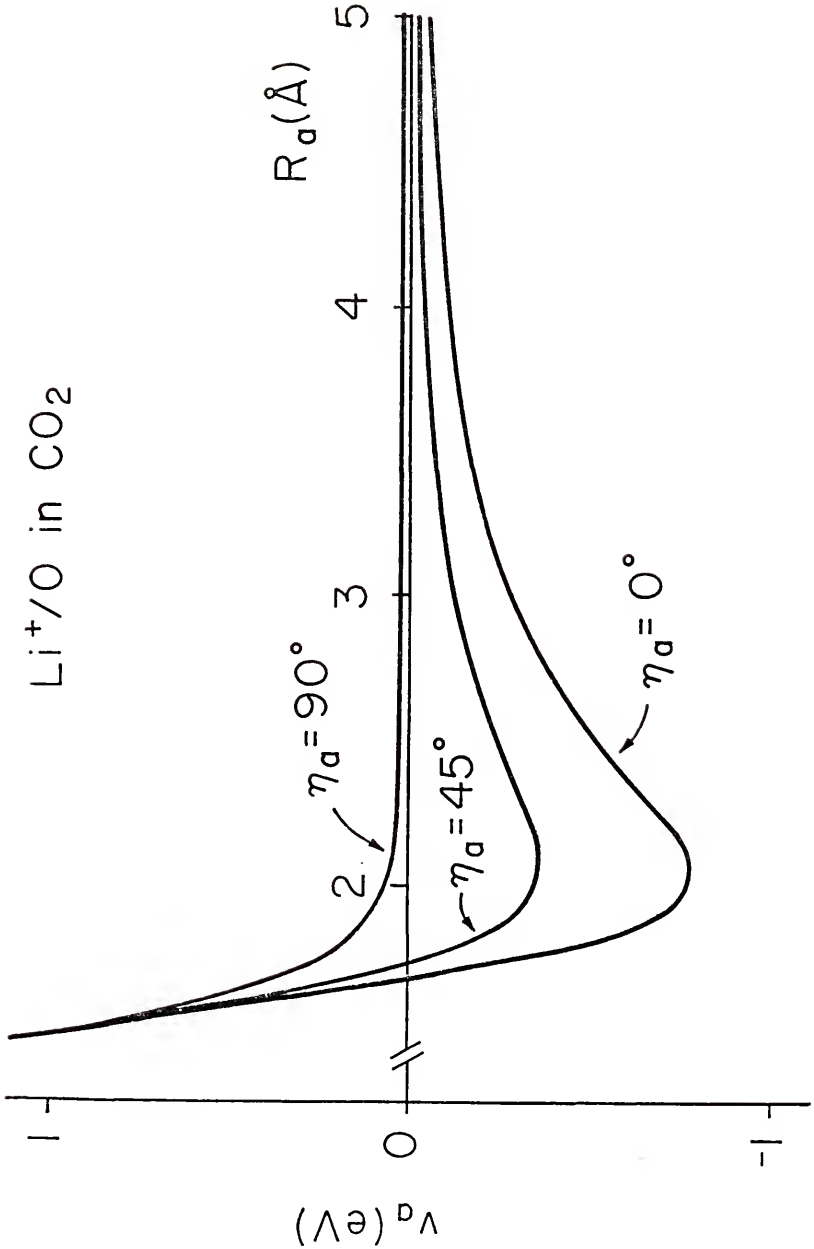
Li+/O in CO2
Ra(Å)
5
4
3
2
ηa=90°
ηa=45°
ηa=0°
1
0
-1
Vd (eV)

CHAPTER IV
ROTATIONAL AND VIBRATIONAL ENERGY TRANSFER IN HYPERTHERMAL COLLISIONS OF Li^+ WITH N_2, CO AND CO_2

The many-body theory of atom-molecule collisions that was presented in Chapter II is applied here to the study of rotational and vibrational energy transfer in the scattering of Li^+ ions from N_2, CO and CO_2. In Section 1 we evaluate the quantities that are required for the calculation of the atom-pair correlation function (APCF) of a diatomic target. In Section 2 we present the theoretical results for the systems Li^+/N_2 and Li^+/CO, and compare them with the experimental measurements of Bottner et al., 1976. In the following section, we briefly outline the steps of the evaluation of the APCF of a linear triatomic molecule. Theoretical probabilities of vibrational excitation and average energy transfers for the system Li^+/CO_2 are presented in Section 4. Comparing these results with those of experiments (Eastes et al., 1977) and analyzing the theoretical model, we gain insight into the dynamical processes and intermolecular forces that dominate atom-molecule scattering in the hyperthermal energy regime. Finally, in Section 5 we calculate the effects of molecular anharmonicity on the vibrational energy transferred to the targets N_2, CO and CO_2.

1. The Atom-Pair Correlation Function of a Diatomic Molecule

The evaluation of the APCF of equation (2.6.8) requires knowledge of the equilibrium positions of the atoms ($\vec{d}_a$) and of the matrix elements ($\vec{C}_{ai}$) of the transformation between Cartesian vibrational displacements

($\vec{u}_a$) and normal coordinates (Q_i). For a diatomic molecule, equation (2.2.1a) shows that there is only one vibrational degree of freedom, and that $\vec{d}_1 = -m_2 d_{12}\vec{d}/m_B$ and $\vec{d}_2 = m_1 d_{12}\vec{d}/m_B$; here m_a is the mass of the target atom **a**, m_B is the mass of the diatomic, d_{12} is the equilibrium bond-length, and $\vec{d}$ is a unit vector in the direction of the molecular axis, from atom 1 to atom 2. From the normal-mode analysis outlined in equations (2.3.8-15) we obtain $\vec{C}_{11} = -[m_2/(m_1 m_B)]^{\frac{1}{2}}\vec{d}$ and $\vec{C}_{21} = [m_1/(m_2 m_B)]^{\frac{1}{2}}\vec{d}$, and for the harmonic vibrational frequency, $\omega_1 = [k_{11} m_B/(m_1 m_2)]^{\frac{1}{2}}$, where k_{11} is the quadratic force-constant.

The rotational energy transfers and widths require the commutators $([\hat{H}_R,)^n \exp(-i\vec{\kappa}\cdot\hat{\vec{d}}_a)]$, for n = 1 and 2. These are readily evaluated for a linear polyatomic in the coordinate representation, where the rotational Hamiltonian is given by (Edmonds, 1974)

$$H_R = \frac{-\hbar^2}{2I_B}\left[\frac{\partial}{\partial(\cos\beta)}(1-\cos^2\beta)\frac{\partial}{\partial(\cos)\beta)} + \frac{\partial^2}{\partial\alpha^2}\right]. \qquad (4.1.1)$$

Here, α and β are the azimuthal and polar angles of $\vec{d}$ in the space fixed (SF) reference frame, respectively, and $I_B = \sum_a m_a d_a^2$ is the moment of inertia of the polyatomic. Taking the z-axis of the SF frame along the direction of $\vec{\kappa}$, so that $\vec{\kappa}\cdot\vec{d} = \kappa d_a \cos\beta$, and performing the necessary differentiations, yields

$$[\hat{H}_R, \exp(-i\vec{\kappa}\cdot\hat{\vec{d}}_a)] = (\hbar^2/2I_B)\exp(-i\kappa d_a\cos\beta)\times$$

$$\times\{\kappa^2 d_a^2(1-\cos^2\beta) - 2i\kappa d_a[\cos\beta - (1-\cos^2\beta)\partial/\partial(\cos^2\beta)]. \qquad (4.1.2)$$

Whenever $|\kappa d_a| >> 1$, only the highest power of $|\kappa d_a|$ need be retained in the above commutator; in these cases, one has that

$$([\hat{H}_R,)^n \exp(-i\vec{\kappa}\cdot\hat{\vec{d}}_a)] \simeq [\hbar^2\kappa^2 d_a^2 \sin^2\beta/(2I_B)]^n \exp(-i\kappa d_a\cos\beta). \qquad (4.1.3)$$

The evaluation of the APCF is completed by calculating the quantum-statistical averages over initial rotational states that are indicated in eqs. (2.6.4b) through (2.6.6). However, the experiments are not yet able to resolve the rotational levels of heavy polyatomics, so that this average may be approximated by a classical one. Since the quantities to be averaged depend only on $\cos\beta$, the classical statistical average reduces to a simple integral over β. Hence, the APCF of a diatomic is given by

$$S^{(aa)}(\vec{\kappa},\varepsilon) = \frac{1}{4\sqrt{\pi}} \sum_{n=-\infty}^{\infty} P_n^{(aa)}(\kappa) \exp\{-[(\langle\langle L_R\rangle\rangle_{CR} - n\hbar\omega_1 - \varepsilon)/ /(2\langle\langle L_R^2\rangle\rangle_{CR}^{\frac{1}{2}})]^2\}/ 2\langle\langle L_R^2\rangle\rangle_{CR}^{\frac{1}{2}}. \quad (4.1.4a)$$

$$P_n^{(aa)}(\kappa) = \int_0^1 d(\cos\beta)\, p_n^{(aa)}(\kappa;\beta), \quad (4.1.4b)$$

$$\langle\langle L_R\rangle\rangle_{CR} = \hbar^2\kappa^2 d_a^2/(2I_B) \quad [P_n^{(aa)}(\kappa)]^{-1} \int_0^1 d(\cos\beta) \times \times p_n^{(aa)}(\kappa;\beta) \sin^2\beta, \quad (4.1.4c)$$

$$\langle\langle L_R^2\rangle\rangle_{CR} = [\hbar^2\kappa^2 d_a^2 / (2I_B)]^2 [P_n^{(aa)}(\kappa)]^{-1} \times \times \int_0^1 d(\cos\beta)\, p_n^{(aa)}(\kappa;\beta) \sin^4\beta - \langle\langle L_R\rangle\rangle_{CR}^2, \quad (4.1.4d)$$

$$p_n^{(aa)}(\kappa;\beta) = I_n(X_{a1}) \exp(-n\alpha_1 - X_{a1}\cosh\alpha_1), \quad (4.1.4e)$$

$$X_{a1} = \hbar\kappa^2 c_{a1}^2 \cos^2\beta/ (2\omega_1 \sinh\alpha_1), \quad (4.1.4f)$$

$$\alpha_1 = \hbar\omega_1/ (2\kappa_B T_v) \quad (4.1.4g)$$

2. Rotational and Vibrational Energy Transfer in Hyperthermal Collisions of Li^+ with N_2 and CO

The doubly differential cross section given in eq. (2.1.5) requires the two-body effective cross sections σ_a. For the experimental conditions of quasielastic scattering ($\varepsilon << E$, so that $|\vec{k}| \approx |\vec{k}'|$) and scattering angles greater than rainbow angles, the σ_a may be approximated by the classical elastic differential cross section for the (A, a) atom-pair collision, evaluated at their relative energy and momentum transfer. Furthermore, since the large-angle scattering of light and fast projectiles is mediated by the short-range repulsive forces, the σ_a may be evaluated for the short-range pair potentials $v_a^{(SR)}$. We will return to the effects of the long-range forces later in this section.

We have calculated doubly differential cross sections for the scattering of Li^+ from N_2 and CO, at the center of mass (CM) collision energies E = 4.23 eV and 7.07 eV and scattering angles θ = 37.2 deg, 43.2 deg and 49.2 deg that were studied by the crossed-molecular-beams experiments of Bottner et al., 1976. The APCF of the target was evaluated for the usual model of harmonic vibration, with the parameters shown in table 4.1 (Herzberg, 1965); the effects of molecular anharmonicity are treated in Sec. 5. For the Li^+/CO system, the σ_a were calculated for the $v_a^{(SR)}$ developed in Sec. 3.3; for the Li^+/N potentials, we used the short-range parameters A_a = 3079.77 eV and B_a = 5.2581 $Å^{-1}$ that were obtained from a multicenter fit to the Li^+/N_2 potential surface of Staemmler, 1975.

Unfortunately, since the experiments were carried out some years before the development of the theory, the measurements have been presented in a form that does not allow a direct comparison with the theoretical

Table 4.1. Parameters for the atom-pair correlation functions of CO and of N_2

	CO	N_2
m_1 (amu)	12.0	14.0
m_2 (amu)	16.0	14.0
d_{12} (Å)	1.128	1.098
$\hbar\omega_1$ (eV)	0.266	0.290
T_V (K)	300.0	300.0

calculations. Firstly, Bottner et al. express the cross section in terms of the final rotational quantum number j_f of the diatomic, and not as functions of the rotational energy transfer ε_R. For a given vibrational transition n, the experimental cross section may be re-expressed in terms of ε_R by means of the relation

$$[\frac{d^2\sigma}{d\Omega d\varepsilon_R}(\vec{n};\ E,\ \theta)]_{exp.} = [\frac{d^2\sigma}{d\Omega dj_f}(\vec{n};\ E,\ \theta)]_{exp.}\ [\frac{\Delta\varepsilon_R}{\Delta j_f}]^{-1}, \qquad (4.2.1)$$

where $\Delta\varepsilon_R/\Delta j_f = \hbar^2\ (2j_f + 1)/(2I_B)$; however, the second factor on the right of eq. (4.2.1) causes an artificial enhancement of $(d^2\sigma/d\Omega d\varepsilon_R)_{exp.}$ for small ε_R. Furthermore, in reducing the cross sections from the laboratory reference frame to the CM frame, Bottner et al. assumed a Gaussian distribution of j_f, in contrast to the Gaussian distribution of ε_R (with an exponent quartic in j_f) that is characteristic of slow rotational motion, in accordance with our theory. Therefore, even if the theoretical cross section is reexpressed in terms of a final rotational quantum number (assuming $j_i = 0$), the experimental distributions are much wider than those expected from the internal dynamics of the diatomic. In this case, it is more meaningful to compare the experimental and theoretical values of the average rotational energy transfered $\langle\varepsilon_R\rangle_{\vec{n}}$, for the vibrational transition $\vec{n}$, and the average total energy transfer $\langle\varepsilon\rangle$ (vibrational plus rotational), which should be independent of the functional form of the final distributions. Since the experiments are quasielastic ($\varepsilon \ll E$), $\kappa \approx [2ME(1 - \cos\theta)]^{\frac{1}{2}}/\hbar$, where M is the reduced mass of the system; hence, from eqs. (2.1.5) and (2.6.8) we find that $\langle\varepsilon_R\rangle_{\vec{n}}$ and $\langle\varepsilon\rangle$ are approximately given by

$$\langle \varepsilon_R \rangle_{\vec{n}} = [\sum_a \sigma_a P_{\vec{n}}^{(aa)}(\kappa) \langle\langle L_R \rangle\rangle][\sum_a \sigma_a P_{\vec{n}}^{(aa)}(\kappa)]^{-1}, \tag{4.2.2a}$$

$$\langle \varepsilon \rangle = [\sum_a \sigma_a \sum_{\vec{n}} P_{\vec{n}}^{(aa)}(\kappa) (\langle\langle L_R \rangle\rangle - \hbar \vec{n} \cdot \vec{\omega}_v)][\sum_a \sigma_a P_{\vec{n}}^{(aa)}(\kappa)]^{-1} \tag{4.2.2b}$$

In table 4.2, we present the calculated and measured values of the average rotational energy transfer $\langle \varepsilon_R \rangle_0$ for no vibrational excitation and of $\langle \varepsilon \rangle$ for the Li^+/N_2 and Li^+/CO systems; the experimental value of $\langle \varepsilon_R \rangle_0$ was obtained from the most probable j_f of the rotational distribution, assuming that $j_i = 0$. A comparison of these results shows that the theoretical model correctly predicts the trends of the rotational and total energy transfers with increasing relative energy and scattering angle, although the model overestimates the rotational excitation of the target. At first sight, one might think that the excess in $\langle \varepsilon_R \rangle_0$ is due to the fact that the long-range ion/atom forces were not included in the calculation of the σ_a. However, eqs. (4.2.2) show that, for quasielastic collisions, the average energy transfers depend on the σ_a only through the ratio σ_1/σ_2. The neglect of the $v_a^{(LR)}$ affects the magnitudes of each σ_a, but does not change σ_1/σ_2 for small impact parameters. In order to test this hypothesis, $\langle \varepsilon_R \rangle_0$ and $\langle \varepsilon \rangle$ were reevaluated for Li^+/CO, using uniform semiclassical ion/atom cross sections (Berry, 1966) with the spherical components of the v_a, which include long-range forces (c.f. eqs. (3.2.3b - 5) . As expected, the long-range potential affects the magnitude of the overall cross section, but changes the average energy transfers by less than 5%.

These results lead us to conclude that the overestimate of rotational excitation is due to the dynamical assumptions on which the model is based,

Table 4.2. Average rotational energy transfer $\langle \varepsilon_R \rangle_0$ for no vibrational excitation and average total energy transfer $\langle \varepsilon \rangle$. The theoretical values are calculated with the real moment of inertia I_B of the diatomic.

E (eV)	θ (deg)	Li^+/CO				Li^+/N_2			
		$\langle \varepsilon_R \rangle$ (eV)		$\langle \varepsilon \rangle$ (eV)		$\langle \varepsilon_R \rangle$ (eV)		$\langle \varepsilon \rangle$ (eV)	
		exp.	th.	exp.	th.	exp.	th.	exp.	th.
4.23	37.1	0.087	0.27	0.13	0.35	0.085	0.25	0.080	0.33
4.23	43.2	0.090	0.36	0.17	0.46	0.092	0.34	0.093	0.43
4.23	49.2	0.095	0.46	0.22	0.57	0.13	0.45	0.14	0.54
7.07	37.2	0.14	0.47	0.25	0.58	0.20	0.45	0.19	0.55
7.07	43.2	0.15	0.64	0.35	0.76	0.24	0.61	0.29	0.72
7.07	49.2	0.16	0.82	0.43	0.94	0.25	0.79	0.33	0.91

namely, single ion/atom collisions and impulsive energy transfer. In particular, the long-range forces give rise to torques on the molecule at large distances; the torques lock the motion of the target about the relative position $\vec{R}$, hinder its rotation and thus hamper rotational excitation. This mechanism is inherently due to multiple interactions between A and the target atoms, and is also of a nonimpulsive nature because the torques act long before and long after the instant of closest approach. However, the lock-in effect may be readily modeled within the single-collision impulsive approximation by replacing the moment of inertia of the molecule I_B, in eq. (4.1.3), with an effective one I_{eff}, obtained as follows.

Table 4.2 shows that, on the average, the calculated $\langle \epsilon_R \rangle_0$ are larger than the experimental values by a factor of 3 for Li^+/N_2 and 4.2 for Li^+/CO. Therefore, the cross sections were reevaluated with $I_{eff} = 3I_B$ for N_2 and $I_{eff} = 4.2I_B$ for CO. This single adjustment, kept the same for all collision energies and scattering angles, yields good agreement between the calculated and measured $\langle \epsilon_R \rangle_0$. We must emphasize that the replacement $I_B \rightarrow I_{eff}$ does not affect the probabilities of vibrational excitation because it is done only in the rotational correlation. Furthermore, once the excess of rotational excitation is corrected, the average total energy transfer predicted by the model agrees with the experimental one, as is seen in table 4.3. This indicates that, at hyperthermal energies and large scattering angles, the vibrational excitation of the diatomic is well described by the single-collision impulsive model. In table 4.4 we present the relative probabilities of vibrational transition, $d\sigma(n; E,\theta) / d\Omega(0; E,\theta)$, for the Li^+N_2 and Li^+/CO systems. Examining these quantities, we find that the vibrational excitation of

Table 4.3. Average rotational energy transfer $\langle \epsilon_R \rangle_0$ for no vibrational excitation and average total energy transfer $\langle \epsilon \rangle$. Theoretical values are calculated with the effective moment of inertia $I_{eff} = 4.2 I_B$ for CO and $I_{eff} = 3.0\ I_B$ for N_2.

E (eV)	θ (deg)	Li^+/CO				Li^+/N_2			
		$\langle \epsilon_R \rangle_0$ (eV)		$\langle \epsilon \rangle$ (eV)		$\langle \epsilon_R \rangle_0$ (eV)		$\langle \epsilon \rangle$ (eV)	
		exp.	th.	exp.	th.	exp.	th.	exp.	th.
4.23	37.1	0.087	0.065	0.13	0.17	0.085	0.086	0.080	0.18
4.23	43.2	0.090	0.089	0.17	0.22	0.092	0.12	0.093	0.24
4.23	49.2	0.095	0.12	0.22	0.28	0.13	0.15	0.14	0.30
7.07	37.2	0.14	0.11	0.25	0.28	0.20	0.15	0.19	0.31
7.07	43.2	0.15	0.16	0.35	0.37	0.24	0.21	0.29	0.40
7.07	49.2	0.16	0.21	0.43	0.45	0.25	0.28	0.33	0.50

Table 4.4. Relative probability of vibrational transition $d\sigma(n; E,\theta)/d\sigma(0; E,\theta)$.

E (eV)	θ (deg)	Li^+/CO			Li^+/N_2		
		n=-1	n=-2	n=-3	n=-1	n=-2	n=-3
4.23	37.1	0.296	0.096	0.027	0.277	0.078	0.018
4.23	43.2	0.350	0.140	0.050	0.334	0.119	0.035
4.23	49.2	0.394	0.185	0.079	0.382	0.164	0.060
7.07	37.2	0.391	0.186	0.082	0.381	0.166	0.063
7.07	43.2	0.435	0.243	0.130	0.430	0.227	0.108
7.07	49.2	0.464	0.289	0.177	0.463	0.280	0.158

both targets increases with increasing scattering angle and energy; however, CO is more readily excited than is N_2. Although experimental values of probabilities of vibrational excitation are not available at the present time, the predictions of the model follow the trends observed in the measured time-of-flight spectra (figs. 3 and 4 of Bottner et al., 1976).

3. Evaluation of the Atom-Pair Correlation Function of a Linear Triatomic Molecule

For a linear triatomic, we may write the equilibrium positions of its atoms as $\vec{d}_a = d_a\vec{d}$, where $\vec{d}$ is a unit vector in the direction of the molecular axis, from atom 1 to atom 3. By means of eq. (2.2.1a), we obtain expressions that relate the d_a to the equilibriumbond-lengths d_{12} and d_{23}, with d_{12}, $d_{23} > 0$; these are

$$d_1 = -(m_2 d_{12} + m_1 d_{13})/m_B, \tag{4.3.1a}$$

$$d_2 = (m_1 d_{12} - m_3 d_{23})/m_B, \tag{4.3.1b}$$

$$d_3 = (m_1 d_{13} + m_2 d_{23})/m_B, \tag{4.3.1c}$$

where $d_{13} = d_{12} + d_{23}$ and m_B is the mass of the molecule. Furthermore, eqs. (2.2.1) show that a linear triatomic has four free vibrational displacements and thus four internal coordinates s_i. Two of these, s_i and s_3, are conventionally taken to be the changes in bond lengths of the atom pairs (1,2) and (2,3), respectively; the other two, s_2 and $s_{2'}$, are then the changes in the bond angles that lie on two mutually perpendicular planes. Due to the cylindrical symmetry of the molecule, s_2 and $s_{2'}$ are

degenerate, so we may choose s_2 to lie on the plane that contains $\vec{\kappa}$ and $\vec{d}$. Since $s_{2'}$ is thus perpendicular to $\vec{\kappa}$ and the APCF depends only on $\vec{\kappa} \cdot \vec{r}_a$, the APCF is independent of $s_{2'}$ and this coordinate need not be considered further. However, an elementary geometrical analysis shows that, for small displacements $\vec{u}_a$,

$$s_2 = [d_{23}(\vec{u}_1)_\perp - d_{13}(\vec{u}_2)_\perp + d_{12}(\vec{u}_3)_\perp]/(d_{12}d_{23}) \tag{4.3.2}$$

where $(\vec{u}_a)_\perp$ is the component of $\vec{u}_a$ in the $(\vec{\kappa}, \vec{d})$ plane and perpendicular to $\vec{d}$; this direction is given by the unit vector

$$\vec{d}_\perp = (\vec{\kappa}/\kappa - \cos\beta\ \vec{d})/\sin\beta, \tag{4.3.3}$$

in which β is the angle between $\vec{\kappa}$ and $\vec{d}$. Using eqs. (2.2.1) and (4.3.2), we find that the Cartesian displacements are related to the internal coordinates by

$$\vec{u}_1 = \{(m_2m_3d_{12}d_{23}^2/I_B)\ s_2\vec{d}_\perp + [(m_2 + m_3)s_1 - m_3s_3]\vec{d}\}/m_B, \tag{4.3.4a}$$

$$\vec{u}_2 = [-(m_1m_3d_{12}d_{23}d_{13}/I_B)s_2\vec{d}_\perp - (m_1s_1 + m_3s_3)\vec{d}]/m_B, \tag{4.3.4b}$$

$$\vec{u}_3 = \{(m_1m_2d_{12}^2d_{23}/I_B)s_2\vec{d}_\perp + [-m_1s_1 + (m_1 + m_2)s_3]\vec{d}\}/m_B; \tag{4.3.4c}$$

here, I_B is the moment of inertia of the triatomic.

We take the harmonic vibrational potential to be the usual generalized quadratic valence-force-field (Jones, 1971, Chap. 1); this is given by

$$V_h(\vec{s}) = \sum_{i=1}^{3} k_{ii}s_i^2/2 + k_{13}s_1s_3. \qquad (4.3.5)$$

Carrying out the normal-mode analysis of eqs. (2.3.8-14), we obtain the harmonic frequencies

$$\omega_{1,3}^2 = \{ b \mp [b^2 + 4m_1m_2m_3m_B(k_{13}^2 - k_{11}k_{33})]^{\frac{1}{2}}\}/(2m_1m_2m_3), \qquad (4.3.6a)$$

$$\omega_2^2 = m_BI_Bk_{22}/(m_1m_2m_3d_{12}^2d_{23}^2), \qquad (4.3.6b)$$

$$b = (m_1 + m_2)m_3k_{11} + m_1(m_2 + m_3)k_{33} + 2m_1m_3k_{13}, \qquad (4.3.6c)$$

and the normal coordinates Q_j, j = 1 to 3, that correspond to the symmetric stretching, bending and assymmetric stretching modes, respectively. Furthermore, we find that the coefficients (a_{ij}) of the transformation from normal to internal displacements s_i are given by

$$a_{1j} = (m_1m_3\omega_j^2 + m_Bk_{13})/c_j \quad \text{for j = 1 and 3,} \qquad (4.3.7a)$$

$$a_{22} = [m_BI_B/(m_1m_2m_3d_{12}^2d_{23}^2)]^{\frac{1}{2}}, \qquad (4.3.7b)$$

$$a_{3j} = [m_1(m_2 + m_3)\omega_j^2 - m_Bk_{11}]/c_j \quad \text{for j = 1 and 3,} \qquad (4.3.7c)$$

$$c_j = \{ m_1m_2m_3\omega_j^2 [m_1(m_2 + m_3)\omega_j^2 - 2m_Bk_{11}] +$$

$$+ m_B[m_1m_3(k_{13} + k_{11})^2 + m_2(m_1k_{13}^2 + m_3k_{13}^2)]^{\frac{1}{2}}\}. \qquad (4.3.7d)$$

Combining eqs. (4.3, 4, 6), we arrive at the vectors $\vec{C}_{aj}$ that relate the

cartesian displacements to the normal ones; the expressions for the $\vec{C}_{aj}$ are rather long and not very illuminating, so they are not reproduced here.

The commutators $([\hat{H}_R,)^n \exp(-i\vec{\kappa} \cdot \hat{\vec{d}}_a)]$ required for the rotational energy transfers and widths, have already been evaluated in Sec. 1, for any linear polyatomic. Equation (4.1.3) shows that if atom a is at the center of mass of the molecule, then $\vec{d}_a = \vec{0}$ so that such an atom does not absorb rotational energy; this is the case, for example, of the carbon atom in CO_2. Finally, the evaluation of the APCF may be completed by approximating the quantal average over the distribution of initial rotational states by means of the classical statistical average, as discussed in Sec. 1.

4. Rotational and Vibrational Energy Transfer in Hyperthermal Collisions of Li^+ with CO

We have calculated average energy transfers and probabilities of vibrational excitation for the system Li^+/CO_2, at the CM collision energies and scattering angles studied in crossed-molecular-beams experiments by Eastes et al., 1977. In these calculations the vibrational motion of CO_2 was approximated by the harmonic model described above; the effects of molecular anharmonicity in CO_2 are discussed in the following section. The values of the parameters required for the APCF of CO_2 (taken from Jones, 1971, Chap. 2) and the harmonic frequencies obtained from eq. (4.3.6) are shown in table 4.5. The target vibrational temperature was taken to be T_v = 300K, as assumed in the experiments. The ion/atom cross sections σ_a were approximated by the classical elastic

Table 4.5 Parameters for the atom-pair correlation function of CO_2

$m_1 = m_3$ (amu)	15.9994
m_2 (amu)	12.0111
$d_{12} = d_{23}$ (Å)	1.161
$k_{11} = k_{33}$ (mdyn/Å)	16.0250
k_{22} (mdyn Å/rad^2)	0.7854
k_{13} (mdyn/Å)	1.263
$\hbar\omega_1$ (eV)	0.1551
$\hbar\omega_2$ (eV)	0.08345
$\hbar\omega_3$ (eV)	0.3214

Table 4.6 Probabilities of vibrational excitation $d\sigma(\vec{n};E,\theta)/d\sigma(\vec{0};E,\theta)$ in Li^+/CO_2 vs. center of mass collision energy E and scattering angle θ.

θ (deg)	$d\sigma(\vec{n};E,\theta)/d\sigma(\vec{0};E,\theta)$					
	$-\vec{n}=(0,1,0)$		$-\vec{n}=(0,2,0)$ and $(1,0,0)$		$-\vec{n}=(0,3,0)$ and $(1,1,0)$	
	exp.	th.	exp.	th.	exp.	th.
	E=2.81eV		$2\theta_r \simeq 30$ deg			
23.1	0.50	0.20	0.45	0.19	0.22	0.022
34.6	0.67	0.46	0.70	0.45	0.36	0.11
	E=4.72eV		$2\theta_r \simeq 19$ deg			
14.6	0.69	0.13	0.51	0.13	0.25	0.010
15.1	0.73	0.14	0.54	0.14	0.28	0.011
16.8	0.77	0.18	0.65	0.17	0.34	0.018
29.4	0.75	0.57	0.89	0.57	0.45	0.18
35.1	0.70	0.82	1.11	0.87	0.58	0.38
	E=6.87eV		$2\theta_r \simeq 15$ deg			
8.7	0.55	0.069	0.35	0.064	0.14	0.003
11.0	0.67	0.11	0.55	0.10	0.36	0.007
12.2	0.78	0.14	0.67	0.13	0.45	0.010
13.3	0.79	0.16	0.70	0.15	0.46	0.015
16.8	0.82	0.26	0.80	0.25	0.52	0.039
20.2	0.88	0.39	0.90	0.38	0.55	0.083
22.6	0.91	0.49	1.01	0.48	0.60	0.13

differential cross sections for the short range ion/atom potentials developed for Li^+/CO_2 in Sec. 3.4.

In table 4.6, we compare the calculated and experimental values of the relative probabilities of excitation of the vibrational modes of CO_2, $d\sigma(\vec{n}; E, \theta)/d\sigma(\vec{0}; E, \theta)$. This comparison shows good agreement in the ordering of the probabilites and in their trends with scattering energy and angle. The magnitudes of the calculated probabilities come closer to the experimental values as the scattering angle θ increases beyong twice the rainbow angle (for the collision energies E = 2.81 eV, 4.72 eV and 6.87 eV the experimentally measured rainbow angles are approximately θ_r = 15.0, 9.5 and 7.5 deg, respectively). This suggests that at angles well beyond $2\theta_r$, collisional vibrational excitation is mediated by single ion/atom impulsive collisions; however, for smaller scattering angles (which correspond to distant collisions) the projectiles do not probe the repulsive cores of the potential to the same extent. As θ decreases, the dynamical effects of the long-range forces become appreciable, so the single-collision impulsive model does not suffice to describe vibrational excitation. This analysis may help explain some puzzling results of experiments with the systems Li^+/CF_4 and Li^+/SF_6 (Ellenbroek et al., 1979 and 1980), where a radical change in the behaviour of the average energy transfer occurs at scattering angles corresponding to about $2\theta_r$. These measurements indicate that the mechanism by which energy is transfered at small angles is quite different than the one that predominates at large angles. Theoretical calculations for the systems Li^+/CF_4 and Li^+/SF_6 are now being planed, in order to test this hypothesis.

In table 4.7 we present the experimental and calculated average energy transfers, for angles greater than $2\theta_r$. We find that the model predicts

Table 4.7 Average energy transfer $\langle\varepsilon\rangle$ for the Li^+/CO_2 system.

E (eV)	θ (deg)	$\langle\varepsilon\rangle$(eV) exp.	th.[a]	th.[b]
2.81	34.6	0.15	0.22	0.20
4.72	29.4	0.17	0.26	0.24
4.72	35.1	0.33	0.36	0.33
6.87	20.2	0.24	0.19	0.17
6.87	22.6	0.26	0.23	0.21

[a] Calculated with the actual moment of inertia I_B.

[b] Calculated with the effective moment of inertia $I_{eff} = 1.2I_B$.

their correct dependence on angle and energy, although there is some overestimate of the rotational excitation of CO_2, as in the case of Li^+/N_2 and Li^+/CO. For example, at E = 6.87 eV and θ = 22.6 deg, the calculated and experimental values of $\langle\varepsilon\rangle$ are in good agreement, but the vibrational contribution to $\langle\varepsilon\rangle$ is too low (c. f. the last line of table 4.6) and the rotational one too high. As discussed in Sec. 3, we expect the model to predict too much rotational excitation because the lock-in effect of the long-range forces is not included. In order to model this effect, the calculations were redone with an effective moment of inertia for CO_2. The value $I_{eff} = 1.2I_B$ was chosen to reproduce the experimental value of $\langle\varepsilon\rangle$ at E = 4.72 eV and θ = 35.1 deg, which is the angle farthest from $2\theta_r$. This single value of I_{eff}, which is independent of scattering angle and energy, brought the calculated average energy transfer into better agreement with the experiment for $\theta >> 2\theta_r$, as is shown in the third column of table 4.7.

Figure 4.3 shows the dependence on scattering angle of the relative probabilities of vibrational excitation of CO_2, at E = 4.72 eV. The increase in excitation with increasing angle agrees with the experimental trends, and we see improved agreement in the magnitudes of the probabilities at angles larger than $2\theta_r$. Examination of fig. 4.3 shows that at smaller angels, the short-range forces also contribute to the vibrational excitation; therefore, a theoretical model that will describe small- and large-angle hyperthermal collisions must include the dynamical effects of short- and long-range forces; this is the subject of the following chapter. However, before proceeding to a new theoretical development, we will calculate the effects of molecular anharmonicity on the vibrational excitation of the targets studied above.

Figure 4.1 Calculated probabilities of vibrational excitation vs. center of mass scattering angle (full line). Experimental results: $\vec{n}=(0,1,0)$, ⊙; $-\vec{n}=(0,2,0)$ and $(1,0,0)$, △; $-\vec{n}=(0,3,0)$ and $(1,1,0)$, ▣ . Dashed curves correspond to angles in the vicinity of or smaller than twice the experimentally measured rainbow angle.

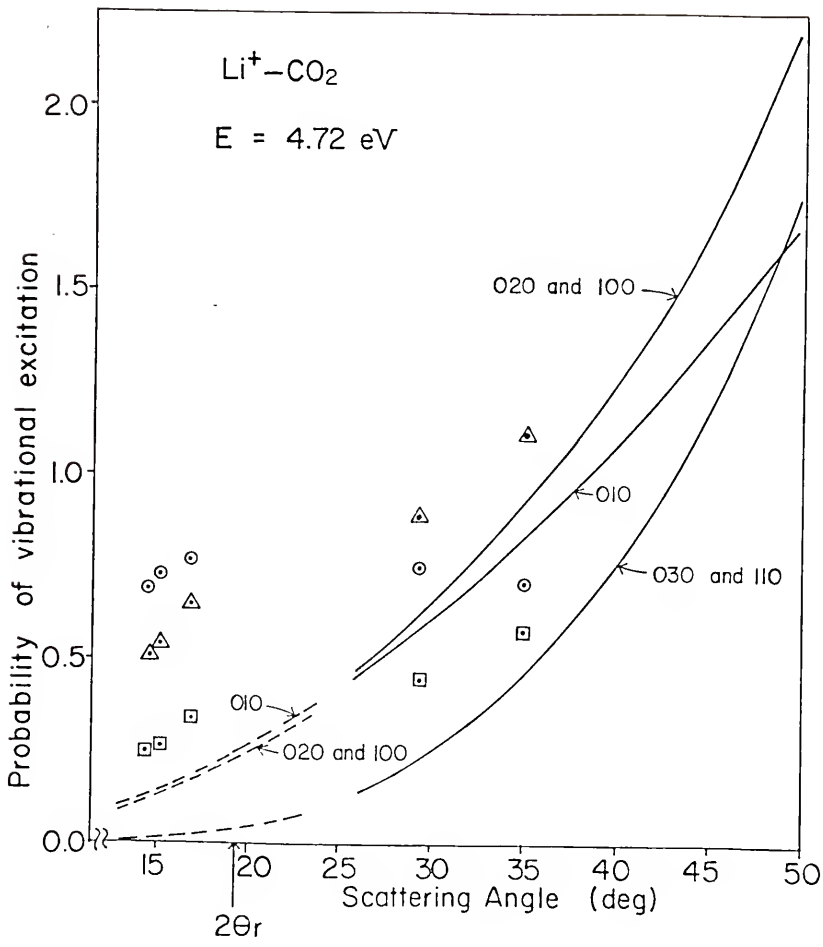
Li+–CO2
E = 4.72 eV
020 and 100
010
030 and 110
010
020 and 100
Probability of vibrational excitation
2.0
1.5
1.0
0.5
0.0
15
20
25
30
35
40
45
50
Scattering Angle (deg)
2θr

5. Effects of Molecular Anharmonicity in N_2, CO and CO_2

As discussed in Sec. 2.5, in hyperthermal atom-polyatomic collisions, the effects of molecular anharmonicity may be interpreted in terms of a shift in the vibrational spectrum of the target, from the harmonic frequencies ω_i to the effective ones $\bar{\omega}_i$. For a diatomic, and for a polyatomic in which the anharmonic couplings between different normal coordinates are zero, the $\bar{\omega}_i$ are given by the simple relation (2.4.17). However, when anharmonic intercoordinate couplings are nonzero, evaluation of the $\bar{\omega}_i$ requires the following procedure. Firstly, the displacement-displacement Green function is obtained by solving the matrix equation (2.4.21). Next, one evaluates the second moment of the exact spectral function; this requires knowledge of the vibrational averages $\langle\langle\hat{Q}_i\hat{Q}_j\rangle\rangle_V$ and $\langle\langle\hat{Q}_i\hat{f}_j\rangle\rangle_V$, which usually can not be obtained in a closed form. Finally, the decoupling coefficients b_{ij} are adjusted to reproduce the second moment of the exact spectral function, which leads to a matrix equation for the b_{ij}, analogous to eq. (2.4.17). In order to avoid extensive calculations that would take us far from the purpose of this dissertation, we now estimate the effects of anharmonicity in CO_2 by considering only the bending mode (Q_2) and neglecting the anharmonic couplings to the stretching modes. Within this model, we can obtain the effective bending frequency $\bar{\omega}_2$ by means of the techniques utilized for a diatomic, as shown below. We will return to the effects of anharmonic couplings between the normal modes, at the end of this section.

Since the vibrational potential is an analytical function of the internal coordinate s_i, we take its anharmonic part V_{anh} to be of the form

$$V_{anh}(s_i) = \sum_{\ell>2} k_i^{(\ell)} s_i^{\ell}, \qquad (4.5.1a)$$

$$k_i^{(\ell)} = \frac{1}{\ell!} \frac{\partial^\ell}{\partial s_i^\ell} V_{anh} \Big|_{s_i = 0}; \tag{4.5.1b}$$

For a diatomic, s_1 is the change in bond length, while for CO_2 s_2 is the change in the valence angle. Hence, the vibrational Hamiltonian for the normal coordinate Q_i is

$$\hat{H}_V = \hat{H}_h + \hat{V}_{anh}, \tag{4.5.2a}$$

$$\hat{H}_h = (\hat{P}_i^2 + \omega_i^2 \hat{Q}_i^2)/2, \tag{4.5.2b}$$

$$\hat{V}_{anh} = \sum_{\ell>2} a_i^\ell k_i^{(\ell)} \hat{Q}_i^\ell; \tag{4.5.2c}$$

here, $a_1 = [(m_1 + m_2)/(m_1 m_2)]^{\frac{1}{2}}$ for a diatomic, while for the bending mode of CO_2 $a_2 = a_{22}$, with a_{22} defined in eq. (4.3.7b). The solution of eq. (2.4.17) requires the averages

$$\langle\langle \hat{Q}_i^2 \rangle\rangle_V = [\mathrm{Tr}\ \hat{\rho}_V(\Theta)]^{-1}\ \mathrm{Tr}[\hat{\rho}_V(\Theta)\hat{Q}_i^2], \tag{4.5.3a}$$

$$\langle\langle \hat{Q}_i \hat{f}_i \rangle\rangle_V = [\mathrm{Tr}\ \hat{\rho}_V(\Theta)]^{-1}\ \mathrm{Tr}[\hat{\rho}_V(\Theta) \sum_{\ell>2} \ell a_i^\ell k_i^{(\ell)} \hat{Q}_i^\ell], \tag{4.5.3b}$$

$$\hat{\rho}_V(\Theta) = \exp(-\Theta \hat{H}_V), \tag{4.5.3c}$$

where $\hat{\rho}_V(\Theta)$ is the density operator for the distribution of initial vibrational states, and $\Theta = 1/(k_B T_V)$. However, from eqs. (4.5.2) we have that

$$\frac{\partial \hat{\rho}_V(\Theta)}{\partial \omega_i} = -\Theta \omega_i \hat{\rho}_V(\Theta) \hat{Q}_i^2, \tag{4.5.4a}$$

$$\frac{\partial \hat{\rho}_V(\Theta)}{\partial a_i} = -\Theta \hat{\rho}_V(\Theta) \sum_{\ell>2} \ell a_i^{\ell-1} k_i^{(\ell)} \hat{Q}_i, \tag{4.5.4b}$$

so eq. (2.4.17) may be written in terms of the vibrational partition function $Z_V(\Theta) = \mathrm{Tr}\hat{\rho}_V(\Theta)$, as follows:

$$\hbar\bar{\omega}_i \coth\bar{\alpha}_i = \frac{-2}{\Theta} \left(\omega_i \frac{\partial}{\partial \omega_i} + a_i \frac{\partial}{\partial a_i}\right) \ell n\, Z_V(\Theta). \tag{4.5.5}$$

In the experiments discussed above, $\hbar\omega_i/(k_B T_V) >> 1$, so that only the lowest vibrational levels are significantly populated. In these states, the vibrational displacements are small, so that $|V_{anh}| << \omega_i^2 Q^2/2$, and $Z_V(\Theta)$ may be evaluated by finite-temperature perturbation theory. Considering V_{anh} as a perturbation on the harmonic density operator $\exp(-\Theta\hat{H}_h)$, we make the ansatz $\hat{\rho}_V(\Theta) = \exp(-\Theta\hat{H}_h)\hat{U}(\Theta)$. Differentiating both sides of this relation with respect to Θ and rearranging terms, we find that $\hat{U}(\Theta)$ satisfies the well-known equation (Messiah, 1961, Vol. 1, Chap. 8)

$$\frac{\partial \hat{U}}{\partial \Theta}(\Theta) = -\hat{V}(\Theta)\hat{U}(\Theta), \tag{4.5.6a}$$

$$\hat{V}(\Theta) = \exp(\Theta \hat{H}_h)\hat{V}_{anh} \exp(-\Theta\hat{H}_h) \tag{4.5.6b}$$

with the boundary condition $\hat{U}(0) = \hat{1}$; this has the formal solution

$$\hat{U}(\Theta) = 1 - \int_0^\Theta d\Theta' \hat{V}(\Theta')\hat{U}(\Theta'). \tag{4.5.7}$$

Iterating eq. (4.5.7) we obtain an expansion of $\hat{\rho}_V(\Theta)$ in terms of the anharmonic potential; this is

$$\hat{\rho}_V(\Theta) = \exp(-\Theta\hat{H}_h)[1 - \int_0^\Theta d\Theta'\hat{V}(\Theta') + \int_0^\Theta d\Theta'\hat{V}(\Theta') \int_0^{\Theta'} d\Theta''\hat{V}(\Theta'')-\cdots]. \qquad (4.5.8)$$

Since the trace of an operator is independent of the choice of basis used to evaluate it, the traces of the terms on the right of eq. (4.5.8) may be readily calculated in the harmonic basis, by means of the algebra of creation and annihilation operators (Messiah, 1961, Vol. 1, Chap. 12). In particular, for a cubic plus quartic anharmonicity ($k_i^{(\ell)} = 0$ for $\ell>4$), we thus find that, to leading order in $k_i^{(3)}$ and $k_i^{(4)}$, the partition function is given by

$$Z_V(\Theta) = 2\text{cosech}\alpha_i - (a_i^4 \hbar^2 k_i^{(4)} \Theta/2\omega_i^2)[(1 + \cosh^2\alpha_i)\ \text{cosech}^2\alpha_i +$$

$$+ (\coth\alpha_i)/\alpha_i]\text{cosech}\alpha_i + [a_i^6(k_i^{(3)})^2 \hbar^2\Theta/32\omega_i^4][5 + 4\sinh^2\alpha_i +$$

$$+ \exp(-2\alpha_i)/2]\ \text{cosech}^3\alpha_i + \ldots \qquad (4.5.9)$$

where $\alpha_i = \Theta\hbar\omega_i/2$. Substituting eq. (4.5.9) into eq. (4.5.5) and performing the indicated differentiations, yields the following expression for the shift in frequency $(\bar{\omega}_i - \omega_i)/\omega_i$ and for the decoupling parameter b_i,

$$(\bar{\omega}_i - \omega_i)/\omega_i \approx -b_i/2\omega_i^2 \approx$$

$$\approx (a_i^4 \hbar\, k_i^{(4)}/\omega_i^3)(\coth\alpha_i + \text{sech}\alpha_i\ \text{cosech}\alpha_i + 1/\alpha_i) -$$

$$- [3a_i^6\ (k_i^{(3)})^2\hbar/8\omega_i^5]\ \{\tanh\ \alpha_i +$$

$$+ [10 + \exp\ (-2\alpha_i)]\ (\text{sech}\ \alpha_i\ \text{cosech}\alpha_i)/8\ \} + \ldots \qquad (4.5.10)$$

Table 4.8. Cubic ($k_i^{(3)}$), quartic ($k_i^{(4)}$) force constants and resulting frequency shifts due to anharmonic forces in N_2, CO and in the bending mode of CO_2, for vibrational temperature T_V = 300 K.

	$k_i^{(3)}$ (eV/Å^3)	$k_i^{(4)}$ (eV/Å^4)	$(\bar{\omega}_i - \omega_i)/\omega_i$ (%)
N_2	-190.0	291.4	0.49
CO	-132.6	176.8	0.30
CO_2	0	-0.4057[a)]	-0.26

a) in eV/rad^4

Using spectroscopic values of the cubic and quartic force constants of N_2, CO (Herzberg, 1965) and of the bending mode of CO_2 (Pariseau et al., 1965), we obtain the frequency shifts presented in table 4.8, for the vibrational temperature T_V = 300K assumed in the experiments. These results indicate that, at hyperthermal collision energies, molecular anharmonicity contributes less than 1% to the vibrational energy transferred to these targets. This is not unexpected, since at high relative energies, the target does not have time to react to the collision; hence, the effects of anharmonicity on the time-evolution of the displacements are not highly significant during the brief time in which energy is transferred. For the same reason, we expect that intercoordinate anharmonic couplings in CO_2 will not play a large role in its vibrational excitation by hyperthermal projectiles. The main effect of these couplings is to cause mixing of the normal coordinates Q_i; however, during the brief transfer-times, the extent of the mixing should be negligible.

CHAPTER V
A SEMICLASSICAL CORRELATION FUNCTION APPROACH TO MOLECULAR COLLISIONS

We develop a new correlation function approach to the description of vibrational and rotational energy transfer in the collision of two polyatomic molecules A and B. In order to focus our attention on vibrational and rotational excitation, we take A and B to have closed electronic shells and we consider the range of collision energies above 1 eV, but below the thresholds for electronic excitation and/or dissociation of the molecules. For large molecules and at high relative energies, the wavelength of relative motion is usually much smaller than the lengths over which the intermolecular potential changes appreciably; in these cases, the relative motion between A and B may be described by means of classical mechanics. However, the experiments mentioned in the Introduction clearly indicate that the internal dynamics of the molecules must be described quantum mechanically. By combining classical relative trajectories with a quantal treatment of the internal degrees of freedom, as reviewed in Sec. 1, one arrives at the well-known semiclassical model of the collision, also called time-dependent or classical path approximation (Child, 1976, Dickinson, 1979). This approach has been recently applied to the study of vibrational excitation in atom-molecule (McCann and Flannery, 1978, 1979, Billing, 1976, 1979a) and molecule-molecule

scattering (Billing, 1978, 1979b, 1980). These studies are based on expanding the internal-wave function in a basis set of states of the isolated molecules, with time-dependent coefficients. The differential equations that describe the time evolution of the coefficients are then integrated numerically to obtain transition amplitudes and probabilities. At the present time, the applications of this method are restricted to thermal collision energies because, in the hyperthermal regime, the number of energetically accessible states is unmanageably large.

The limitations of the previous approaches are avoided with the use of correlation function techniques, which we introduce in Sec. 2. In particular, we find that the differential probability of energy transfer (DPET) is closely related to the time-correlation function of the semiclassical evolution operator. In Sec. 4, we evaluate this operator by means of a procedure that contains the intermolecular potential to infinite order. In the following three sections, we calculate the correlation function of large polyatomics, without need of internal-state expansions. In Sec. 8, we thus obtain simple analytical expressions for the DPET in terms of certain vibrational and rotational action integrals. The actions correspond to the forces that the intermolecular potential exerts on the molecular atoms, throughout the course of the relative motion. Since the action integrals contain the full potential, the present approach is applicable to hyperthermal molecular collisions over a wide range of scattering angles. A further advantage of the present approach lies in the fact

that the correlation function contains from the outset the averages over initial experimental distributions; hence, one needs to calculate only quantities that are directly related to experimental measurements.

1. The Semiclassical Approximation

In the collision of two large molecules with reduced mass $M = M_A M_B/(M_A+M_B)$ and at hyperthermal relative energy E, the wavelength for relative motion $\lambda=2\pi\hbar/(2ME)^{\frac{1}{2}}$ is usually much smaller than the lengths over which the intermolecular potential changes appreciably; in these cases the relative motion may be described by a classical trajectory $\vec{R}(t)$. Indicating operators with carats, in the coordinate representation the relative kinetic energy operator is approximately given by the classical expression

$$\langle\vec{R}'|\hat{K}|\vec{R}\rangle \approx \delta(\vec{R}-\vec{R}')\ K(t), \tag{5.1.1a}$$

$$K(t) = \vec{P}^2(t)/(2M), \tag{5.1.1b}$$

where $\vec{P}(t)$ is the relative momentum. Ideally, the classical dynamical variables $\vec{R}(t)$ and $\vec{P}(t)$ must be obtained from the solution of 6N Hamilton's equations of motion for the N-body problem (Goldstein, 1956, Chap. 7), where $N = N^{(A)} + N^{(B)}$ and $N^{(X)}$ is the number of atoms of the polyatomic X = A and B. For many experimental conditions of interest (e.g. quasielastic scattering, small detection angles, etc.), one may introduce approximations into the dynamics of relative motion that considerably simplify the evaluation of $\vec{R}(t)$; these approximations are not essential to the present development, so we postpone their consideration to Sec. 8.

The classical trajectory (whether exact or approximate) depends parametrically on the set of initial conditions. These are usually taken to be the initial values of the impact parameter, the relative momentum, the azimuthal angle of $\vec{R}(-\infty)$, and the initial values of the action and angle variables of the internal motions of A and of B (Porter and Raff, 1976). In most scattering experiments, only a subset of the final conditions is specified; in particular, the time-of-flight experiments mentioned in the Introduction only measure the magnitudes of the final deflection angle and of the relative velocity. In these cases, it may occur that more than one set of values of initial conditions originate different trajectories $\vec{R}^{(\ell)}(t), \ell = 1, 2, 3, \ldots$, that lead to the measured final conditions; this is the origin of the well-known rainbow effect in elastic scattering. In order to simplify the notation, throughout most of the present treatment we omit the index ℓ; we explicitly consider different trajectories that lead to the same final conditions only when they affect the theoretical development.

Within the semiclassical model, the Hamiltonian operator that governs the internal dynamics of the molecules during the collision is given by

$$\hat{H}(t) = K(t) + \hat{H}_M + \hat{V}(t), \tag{5.1.2a}$$

$$\hat{V}(t) \equiv V(\vec{R}(t), \hat{\vec{r}}^M). \tag{5.1.2b}$$

Here, $\hat{H}_M$ is the sum of the internal Hamiltonians of the noninteracting polyatomics and $V(\vec{R}, \vec{r}^M)$ is the intermolecular potential. The

potential depends on the position of A relative to the center of mass (CM) of B, and on $\vec{r}^{M}=\{\vec{r}^{(A)}, \vec{r}^{(B)}\}$, where $\vec{r}^{(X)}$ denotes the set of positions of the atoms of molecule X = A or B with respect to the CM of X. The time dependence of $\hat{V}(t)$ arises from that of the classical relative trajectory; furthermore, $\hat{V}(t)$ is an operator that acts on the internal states of the polyatomics.

Initially, A and B are isolated from each other and in the state $|\nu>$, where ν denotes the collection of their quantum numbers (rotational and vibrational), we then have that

$$\hat{H}_M |\nu> = E_\nu |\nu>, \tag{5.1.3}$$

in which E_ν is the sum of the internal energies of A and of B. During the collision $|\nu>$ evolves into $|\nu ,t>$, in accordance with the semiclassical Hamiltonian, as indicated below.

$$[i\hbar\partial/\partial t - \hat{H}(t)]|\nu,t> = 0, \tag{5.1.4a}$$

$$\lim_{t\to-\infty} |\nu,t> = |\nu>. \tag{5.1.4b}$$

Therefore, the probability that A and B will make a transition between the initial state $|\nu>$ and a final one $|\nu'>$ is given by

$$W_{\nu'\nu} = \lim_{t\to\infty} |<\nu'|\nu,t>|^2 = \tag{5.1.5a}$$

$$= \lim_{\substack{t\to\infty \\ t_i\to-\infty}} |<\nu',t_i|\nu,t>|^2. \tag{5.1.5b}$$

Before proceeding to the evaluation of $W_{\nu'\nu}$, it will prove convenient to separate the time evolution of $|\nu,t\rangle$ into a part that corresponds to the motion of the noninteracting polyatomics and another one that explicitly contains the intermolecular forces. This separation is readily achieved in the interaction representation, as follows (Messiah, 1961, Vol. 1, Chap. 8).

Firstly, one writes for the Hamiltonian

$$\hat{H}(t) = \hat{H}_i + \Delta K(t) + \hat{V}(t), \tag{5.1.6a}$$

$$\hat{H}_i = \lim_{t\to-\infty} \hat{H}(t) = \vec{P}_i^2/(2M) + \hat{H}_M, \tag{5.1.6b}$$

$$\Delta K(t)=[\vec{P}^2(t) - \vec{P}_i^2]/(2M), \tag{5.1.6c}$$

where $\vec{P}_i$ is the initial relative momentum. Next, the state $|\nu,t\rangle$ is written as

$$|\nu,t\rangle = \exp[-i\hat{H}_i(t-t_i)/\hbar]\hat{U}(t,t_i)|\nu,t_i\rangle, \tag{5.1.7}$$

where $\hat{U}(t,t_i)$ is the time-evolution operator in the interaction representation. Substituting eq. (5.1.7) into eqs. (5.1.4), one finds that $\hat{U}(t,t_i)$ is determined by

$$[i\hbar\partial/\partial t - \hat{H}'(t,t_i)]\hat{U}(t,t_i) = \hat{0}, \tag{5.1.8a}$$

$$\hat{U}(t,t) = \hat{1}, \tag{5.1.8b}$$

$$\hat{H}'(t,t_i) = \Delta K(t) + \exp[i\hat{H}_i(t-t_i)/\hbar]\hat{V}(t)\exp[-i\hat{H}_i(t-t_i)/\hbar], \tag{5.1.8c}$$

where we have used the fact that $[\Delta K, \hat{H}_M] = \hat{0}$ because ΔK contains only classical dynamical variables. Finally, replacing eq. (5.1.7) into eq. (5.1.5b) and using eq. (5.1.3), one obtains

$$W_{\nu'\nu} = |\langle\nu'|\hat{U}(\infty,-\infty)|\nu\rangle|^2. \tag{5.1.9}$$

Whenever more than one trajectory $\hat{R}^{(\ell)}(t)$ leads to the same subset of final conditions eq. (5.1.9) may be extended as follows. To each trajectory there corresponds an evolution operator $\hat{U}^{(\ell)}(t,t_i)$ with an associated transition amplitude $\langle\nu'|\hat{U}^{(\ell)}(\infty, -\infty)|\nu\rangle$. As we shall see below, the transition amplitudes contain phases that depend on the initial conditions. In most cases of interest, for different trajectories the phases differ by a large amount, so that one may use the "primitive" semiclassical approximation (Berry and Mount, 1972),

$$W_{\nu'\nu} = |\langle\nu'|\sum_{\ell} c_\ell \hat{U}^{(\ell)}(\infty,-\infty)|\nu\rangle|^2. \tag{5.1.10}$$

Here, the coefficients c_ℓ are related to the Jacobian of the transformation from initial to final classical dynamical variables. Whenever the phase differences are small, the "primitive" approximation of eq. (5.1.10) must be replaced by a uniform one.

2. The Differential Probability of Energy Transfer

The aforementioned time-of-flight experiments do not measure directly the state-to-state transition probabilities $W_{\nu'\nu}$; instead, the experimentalist obtains doubly differential cross sections (per unit solid-angle and per unit energy). These correspond to averages

over initial distributions of internal states of A and B, in accordance with the way in which the molecular beams are prepared in their sources. Furthermore, the instruments are usually not calibrated to yield absolute cross sections, so that the measurements are reported in the form of relative probabilities of transition and/or average energy transfers, as functions of scattering angle and energy. In these cases, the theoretical quantity most readily comparable with experimental results is the differential probability of energy transfer, averaged over the initial distributions. This quantity is related to the $W_{\nu',\nu}$ in the following way.

Firstly, consider the probability that, if A and B are in the initial state $|\nu>$, an amount of energy equal to or smaller than ε will be transferred in the collision, leaving A and B in any final state $|\nu'>$; this is given by

$$P_{\nu}(\varepsilon) = \sum_{\nu'} W_{\nu',\nu}\, \Theta[\varepsilon - (E_{\nu'} - E_{\nu})], \tag{5.2.1}$$

where the step-function Θ selects only those transitions that are energetically allowed. Taking the derivative of eq. (5.2.1) with respect to ε yields the differential probability of energy transfer from the initial state $|\nu>$ that is shown below,

$$\frac{dP}{d\varepsilon}_{\nu} = \sum_{\nu'} W_{\nu',\nu}\, \delta[\varepsilon - (E_{\nu'} - E_{\nu})]. \tag{5.2.2}$$

Finally, averaging $dP_{\nu}/d\varepsilon$ over the initial distribution w_{ν}, we obtain the differential probability of energy transfer to be compared with experiments, namely

$$\frac{dP}{d\varepsilon} = \sum_{\nu} w_{\nu} \sum_{\nu'} W_{\nu',\nu}\delta[\varepsilon-(E_{\nu'}-E_{\nu})]. \qquad (5.2.3)$$

The right side of this last equation may now be expressed in terms of a time-correlation function by means of the procedure presented in Sec. 1.2. Briefly, the integral representation of the δ-function,

$$\delta[\varepsilon-(E_{\nu'}-E_{\nu})] = \int_{-\infty}^{\infty} \frac{dt}{2\pi\hbar} \exp[-i(\varepsilon-E_{\nu'}+E_{\nu})t/\hbar], \qquad (5.2.4)$$

is introduced into one of the matrix elements of eq. (5.1.9), so that with the aid of eq. (5.1.3) we have that

$$\langle\nu'|\hat{U}(\infty,-\infty)|\nu\rangle\delta[\varepsilon-(E_{\nu'}-E_{\nu})] =$$

$$= \int_{-\infty}^{\infty} \frac{dt}{2\pi\hbar} \exp(-i\varepsilon t/\hbar)\ \langle\nu'|\exp(i\hat{H}_M t/\hbar)\hat{U}(\infty,-\infty)\exp(-i\hat{H}_M t/h)|\nu\rangle. \qquad (5.2.5)$$

Substituting eq. (5.2.5) into $W_{\nu',\nu}$ and the latter into eq. (5.2.3) the sum over the final states may be removed from $dP/d\varepsilon$ due to the completeness relation $\sum_{\nu'} |\nu'\rangle\langle\nu'| = \hat{1}$. We thus find that

$$\frac{dP}{d\varepsilon} = \int_{-\infty}^{\infty} \frac{dt}{2\pi\hbar}\ F(t)\ \exp(-i\varepsilon t/\hbar), \qquad (5.2.6a)$$

$$F(t) = \langle\langle\hat{U}_M^{\dagger}(0)\hat{U}_M(t)\rangle\rangle, \qquad (5.2.6b)$$

$$\hat{U}_M(t) = \exp(i\hat{H}_M t/\hbar)\hat{U}(\infty,-\infty)\exp(-i\hat{H}_M t/\hbar), \qquad (5.2.6c)$$

where the double brackets denote the quantal and statistical averages over the initial distributions, as indicated below

$$<< \ldots >> = \sum_{\nu} w_{\nu} <\nu| \ldots |\nu>. \qquad (5.2.7)$$

Whenever more than one trajectory leads to the same subset of final conditions, from eq. (5.1.10) we see that the correlation function F(t) becomes

$$F(t) = <<\sum_{\ell,\ell'} c^{*}_{\ell} c_{\ell'} [\hat{U}_M^{(\ell)}(0)]^{\dagger} \hat{U}_M^{(\ell')} (t)>> . \qquad (5.2.8)$$

In Sec. 4 we find that terms of the above sum with $\ell \neq \ell'$ contain large phases that depend on the initial conditions. Since experimental measurements correspond to initial averages over random phases, the terms with $\ell \neq \ell'$ average to zero, so eq. (5.2.8) simplifies to

$$F(t) \approx <<\sum_{\ell} |c_{\ell}|^2 [\hat{U}_M^{(\ell)}(0)]^{\dagger} \hat{U}_M^{(\ell)} (t) >>. \qquad (5.2.9)$$

Equations (5.2.6,9) indicate that the differential probability of energy transfer is given by the Fourier transform of the time-correlation function of the semiclassical evolution operator; furthermore, the time dependence of F(t) is determined solely by the internal motions of the noninteracting molecules. The advantage of the present approach lies in the fact that the correlation function may be readily evaluated for most polyatomics, without need for expansions in internal states, as is shown in the following sections.

We must emphasize that F(t) includes two types of time dependence whose natures are radically different. Firstly, $\hat{U}_M(t)$ implicitly contains the evolution of the polyatomics during the collision and under the influence of the intermolecular forces, as prescribed by $\hat{U}(t,t_i)$. The second type of time dependence, which is explicitly indicated in

eq. (5.2.6c), arises from the δ-function that corresponds to the conservation of the total energy of the system. This difference must be carefully considered when one desires to introduce approximations to the dynamics. For example, at high collision energies, one may be justified in assuming that the internal degrees of freedom are frozen during brief collision times, and one may approximate $\hat{U}(t,t_i)$ accordingly. In contrast, if the explicit time dependence of $\hat{U}_M(t)$ were to be neglected, the resulting model would exclude all of the inelastic processes that are allowed by energy conservation (c. f. eq. (5.2.6a)).

The evaluation of F(t) requires the following procedure. Firstly, the Hamiltonians of the noninteracting molecules are defined, in order to obtain the Hamiltonian that governs the collisional evolution of the system in the interaction representation; next, the differential equation (5.1.8a) is integrated to yield $\hat{U}(t,t_i)$; these are the subjects of Sec. 4. From $\hat{U}(\infty,-\infty)$ the correlation function is constructed as shown in Sec. 5. One then evaluates the vibrational and the rotational correlations by the methods described in Secs. 6 and 7, respectively. However, before initiating this procedure, it will prove convenient to express the intermolecular potential in a way that highlights the forces that are responsible for rotational and for vibrational excitation, as follows.

3. Expansion of the Intermolecular Potential in Vibrational Displacements

For each atom x of the polyatomic X = A and B, we introduce an equilibrium position $\vec{d}_x$ and a vibrational displacement $\vec{u}_x$, referred to the CM of its molecule. Hence, we have that $\vec{r}^M = \vec{d}^M + \vec{u}^M$, where $\vec{d}^M$ and $\vec{u}^M$ denote the collection of equilibrium positions and of displacements, respectively.

Since we are interested in collisions that do not lead to dissociation or to rearrangement, we may expand $V(\vec{R},\vec{r}^M)$ in a Taylor series in $\vec{u}^M$ about $\vec{d}^M$. Furthermore, for vibrational excitations well below the dissociation thresholds, $|\vec{u}_x| << |\vec{d}_x|$; in these cases, terms of order $(|\vec{u}_x|/|\vec{d}_x|)^n$ with $n > 1$ may be neglected so that

$$V(\vec{R},\vec{r}^M) \approx V_e(\vec{R},\Gamma) - \sum_{x=1}^{N} \vec{f}_x(\vec{R},\Gamma) \cdot \vec{u}_x, \tag{5.3.1a}$$

$$V_e(\vec{R},\Gamma) = V(\vec{R},\vec{d}^M), \tag{5.3.1b}$$

$$\vec{f}_x(\vec{R},\Gamma) = -\frac{\partial V}{\partial \vec{r}_x}\bigg|_{\vec{r}^M=\vec{d}^M}. \tag{5.3.1c}$$

Here, $V_e(\vec{R},\Gamma)$ is the potential evaluated at the internal equilibrium configurations of each polyatomic and it depends on their orientation in the space fixed (SF) reference frame. We indicate this orientation by $\Gamma = \{\Gamma^{(A)}, \Gamma^{(B)}\}$, where $\Gamma^{(X)}$ represents the set of Euler angles of molecule X = A or B. Examining eqs. (5.3.1) we see that V_e mediates rotational transitions, but not vibrational excitation because it is independent of $\vec{u}^M$. However, vibrational energy transfer is due to the intermolecular forces $\vec{f}_x$ exerted on the atoms.

We remark that eqs. (5.3.1) are not equivalent to expanding the anisotropic part of $V(\vec{R},\vec{r}^{M})$ about the spherically averaged potential, as has been proposed in other semiclassical models (see Dickinson, 1979, for example). Here, V_e and $\vec{f}_x$ may be highly anisotropic, due to the many-body nature of the polyatomics. At hyperthermal collision energies, the anisotropy of the potential may not be treated as a perturbation because the inner regions of $V(\vec{R},\vec{r}^{M})$ are deeply probed for small impact parameters. Furthermore, the truncation of the Taylor series of V to first order in the $\vec{u}_x$ is not essential to the present development; the procedure described below may be directly extended to a finite expansion of V to any order in the $\vec{u}_x$.

4. The Evolution Operator in the Interaction Representation

In order to obtain the interaction Hamiltonian of eqs. (5.1.8c) we must first specify the Hamiltonian $\hat{H}_M$ that governs the internal dynamics of the noninteracting polyatomics. For most molecules (except those that contain several hydrogen atoms), typical rotational periods are much longer than vibrational ones. This indicates that rotational and vibrational motions should be studied separately from one another. Therefore, we take the internal Hamiltonian to be of the form

$$\hat{H}_M = \hat{H}_V + \hat{H}_R , \tag{5.4.1a}$$

$$\hat{H}_V = \hat{H}_V^{(A)} + \hat{H}_V^{(B)} , \tag{5.4.1b}$$

$$\hat{H}_R = \hat{H}_R^{(A)} + \hat{H}_R^{(B)} , \tag{5.4.1c}$$

and we require that the rotational ($\hat{H}_R^{(X)}$) and the vibrational ($\hat{H}_V^{(X)}$) Hamiltonians of each polyatomic satisfy the relation

$$[\hat{H}_R^{(X)}, \hat{H}_V^{(X)}] = \hat{0}. \tag{5.4.2}$$

This means that $[\hat{H}_V, \hat{\vec{d}}^M] = \hat{0}$, although $[\hat{H}_R, \hat{\vec{u}}^M] \neq 0$ because the $\hat{\vec{u}}_x$ depend on the orientation of A and of B in the SF frame.

Since we are interested in transitions between internal states that are well below the dissociation thresholds, we use the standard model of harmonic vibrational motions (Wilson, 1955, Chap. 8). Carrying out the normal-mode analysis outlined in eqs. (2.3.8-14), for each molecule X we obtain the vibrational frequences $\omega_j^{(X)}$ and the vector coefficients ($\vec{C}_{xj}^{(X)}$) of the transformation between normal ($Q_j^{(X)}$) and Cartesian displacements. In order to abbreviate the notation, we collect these quantities, as follows: $\{\vec{C}_{xj}\} = \{\vec{C}_{xj}^{(A)}, \vec{C}_{xj}^{(B)}\}$, $\{\omega_j\} = \{\omega_j^{(A)}, \omega_j^{(B)}\}$ and $\{Q_j\} = \{Q_j^{(A)}, Q_j^{(B)}\}$, so that we may write

$$\vec{u}_x = \sum_j \vec{C}_{xj}(\Gamma)\, Q_j, \tag{5.4.3}$$

Here, the $\vec{C}_{xj}(\Gamma)$ contain all the dependence of the $\vec{u}_x$ on the orientation of the polyatomics.

The vibrational degrees of freedom are quantized by introducing creation ($\hat{a}_j^+$) and annihilation ($\hat{a}_j$) operators that are defined by the relations (Messiah, 1961, Vol. 1, Chap. 12)

$$\hat{Q}_j = [\hbar/(2\omega_j)]^{\frac{1}{2}}(\hat{a}_j + \hat{a}_j^+), \tag{5.4.4a}$$

$$\hat{P}_j = -i(\hbar\omega_j/2)^{\frac{1}{2}}(\hat{a}_j - \hat{a}_j^+), \tag{5.4.4b}$$

where P_j is the canonical momentum conjugate to Q_j. From the commutator $[\hat{Q}_j,\hat{P}_{j'}] = i\hbar\delta_{jj'}$, one finds that

$$[\hat{a}_j,\hat{a}_{j'}^{\dagger}] = \delta_{jj'}\hat{1} \tag{5.4.5}$$

and for the vibrational Hamiltonian,

$$\hat{H}_V = \sum_j \hbar\omega_j(\hat{a}_j^{\dagger}\hat{a}_j+1/2). \tag{5.4.6}$$

Using eqs. (5.4.5,6) Heisenberg's equation of motion for the $\hat{a}_j(t)$ are integrated to give

$$\hat{a}_j(t) = \hat{a}_j \exp(-i\omega_j t). \tag{5.4.7}$$

Replacing eq. (5.4.4a) into eq. (5.4.3) and the latter into eqs. (5.3.1) we obtain the following expression for the intermolecular potential.

$$V(\vec{R},\hat{\vec{r}}^M) = V_e(\vec{R},\hat{\Gamma}) + \sum_j V_j(\vec{R},\hat{\Gamma})(\hat{a}_j+\hat{a}_j^{\dagger}), \tag{5.4.8a}$$

$$V_j(\vec{R},\Gamma) = -[\hbar/(2\omega_j)]^{1/2} \sum_x \vec{f}_x(\vec{R},\Gamma) \cdot \vec{C}_{xj}(\Gamma). \tag{5.4.8b}$$

Here, V_j is the component of the intermolecular potential that acts on the normal mode j and forces it to undergo a vibrational transition. Substituting eq. (5.4.8) into (5.1.8c) and using eq. (5.4.7), we find that the interaction Hamiltonian is given by

$$\hat{H}'(t,t_i) = \Delta K(t)_C + V_e(\vec{R}(t)_C, \hat{\Gamma}(t,t_i)_R) + \\ + \sum_j V_j(\vec{R}(t)_C,\hat{\Gamma}(t,t_i)_R)[\hat{a}_j(t-t_i)_V + \hat{a}_j^{\dagger}(t-t_i)_V]. \tag{5.4.9}$$

In eq. (5.4.9), we have explicitly indicated the origin of the time dependence of the quantities during the collision; here the subscripts C, R, and V, represent classical relative, quantal rotational and vibrational motions, respectively. However, rotational motions of large polyatomics are much slower than vibrational ones; furthermore, at hyperthermal relative energies, collision times are much shorter than typical rotational periods. In these cases, the time dependence of $\hat{\Gamma}(t,t_i)$ may be neglected in comparison with those of $\vec{R}(t)$ and $\hat{a}_j(t,t_i)$; hence,

$$\hat{H}'(t,t_i) \simeq \Delta K(t) + V_e(\vec{R}(t),\hat{\Gamma}) + \\ + \sum_j V_j(\vec{R}(t),\hat{\Gamma}) \{\hat{a}_j \exp[-i\omega_j(t-t_i)] + \hat{a}_j^\dagger \exp[i\omega_j(t-t_i)]\}, \tag{5.4.10}$$

where Γ denotes the initial orientations of A and of B in the SF frame. This model corresponds to assuming that vibrational transitions occur at fixed orientations of the polyatomics, with the rotational motions frozen throughout the duration of the collision. A similar approximation may not be done on the vibrational degrees of freedom because typical vibrational periods are usually shorter than collision times. We should remark that the replacement $\hat{\Gamma}(t,t_i) \to \hat{\Gamma}(t_i,t_i)$ is not essential to our development, but it considerably simplifies the evaluation of the evolution operator $\hat{U}(t,t_i)$, as we shall see below.

In general, the solution of eqs. (5.1.8a,b) can not be obtained in a closed form; instead, by means of straightforward but rather lengthy manipulations, one obtains the following expansion (Magnus, 1954),

$$\hat{U}(t,t_i) = \exp\{-i\int_{t_i}^{t} dt'\hat{H}(t',t_i)/\hbar + \int_{t_i}^{t} dt'\int_{t_i}^{t'} dt''[\hat{H}'(t',t_i),\hat{H}'(t'',t_i)]/2\hbar^2 + \ldots\} \tag{5.4.11}$$

Here, the nth term of the exponent contains n time-integrals of n-tuple commutators of $\hat{H}'$ with itself evaluated at different times. Since $[\hat{\Gamma}, \hat{H}_R] \neq \hat{0}$, one has that $[[\hat{\Gamma}(t),\hat{\Gamma}(t')],\hat{\Gamma}(t'')]] \neq \hat{0}$, so the exponent in eq. (5.4.11) contains a large number of terms. However, using eqs. (5.4.5,7), for the approximate Hamiltonian of eq. (5.4.10) we find that

$$[\hat{H}'(t,t_i),\hat{H}'(t',t_i)] = -2i\sum_j V_j(\vec{R}(t),\hat{\Gamma})V_j(\vec{R}(t'),\hat{\Gamma})\sin\omega_j(t-t'). \tag{5.4.12}$$

In this case, the n-tuple commutators of $\hat{H}'$ with itself are identically zero whenever n>2. Therefore, for heavy polyatomics, $\hat{U}(\infty,-\infty)$ is exactly given by

$$\hat{U}(\infty,-\infty) = \exp\{-i[A_K + \hat{A}_e + \sum_j \hat{B}_j + \hat{A}_j\hat{a}_j + \hat{A}_j^\dagger\hat{a}_j^\dagger]\}, \tag{5.4.13a}$$

$$A_K = \int_{-\infty}^{\infty} dt\{[\vec{P}(t)]^2 - \vec{P}_i^2\}/(2M\hbar), \tag{5.4.13b}$$

$$\hat{A}_e = \int_{-\infty}^{\infty} dt\ V_e(\vec{R}(t),\hat{\Gamma})/\hbar, \tag{5.4.13c}$$

$$\hat{A}_j = \int_{-\infty}^{\infty} dt\ V_j(\vec{R}(t),\hat{\Gamma})\exp[-i(\omega_j t + \delta_j)]/\hbar, \tag{5.4.13d}$$

$$\hat{B}_j = \int_{-\infty}^{\infty} dt \int_{-\infty}^{\infty} dt'\ V_j(\vec{R}(t),\hat{\Gamma})V_j(\vec{R}(t'),\hat{\Gamma})\ \sin[\omega_j(t-t')]/\hbar^2, \tag{5.4.13e}$$

where δ_j corresponds to the initial vibrational phase of mode j. In eqs. (5.4.13), A_e and A_j represent the action that the intermolecular forces exert on the rotational degrees of freedom and on the normal modes, respectively, throughout the course of the collision. We remark that the above expression of $\hat{U}(\infty,-\infty)$ contains the potential to

infinite order. At hyperthermal collision energies, a perturbation expansion of $\hat{U}$ in powers of V is not applicable because the highly repulsive cores are deeply probed for small impact parameters.

Before proceeding to the evaluation of the correlation function, we should comment on the "primitive" semiclassical approximation discussed at the end of Sec. 1. Using eqs. (5.4.13) one can readily obtain the state-to-state transition amplitudes $\langle v' | \hat{U}(\infty,-\infty) | v \rangle$. Examination of eqs. (5.4.13) shows that the amplitudes have the phase A_K that corresponds to the net action along the classical trajectory. Whenever different trajectories $R^{(\ell)}(t)$, $\ell = 1, 2, \ldots,$ lead to the same final conditions measured in the experiments, the applicability of the "primitive" approximation of eq. (5.1.10) may be judged by calculating the $A_K^{(\ell)}$ for each ℓ and comparing their magnitudes. Alternatively, since $\langle v' | \hat{U}(\infty,-\infty) | v \rangle$ may be considered to be a functional of an arbitrary trajectory $\vec{R}(t)$, one could use eqs. (5.4.13) as a starting point of the development of uniform semiclassical approximations; for examples see Berry and Mount, 1972 and Pechukas, 1969.

5. Vibrational and Rotational Correlation

Substituting eqs. (5.5.13) into eq. (5.2.6c) and the latter into eq. (5.2.6b), we obtain the following expression for the correlation function,

$$F(t) = \langle\langle \exp[i\hat{A}_e(0)] \hat{F}_V(t) \exp[-i\hat{A}_e(t)_R] \rangle\rangle_R, \qquad (5.5.1a)$$

$$\hat{F}_V(t) = \langle\langle \exp[i \sum_j \hat{B}_j(0) + \hat{A}_j(0)\hat{a}_j(0) + \hat{A}_j^\dagger(0)\hat{a}_j^\dagger(0)] \times$$

$$\times \exp[-i \sum_j \hat{B}_j(t)_R + \hat{A}_j(t)_R \hat{a}_j(t)_V + \hat{A}_j^\dagger(t)_R \hat{a}_j^\dagger(t)_V] \rangle\rangle_V, \tag{5.5.1b}$$

where we have used the fact that $[A_K, \hat{H}_M] = 0$ because A_K depends only on classical dynamical variables. Here, the operators evolve in time in accordance with the Hamiltonians of the noninteracting molecules, as they are prepared in their respective sources. In eq. (5.5.5b) we have explicitly indicated the nature of the time dependence with the subscripts R and V representing the rotational and vibrational motions, respectively.

The vibrational correlation $\hat{F}_V(t)$ can now be calculated in the body fixed (BF) frames of A and of B, in which case it depends on the set of Euler angles (Γ) that describe the orientations of these frames with respect to the SF one. However, considerable simplifications occur when the rotational motions of A and of B are much slower than their respective vibrational ones. In these cases, we need only consider the vibrational correlation for fixed orientations of the molecules in space. Hence, within $\hat{F}_V(t)$, the slow evolution of $\hat{B}_j(t)_R$ and of $\hat{A}_j(t)_R$, which are due to that of $\hat{\Gamma}(t)_R$, may be neglected in comparison with the evolution of the rapidly oscillating $\hat{a}_j(t)_V$. We can then approximate $\hat{B}_j(t)_R \simeq \hat{B}_j(0)$ and $\hat{A}_j(t)_R \simeq \hat{A}_j(0)$, so that the vibrational correlation simplifies as follows,

$$\hat{F}_V(t) \simeq \langle\langle \exp[i \sum_j \hat{A}_j(0)\hat{a}_j(0) + \hat{A}_j^\dagger(0)\hat{a}_j^\dagger(0)] \times$$

$$\times \exp[-i \sum_j \hat{A}_j(0)\hat{a}_j(t)_V + \hat{A}_j^\dagger(0)\hat{a}_j^\dagger(t)_V] \rangle\rangle_V. \tag{5.5.2}$$

6. The Vibrational Correlation

Since the normal modes are independent, $\hat{F}_V(t)$ can be factored into the product of correlation functions of each mode, so that

$$\hat{F}_V(t) = \prod_j \hat{F}_V^{(j)}(t), \tag{5.6.1a}$$

$$\hat{F}_V^{(j)}(t) = \langle\langle e^{\hat{X}} e^{\hat{Y}} \rangle\rangle_V, \tag{5.6.1b}$$

$$\hat{X} = i[\hat{A}_j(0)\hat{a}_j(0) + \hat{A}_j^{\dagger}(0)\hat{a}_j^{\dagger}(0)], \tag{5.6.1c}$$

$$\hat{Y} = -i[\hat{A}_j(0)\hat{a}_j(t) + \hat{A}_j^{\dagger}(0)\hat{a}_j^{\dagger}(t)]. \tag{5.6.1d}$$

Here, we have introduced the operators $\hat{X}$ and $\hat{Y}$ in order to abbreviate the notation. For each mode, the vibrational correlation is evaluated by means of the following procedure (Micha, 1979b).

From eqs. (5.4.5,7) one readily finds that $[\hat{X},\hat{Y}]$ is a complex function of time that contains neither $\hat{a}_j$ nor $\hat{a}_j^{\dagger}$. Hence one can use the relation

$$e^{\hat{X}} e^{\hat{Y}} = \exp(\hat{X} + \hat{Y} + [\hat{X},\hat{Y}]/2), \tag{5.6.2}$$

which is valid whenever $[\hat{X},\hat{Y}]$ commutes with $\hat{X}$ and with $\hat{Y}$. Next, one applies the Bloch theorm (Messiah, 1961, Vol. 1, Chap. 12),

$$\langle\langle e^{\hat{Z}} \rangle\rangle_V = \exp\langle\langle \hat{Z}^2/2 \rangle\rangle_V, \tag{5.6.3}$$

for $\hat{Z}$ a linear combination of $\hat{a}_j$ and $\hat{a}_j^{\dagger}$, to obtain

$$\langle\langle e^{\hat{X}} e^{\hat{Y}} \rangle\rangle_V = \exp\langle\langle \hat{X}^2 + \hat{X}\hat{Y} \rangle\rangle_V. \tag{5.6.4}$$

Finally, the averages of $\hat{X}^2$ and $\hat{X}\hat{Y}$ are evaluated for the experimental Boltzmann distribution, by means of elementary techniques (Messiah, ibid). We thus find that

$$\hat{F}_V^{(j)}(t) = \exp\{\hat{A}_j^{\dagger}(0)\hat{A}_j(0)\{\coth\alpha_j + [\exp(\alpha_j + i\omega_j t) + \exp(-\alpha_j - i\omega_j t)]/(2\sinh\alpha_j)\}\}, \tag{5.6.5}$$

where $\alpha_j = \hbar\omega_j^{(X)}/(2k_B T_V^{(X)})$, k_B is Boltzmann's constant and $T_V^{(X)}$ is the vibrational temperature of the distribution of molecule X = A, B. Equation (5.6.5) may be cast into a more convenient form with the aid of the generator of modified Bessel functions (I_n) of the first kind (Abramowitz and Stegun, 1972, Chap. 9),

$$\exp[x(y + 1/y)2] = \sum_{n=-\infty}^{\infty} y^n I_n(x), \tag{5.6.6}$$

with $y = \exp(-\alpha_j - i\omega_j t)$. Substitution of eq. (5.6.6) into (5.6.5) and of the latter into eq. (5.6.1a) yields the following expression for the vibrational correlation

$$\hat{F}_V(t) = \sum_{\vec{n}} p_{\vec{n}}(\hat{\Gamma})\exp(-i\vec{n}\cdot\vec{\omega}_V t), \tag{5.6.7a}$$

$$p_{\vec{n}}(\hat{\Gamma}) = \prod_j I_{n_j}(\hat{X}_j)\exp(-n_j\alpha_j - \hat{X}_j\cosh\alpha_j), \tag{5.6.7b}$$

$$\hat{X}_j = \hat{A}_j^{\dagger}(0)\hat{A}_j(0)/(2\sinh\alpha_j), \tag{5.6.7c}$$

where we have introduced the abbreviations $\vec{n} = \{n_j\}$ and $\omega_V = \{\omega_j\}$. Here, we explicitly indicate that $p_{\vec{n}}$ is a function of the initial orientations of the polyatomics, since A_j depends on Γ (c f. eq. 5.4.13d).

In analogy with eq. (5.2.6a), the Fourier transform of $\hat{F}_V(t)$ is the differential probability of vibrational energy transfer for fixed orientations of A and of B,

$$dP_V(\Gamma)/d\varepsilon = \sum_{\vec{n}} p_{\vec{n}}(\Gamma)\delta(\varepsilon + \hbar\vec{n}\cdot\vec{\omega}_V). \tag{5.6.8}$$

This consists of a group of δ-function peaks located at the vibrational energy transferred $\varepsilon_V = -\hbar\vec{n}\cdot\vec{\omega}_V$. Therefore, n_j corresponds to the change in quantum number (initial minus final) of normal mode j; furthermore, the probability that the collision will cause the vibrational transition $\vec{n}$ is given by $p_{\vec{n}}(\Gamma)$. In practice, these peaks are broadened by the rotational correlation, as we proceed to show.

7. The Rotational Correlation

The rotational correlation of heavy polyatomics may be obtained by means of the short-time expansion technique presented in Chap. I. In particular, substituting eq. (5.6.7a) into (5.5.1a) and following the procedure described in Sec. 1.2, we find that

$$F(t) = \sum_{\vec{n}} \exp(-i\vec{n}\cdot\vec{\omega}_V t)\langle\langle \exp[i\hat{A}_e(0)]p_{\vec{n}}(\hat{\Gamma}) \times$$

$$\times \exp(iL_R t/\hbar)\exp[-i\hat{A}_e(0)]\rangle\rangle_R. \tag{5.7.1}$$

where L_R is the Liouville superoperator for rotation. This is defined by its action on any operator $\hat{Y}$, as follows:

$$L_R^n \hat{Y} = ([\hat{H}_R,)^n \hat{Y}]\ ; \tag{5.7.2}$$

here, $\hat{H}_R$ is the sum of the rotational Hamiltonians of the polyatomics.

Whenever the rotational motions of A and of B are much slower than their respective vibrational ones, we perform a short-time approximation to the rotational correlation of each vibrational transition. As discussed in Sec. 1.4, this corresponds to expanding the second exponential on the right side of eq. (5.7.1) in terms of the cumulant rotational averages $\langle L_R^n \rangle$ and retaining only the first two cumulants, so that

$$F(t) \approx \sum_{\vec{n}} \langle\langle p_{\vec{n}}(\hat{\Gamma}) \rangle\rangle_R \exp[i(\langle L_R \rangle/\hbar - \vec{n}\cdot\vec{\omega}_V)t - \langle L_R^2 \rangle t/(2\hbar^2)]. \quad (5.7.3)$$

From eqs. (1.4.5a,b) and (5.7.2) we find that these cumulants are

$$\langle L_R \rangle = \langle\langle \exp(i\hat{A}_e) p_{\vec{n}}(\hat{\Gamma}) [\hat{H}_R, \exp(-i\hat{A}_e)] \rangle\rangle_R / \langle\langle p_{\vec{n}}(\hat{\Gamma}) \rangle\rangle_R, \quad (5.7.4a)$$

$$\langle L_R^2 \rangle = \langle\langle \exp(i\hat{A}_e) p_{\vec{n}}(\hat{\Gamma}) [\hat{H}_R, [\hat{H}_R, \exp(-i\hat{A}_e)]] \rangle\rangle_R / \langle\langle p_{\vec{n}}(\hat{\Gamma}) \rangle\rangle_R - \langle L_R \rangle^2, \quad (5.7.4b)$$

where $\hat{A}_e$ is evaluated at t=0. The commutators indicated in eqs. (5.7.4) are obtained, as follows.

In order to simplify the notation, we first consider the commutator $[\hat{H}_R^{(X)}, \exp(-i\hat{A}_e)]$ for one of the polyatomics X = A or B, and we omit the index X. This does not cause any loss in generality because a commutator is transitive with respect to the addition of operators. Furthermore, we take the polyatomics to be symmetric tops (which includes linear and spherical molecules as particular cases), although the method presented below can be directly extended to

nonsymetric molecules. Hence, in the coordinate representation the rotational Hamiltonian of either polyatomic may be written as (Edmonds, 1974, Chap. 4)

$$\hat{H}_R = E_1(\hat{L}_+\hat{L}_- + \hat{L}_z^2 - \hat{L}_z) + E_2 \hat{L}_\gamma^2 , \tag{5.7.5a}$$

$$\hat{L}_\pm = \exp(\pm i\alpha)(\pm\partial/\partial\beta + i\cot\beta\partial/\partial\alpha), \tag{5.7.5b}$$

$$\hat{L}_z = -i\partial/\partial\alpha, \tag{5.7.5c}$$

$$\hat{L}_\gamma = -i\partial/\partial\gamma, \tag{5.7.5d}$$

$$E_1 = \hbar^2/2I_1, \tag{5.7.5e}$$

$$E_2 = \hbar^2(I_1 - I_2)/(I_1 I_2), \tag{5.7.5f}$$

where I_1 and I_2 are the moments of inertia about the principal axes of the molecule, with 1 indicating the axis of symmetry. In eqs. (5.7.5) α, β and γ are the Euler angles that describe the orientation of the molecule with respect to the SF reference frame; α and β indicate the azimuthal and polar angles, respectively, of the axis of symmetry, while γ corresponds to a rotation about this axis.

Before proceeding to the evaluation of $[\hat{H}_R, \exp(-i\hat{A}_e)]$, it will prove convenient to consider the simpler commutator $[\hat{A}_e,[\hat{H}_R,\hat{A}_e]]$. By means of the operator identities

$$[\hat{A}\hat{B},\hat{C}] = \hat{A}[\hat{B},\hat{C}] + [\hat{A},\hat{C}]\hat{B}, \tag{5.7.6a}$$

$$[\hat{A},\hat{B}\hat{C}] = [\hat{A},\hat{B}]\hat{C} + \hat{B}[\hat{A},\hat{C}], \tag{5.7.6b}$$

we find that

$$[\hat{A}_e,[\hat{H}_R,\hat{A}_e]]=2\ E_1[(\partial A_e/\partial\beta)^2 + \mathrm{cosec}^2\beta\ (\partial A_e/\partial\alpha)^2] +$$

$$+\ 2\ E_2(\partial A_e/\partial\gamma)^2. \qquad (5.7.7)$$

We now invoke the general expression (Messiah, 1961, Chap. 8)

$$[\hat{H}_R,\exp(-i\hat{A}_e)] = -\exp(-i\hat{A}_e)\sum_{n=0}^{\infty} i^{n+1}([\hat{A}_e,)^n[\hat{H}_R,\hat{A}_e]]/(n+1)!, \qquad (5.7.8)$$

which can be obtained by expanding the leftmost exponential in a power series of its exponent, followed by commuting $\hat{H}_R$ through each term. Equations (5.4.13c) and (5.7.7) show that in the coordinate representation $\hat{A}_e$ and $[\hat{A}_e,[\hat{H}_R,\hat{A}_e]]$ are functions of α, β and γ but they are not differential operators, so that $\hat{A}_e$ commutes with $[\hat{A}_e,[\hat{H}_R,\hat{A}_e]]$. Therefore, terms on the right side of eq. (5.7.8) which have $n > 1$ are identically zero and $[\hat{H}_R,\exp(-i\hat{A}_e)]$ is exactly given by

$$[\hat{H}_R,\exp(-i\hat{A}_e)] = \exp(-i\hat{A}_e)\{-i[\hat{H}_R,\hat{A}_e]+[\hat{A}_e,[\hat{H}_R,\hat{A}_e]]/2\}. \qquad (5.7.9)$$

Furthermore, eq. (5.4.13c) indicates that A_e is of the order $\kappa\ell$, where κ is the momentum transferred in the collision and ℓ is the range of the intermolecular potential; thus $[\hat{H}_R,\hat{A}_e]$ is of the order of $\kappa\ell$ while $[\hat{A}_e,[\hat{H}_R,\hat{A}_e]]$ is of order $(\kappa\ell)^2$. In hyperthermal collisions of large molecules $\kappa\ell>>1$, so we may retain only the highest powers of $\kappa\ell$ and write

$$[\hat{H}_R,\exp(-i\hat{A}_e)] \simeq \exp(-i\hat{A}_e)[\hat{A}_e,[\hat{H}_R,\hat{A}_e]]/2. \qquad (5.7.10)$$

By repeated applications of eq. (5.7.9) we also find that, to leading order in $\kappa\ell$,

$$([\hat{H}_R,)^n \exp(-i\hat{A}_e)] \simeq \exp(-i\hat{A}_e)([\hat{A}_e,[\hat{H}_R,\hat{A}_e]]/2)^n. \tag{5.7.11}$$

Generalizing eqs. (5.7.7,11) to the total rotational Hamiltonian $\hat{H}_R = \hat{H}_R^{(A)} + \hat{H}_R^{(B)}$ and replacing the generalized expressions into eqs. (5.7.4), we obtain the quantities required for the correlation function of symmetric top polyatomics; these are

$$P_{\vec{n}} = \langle\langle p_{\vec{n}}(\hat{\Gamma})\rangle\rangle_R, \tag{5.7.12a}$$

$$\langle L_R\rangle = \langle\langle p_{\vec{n}}(\hat{\Gamma})G(\hat{\Gamma})\rangle\rangle_R / P_{\vec{n}}, \tag{5.7.12b}$$

$$\langle L_R^2\rangle = \langle\langle p_{\vec{n}}(\hat{\Gamma})[G(\hat{\Gamma})]^2\rangle\rangle_R / P_{\vec{n}} - \langle L_R\rangle^2, \tag{5.7.12c}$$

$$G(\Gamma) = \sum_{X=A,B} E_1^{(X)}[(\partial A_e/\partial\beta^{(X)})^2 + \mathrm{cosec}^2\beta^{(X)}(\partial A_e/\partial\alpha^{(X)})^2] + E_2^{(X)}(\partial A_e/\partial\alpha^{(X)})^2. \tag{5.7.12d}$$

Examining eqs. (5.7.12) we find that the evaluation of the averages over initial rotational distributions is quite straightforward, for the following reason. Since all the operators on the right sides of these equations are functions only of Γ and not of $\partial/\partial\Gamma$, in the coordinate representation their matrix elements reduce to simple integrals over the six Euler angles; the integrals can be readily obtained by numerical quadrature.

8. Discussion

Substituting eq. (5.7.3) into (5.2.6a) and evaluating the Fourier transform of F(t) yields the following expression for the differential probability of energy transfer,

$$\frac{dP}{d\varepsilon} = (4\sqrt{\pi})^{-1} \sum_{\vec{n}} P_{\vec{n}} \exp\{-[(\langle L_R \rangle - \hbar\vec{n}\cdot\vec{\omega}_V - \varepsilon)/ /(2\langle L_R^2 \rangle^{1/2})]^2\}/(2\langle L_R^2 \rangle^{1/2}). \quad (5.8.1)$$

This consists of a group of normalized Gaussian peaks centered at the energy transferred (vibrational $-\hbar\vec{n}\cdot\vec{\omega}_V$ plus average rotational $\langle L_R \rangle$) to the vibrational transition indicated by $\vec{n}$; each peak is rotationally broadened by an amount $2\langle L_R^2 \rangle$. Eqs. (5.7.12b,c) show that the average rotational energy transfers and widths depend on $\vec{n}$; furthermore, $\langle L_R \rangle$ and $\langle L_R^2 \rangle$ are related to the integral of the intermolecular potential (A_e) along the classical trajectory, with the potential evaluated at the internal equilibrium configurations of the polyatomics. Examining eq. (5.8.1), we conclude that the probability that the collision will cause the vibrational transition $\vec{n}$ (averaged over initial distributions) is given by $P_{\vec{n}}$, as defined in eqs. (5.7.12a) and (5.6.7b,c). The latter equations show that the probability of vibrational transition is a function of the integrals A_j defined in eq. (5.4.13d). These integrals correspond to the action that the intermolecular forces exert on the normal modes throughout the course of the collision.

Next, we briefly consider an additional advantage of our development. As discussed in Sec. 1, in principle the classical relative trajectory $\vec{R}(t)$ must be obtained from the solution of Hamilton's equations of motion for the full many-body problem. However, the differential probability of energy transfer given in eq. (5.8.1) is a functional of $\vec{R}(t)$, so that one can easily introduce approximate models of the relative dynamics. By comparing the values of $dP/d\varepsilon$ obtained from these models with those that correspond to the exact trajectory, one can gain insight into the mechanisms that govern energy transfer processes in molecular collisions.

BIBLIOGRAPHY

Abramowitz, M. and I. A. Stegun (1972) *Handbook of Mathematical Functions*, Dover, New York.

Bader, R.F.W. (1980) J. Chem. Phys. 73, 2871.

Beard, L. H. (1979) Ph.D. thesis, Chemistry Department, University of Florida.

Berry, M. V. (1966) Proc. Phys, Soc. 89, 479.

Berry, M. V. and K. E. Mount (1972) Rep. Prog. Phys. 35, 315.

Billing, G.D. (1976) Chem. Phys. 14, 267.

Billing, G.D. (1978) Chem. Phys. 33, 227.

Billing, G.D. (1979a) Chem. Phys. Letters 36, 127.

Billing, G.D. (1979b) Chem. Phys. 41, 11.

Billing, G.D. (1980) Chem. Phys. 46, 123.

Bottner, R., U. Ross and J. P. Toennies (1976) J. Chem. Phys. 65, 733.

Brumer, P. and M. Shapiro (1975) J. Chem. Phys. 63, 427.

Buckingham, A. D. and B. J. Orr (1967) Quart. Rev. 21, 195.

Carr, W. J., R. A. Coldwell-Horsfall and A. E. Fein (1961) Phys. Rev. 124, 747.

Carr, W. J. and A. A. Maradudin (1964) Phys. Rev. A133, 371.

Chase, D. M. (1956) Phys. Rev. 104, 838.

Child, M. S. (1976) in *Dynamics of Molecular Collisions*, Park B, W. H. Miller, Ed., Plenum, New York.

Churchill, R. V., J. W. Brown and R. F. Verhey (1974) *Complex Variables and Applications*, McGraw-Hill, New York.

Clark, A. P., A. S. Dickinson and D. Richards (1977) Adv. Chem. Phys. 36, 63.

Clary, D. C. (1980) Chem. Phys. Letters 74, 454.

Clementi, E. (1965) *Tables of Atomic Wave-Functions*, IBM, N.P.

Davies, S. L., J. E. Boggs and S. C. Mehotra (1979) J. Chem. Phys. 71, 1418.

Dickinson, A. S. (1979) Com. Phys. Commun. 17, 51.

Dorn, W. S. and D. D. McCracken (1972) *Numerical Methods with FORTRAN IV Case Studies*, Wiley, New York.

Eastes, W., U. Ross and J. P. Toennies (1977) J. Chem. Phys. 66, 1919.

Eastes, W., U. Ross and J. P. Toennies (1979a) Chem. Phys. 39, 407.

Eastes, W., U. Ross and J. P. Toennies (1979b) J. Chem. Phys. 70, 1652.

Edmonds, A. R. (1974) *Angular Momentum in Quantum Mechanics*, Princeton Univ. Press, Princeton.

Ellenbroek, T., U. Gierz and J. P. Toennies (1980) Chem. Phys. Letters 70, 459.

Ellenbroek, T., J. P. Toennies and M. Wilde (1979) *Book of Abstracts*, XI ICPEAC, Kyoto.

Faubel, M. and J. P. Toennies (1977) Adv. Atomic Mol. Phys. 13, 229.

Gaydaenko, V. I. and V. K. Nikulin (1970) Chem. Phys. Letters 7, 360.

Gianturco, F. A. (1979) *The Transfer of Molecular Energies by Collision*, Springer-Verlag, Berlin.

Goldflam, R., S. Green and D. J. Kouri (1977) J. Chem. Phys. 67, 5661.

Goldstein, H. (1950) *Classical Mechanics*, Addison-Wesley, Cambridge.

Gordon, R. G. and Y. S. Kim (1972) J. Chem. Phys. 56, 3122.

Green, S., B. J. Garrison and W. A. Lester, Jr. (1975) J. Chem. Phys. 63, 1154.

Green, S. and R. G. Gordon, POTLSURF, Quantum Chemistry Program Exchange, University of Indiana, Bloomington, Program 251.

Herzberg, G. (1965) *Spectra of Diatomic Molecules*, Van Nostrand, Princeton.

Hirschfelder, J., C. Curtiss and R. Bird (1967) *Molecular Theory of Gases and Liquids*, J. W. Wiley, New York.

Jackson, J. D. (1975) *Classical Electrodynamics*, J. Wiley, New York.

Jones, L. H. (1971) *Inorganic Vibrational Spectroscopy*, M. Dekker, New York.

Kascheev, V. N. and M. A. Krivoglaz (1961) Sov. Phys. Solid State 3, 1107.

Khare, V. (1977) J. Chem. Phys. 67, 3897.

Khare, V. (1978) J. Chem. Phys. 68, 4631.

Kim, Y. S. and R. G. Gordon (1974a) J. Chem. Phys. 60, 4323.

Kim, Y. S. and R. G. Gordon (1974b) J. Chem. Phys. 61, 1.

Kubo, R. (1962) J. Phys. Soc. Japan 17, 1100.

Kuruoglu, Z. C. and D. A. Micha (1980) J. Chem. Phys. 72, 3327.

Lester, W. A., Jr. (1976) in *Dynamics of Molecular Collisions*, Part A, W. H. Miller, Ed., Plenum, New York.

Magnus, W. (1954) Commun. Pure Appl. Math. 7, 649.

Maradudin, A. A. and V. Ambegaokar (1964) Phys. Rev. A135, 1071.

March, N. H. and M. P. Tosi (1976) *Atomic Dynamics in Liquids*, J. Wiley, New York.

Margenau, H. and N. R. Kestner (1971) *Theory of Intermolecular Forces*, Pergamon, Oxford.

Marion, J. B. (1971) *Classical Dynamics of Particles and Systems*, Academic Press, New York.

Marshall, W. and S. W. Lovesey (1971) *Theory of Thermal Neutron Scattering*, Oxford University Press, Oxford.

McCann, K. J. and M. R. Flannery (1975) J. Chem. Phys. 63, 4695.

McCann, K. J. and M. R. Flannery (1978) J. Chem. Phys. 69, 5275.

McCann, K. J. and M. R. Flannery (1979) Chem. Phys. Letters 60, 523.

McDowell, M. R. C. and J. P. Coleman (1970) *Introduction to the Theory of Ion-Atom Collisions*, North Holland, Amsterdam.

McGuire, P. M. and D. J. Kouri (1974) J. Chem. Phys. 60, 2488.

McLean, A. D. and M. Yoshimine (1967) *Tables of Linear Molecule Wave-Functions*, IBM, N.P.

Messiah, A. (1961) *Quantum Mechanics*, North Holland, Amsterdam.

Micha, D. A. (1979a) J. Chem. Phys. 70, 565.

Micha, D. A. (1979b) J. Chem. Phys. 70, 3165.

Micha, D. A. (1981a) *Overview of Nonreactive Scattering*, to appear in *Potential Energy Surfaces and Dynamics Calculations*, D. G. Truhlar, Ed., Plenum, New York.

Micha, D. A. (1981b) *Scattering of ions by Polyatomics and Solid Surfaces: Multicenter Short-Range Interactions,* to appear in *Potential Energy Surfaces and Dynamics Calculations,* D. G. Truhlar, Ed., Plenum, New York.

Micha, D. A. (1981c) J. Chem. Phys. 74, 2054.

Micha, D. A., E. Vilallonga and J. P. Toennies (1979) Chem. Phys. Letters 62, 238.

Miller, W. H. (1975) Adv. Chem. Phys. 30, 77.

Miller, W. H. (1976) *Dynamics of Molecular Collisions,* Plenum, New York.

Munster, A. (1969) *Statistical Thermodynamics,* Springer-Verlag, Berlin.

Newton, R. G. (1966) *Scattering Theory of Waves and Particles,* McGraw-Hill, New York.

Ostrowski, A. M. (1966) *Solutions of Equations and Systems of Equations,* Academic Press, New York.

Pack, R. T. (1974) J. Chem. Phys. 60, 633.

Pariseau, M. A. I. Suzuki and J. Overend, (1965) J. Chem. Phys. 42, 2334.

Parker, G. A., R. L. Snow and R. T. Pack (1975) Chem. Phys. Letters 33, 399.

Parker, G. A., R. L. Snow and R. T. Pack (1976) J. Chem. Phys. 64, 1668.

Pathak, K. N. (1965) Phys. Rev. A139, 1564.

Pechukas, P. (1969) Phys. Rev. 181, 166.

Pople, J. A. and D. L. Beveridge (1970) *Approximate Molecular Orbital Theory,* McGraw-Hill, New York.

Porter, R. N. and L. M. Raff (1976) in *Dynamics of Molecular Collisions* Part B, W. H. Miller, Ed., Plenum, New York.

Rabitz, H. (1976) in *Dynamics of Molecular Collisions,* Part A, W. H. Miller, Ed., Plenum, New York.

Rae, A. I. M. (1973) Chem. Phys. Letters 18, 574.

Rodberg, L. S. and R. M. Thaler (1967) *Introduction to the Quantum Theory of Scattering,* Academic Press, New York.

Schatz, G. C. (1980) J. Chem. Phys. 72, 3929.

Secrest, D. (1975) J. Chem. Phys. 62, 710.

Slater, J. C. (1968) *Quantum Theory of Matter,* McGraw-Hill, New York.

Staemmler, V. (1975) Chem. Phys. 7, 17.

Thomas, L. D., W. P. Kraemer and G. A. F. Diercksen (1978) Chem. Phys. 30, 33.

Thompson, B. V. (1963) Phys, Rev. 131, 1420.

Toennies, J. P., (1976) Ann. Rev. Phys. Chem. 27, 225.

Tully, J. C. (1976) in *Dynamics of Molecular Collisions*, Part B, W. H. Miller, Ed., Plenum, New York.

Van Hove, L. (1954) Phys. Rev. 95, 249.

Vilallonga, E., D. A. Micha and J. P. Toennies (1979) Chem. Phys. Letters 68, 352.

Wilson, E. B., J. C. Decius and P. C. Cross (1955) *Molecular Vibrations*, McGraw-Hill, New York.

Zubarev, D. N. (1960) Sov. Phys. Uspekhi, 3, 320.

BIOGRAPHICAL SKETCH

Eduardo Fermin Vilallonga was born on October 19, 1953,in Buenos Aires, Argentina. He received his secondary education at the Colegio Nacional de Buenos Aires. In December, 1971,he came to the United States to attend the University of Florida, Gainesville, where he obtained the Bachelor of Science degree, summa cum laude, in physics in June, 1975. From September 1975 until the present, he has been a graduate student in the Department of Physics and in the Quantum Theory Project of the University of Florida. In September, 1978, he attended the International Summer Institute in Quantum Chemistry and Solid State Physics held at the University of Uppsala, Sweden. In September, 1979, he participated in a research collaboration trip to the Max Planck Institut für Strömungsforschung, Göttingen, Fed. Rep. Germany. In September, 1980, he attended the NATO Advanced Study Institute on Atomic and Molecular Collision Theory held at Cortona, Italy.

I certify that I have read this study and that in my opinion it conforms to acceptable standards of scholarly presentation and is fully adequate, in scope and quality, as a dissertation for the degree of Doctor of Philosophy.

David A. Micha, Chairman
Professor of Chemistry and Physics

I certify that I have read this study and that in my opinion it conforms to acceptable standards of scholarly presentation and is fully adequate, in scope and quality, as a dissertation for the degree of Doctor of Philosophy.

Thomas L. Bailey
Professor of Physics

I certify that I have read this study and that in my opinion it conforms to acceptable standards of scholarly presentation and is fully adequate, in scope and quality, as a dissertation for the degree of Doctor of Philosophy.

Charles F. Hooper, Jr.
Professor of Physics

I certify that I have read this study and that in my opinion it conforms to acceptable standards of scholarly presentation and is fully adequate, in scope and quality, as a dissertation for the degree of Doctor of Philosophy.

James W. Dufty
Professor of Physics

I certify that I have read this study and that in my opinion it conforms to acceptable standards of scholarly presentation and is fully adequate, in scope and quality, as a dissertation for the degree of Doctor of Philosophy.

Earle E. Muschlitz, Jr.
Professor of Chemistry

This dissertation was submitted to the Graduate Faculty of the Department of Physics in the College of Liberal Arts and Sciences and to the Graduate Council, and was accepted as partial fulfillment of the requirements for the degree of Doctor of Philosophy.

June, 1981

_____

Dean for Graduate Studies and Research

UNIVERSITY OF FLORIDA
3 1262 08666 918 0